

**ISTANBUL TECHNICAL UNIVERSITY ★ GRADUATE SCHOOL OF SCIENCE**  
**ENGINEERING AND TECHNOLOGY**

**EFFECTS OF VARIABLE VALVE TIMING ON THE EXHAUST THERMAL  
MANAGEMENT OF A TURBOCHARGED & INTERCOOLED DIESEL  
ENGINE**

**Ph.D. THESIS**

**Hasan Üstün BAŞARAN**

**Department of Naval Architecture and Marine Engineering**

**Naval Architecture and Marine Engineering Program**

**AUGUST 2016**



**ISTANBUL TECHNICAL UNIVERSITY ★ GRADUATE SCHOOL OF SCIENCE**  
**ENGINEERING AND TECHNOLOGY**

**EFFECTS OF VARIABLE VALVE TIMING ON THE EXHAUST THERMAL  
MANAGEMENT OF A TURBOCHARGED & INTERCOOLED DIESEL  
ENGINE**

**Ph.D. THESIS**

**Hasan Üstün BAŞARAN**  
**(508102003)**

**Department of Naval Architecture and Marine Engineering**

**Naval Architecture and Marine Engineering Program**

**Thesis Advisor: Prof. Dr. Osman Azmi ÖZSOYSAL**

**AUGUST 2016**



**İSTANBUL TEKNİK ÜNİVERSİTESİ ★ FEN BİLİMLERİ ENSTİTÜSÜ**

**DEĞİŞKEN VALF ZAMANLAMASININ TÜRBOŞARJLI &  
ARASOĞUTUCULU BİR DİZEL MOTORUN EGZOZ ISIL YÖNETİMİ  
ÜZERİNDEKİ ETKİLERİ**

**DOKTORA TEZİ**

**Hasan Üstün BAŞARAN  
(508102003)**

**Gemi İnşaatı ve Gemi Makinaları Mühendisliği Anabilim Dalı**

**Gemi İnşaatı ve Gemi Makinaları Mühendisliği Programı**

**Tez Danışmanı: Prof. Dr. Osman Azmi ÖZSOYSAL**

**AĞUSTOS 2016**



Hasan Üstün BAŞARAN, a Ph.D. student of ITU Graduate School of Science Engineering and Technology student ID 508102003, successfully defended the thesis entitled “EFFECTS OF VARIABLE VALVE TIMING ON THE EXHAUST THERMAL MANAGEMENT OF A TURBOCHARGED & INTERCOOLED DIESEL ENGINE”, which he prepared after fulfilling the requirements specified in the associated legislations, before the jury whose signatures are below.

**Thesis Advisor :**      **Prof. Dr. Osman Azmi ÖZSOYSAL**      .....  
Istanbul Technical University

**Jury Members :**      **Prof. Dr. Oğuz Salim SÖĞÜT**      .....  
Istanbul Technical University

**Prof. Dr. Selma ERGİN**      .....  
Istanbul Technical University

**Prof. Dr. Bahri ŞAHİN**      .....  
Yıldız Technical University

**Prof. Dr. İzzet Deniz ÜNSALAN**      .....  
Dokuz Eylül University

**Date of Submission : 15 July 2016**  
**Date of Defense : 17 August 2016**



*To my family,*



## **FOREWORD**

Emissions from diesel engines have become one of the most important environmental problems in the world today. The emission regulations have become stricter and stricter in the last 30 years and diesel engines are no longer allowed to release high rates of NO<sub>x</sub>, CO and particulate matter to the atmosphere.

One of the important solution to reduce emissions from diesel engines is to use exhaust thermal management systems. However, exhaust thermal management systems have a major drawback. They generally acquire effective emission conversion efficiencies when exhaust gas temperatures are above 250°C. As the diesel engines have lower than 250°C exhaust gas temperatures at low engine speed and low engine loading cases, utilizing these systems cannot be as efficient as expected on these performance points.

One of the current methods to achieve higher than 250°C temperatures is to use variable valve timing. Therefore, the intention in this study is to utilize variable valve timing on a diesel engine system to attain greater than 250°C exhaust gas temperatures and to obtain more effective aftertreatment management for more engine performance area.

I would like to begin by expressing my deepest appreciation and gratitude to my advisor, Prof. Dr. Osman Azmi ÖZSOYSAL, whose encouragement, guidance and support substantially contributed me to prepare this thesis. I would also like to thank TÜBİTAK for providing me scholarship via 2211-National Ph.D. Scholarship Programme during my Ph.D. studentship. Last but not least, I would like to thank my father, Alaettin BAŞARAN and my brother, Raşit Can BAŞARAN, for their love and support they have given to me during this study.

August 2016

Hasan Üstün BAŞARAN  
(Naval Arch. & Marine Engineer)



## TABLE OF CONTENTS

	<u>Page</u>
<b>FOREWORD</b> .....	<b>ix</b>
<b>TABLE OF CONTENTS</b> .....	<b>xi</b>
<b>ABBREVIATIONS</b> .....	<b>xiii</b>
<b>SYMBOLS</b> .....	<b>xv</b>
<b>LIST OF TABLES</b> .....	<b>xvii</b>
<b>LIST OF FIGURES</b> .....	<b>xix</b>
<b>SUMMARY</b> .....	<b>xxi</b>
<b>ÖZET</b> .....	<b>xxiii</b>
<b>1. INTRODUCTION</b> .....	<b>1</b>
1.1 Motivation .....	2
1.2 Literature Review .....	7
1.2.1 VVT effect on gasoline engines .....	7
1.2.2 VVT effect on diesel engines .....	8
1.2.3 VVT effect on the exhaust thermal management of diesel engines.....	12
1.3 Purpose of Thesis .....	16
<b>2. DIESEL ENGINE SPECIFICATIONS AND THE SIMULATION MODEL</b> 19	
2.1 Diesel Engine Specifications.....	19
2.2 The Simulation Model.....	20
2.2.1 Steps of LES engine model.....	21
2.2.2 LES engine model data insertion .....	22
<b>3. MATHEMATICAL FORMULATIONS</b> .....	<b>25</b>
3.1 Governing Equations of Gas Flow .....	25
3.2 Calculation of the Engine Performance Parameters.....	27
3.3 Calculation of Diesel Engine Friction .....	29
3.3.1 Rotating friction .....	29
3.3.2 Reciprocating friction .....	30
3.3.3 Valve train friction .....	31
3.3.4 Auxiliary friction.....	32
3.4 Pipe Wall Friction and Heat Transfer.....	32
3.5 In-cylinder Calculations .....	33
3.6 Combustion System.....	34
3.7 Cylinder Heat Transfer.....	36
3.8 Charge Cooler .....	37
3.9 Cylinder Scavenging .....	37
3.10 Flow Through Valves and Ports .....	38
3.11 Turbocharger .....	39
<b>4. VVT APPLICATION ON THE SYSTEM</b> .....	<b>41</b>
4.1 Validation of the Model .....	41
4.2 Examining the Effect of IVC on Diesel Engine Performance.....	47
4.2.1 Exhaust flow rate .....	48

4.2.2 Fuel injection rate.....	49
4.2.3 FMEP, PMEP and IMEP <sub>power</sub> variation along IVC sweep.....	50
4.2.4 Pressure-volume diagrams .....	51
4.3 TET and Exhaust Flow Diagrams for Different Engine Speeds and Engine Loadings .....	55
4.4 Effects of Other VVT Methods on the System .....	57
4.4.1 Late intake valve opening .....	58
4.4.2 Early exhaust valve closing.....	60
4.4.3 Early exhaust valve opening .....	61
4.5 Application of Combined EIVC and EEVO on the System.....	65
4.6 Application of Variable Inlet and Exhaust Maximum Valve Lifts .....	67
4.6.1 Change of inlet maximum valve lift.....	68
4.6.2 Change of exhaust maximum valve lift.....	69
4.6.3 Using lower inlet and higher exhaust maximum valve lifts.....	71
4.7 Application of EIVC & EEVO with Low Inlet and High Exhaust Max. Lifts	75
<b>5. CONCLUSIONS.....</b>	<b>81</b>
5.1 Conclusions .....	81
5.2 Recommendations for Future Work .....	84
<b>REFERENCES.....</b>	<b>87</b>
<b>APPENDICES .....</b>	<b>95</b>
<b>CURRICULUM VITAE .....</b>	<b>101</b>

## ABBREVIATIONS

<b>ABDC</b>	: After Bottom Dead Center
<b>AFR</b>	: Air Fuel Ratio
<b>arb</b>	: Arbitrary unit
<b>ATDC</b>	: After Top Dead Center
<b>BBDC</b>	: Before Bottom Dead Center
<b>BDC</b>	: Bottom Dead Center
<b>BTDC</b>	: Before Top Dead Center
<b>bmep</b>	: Brake mean effective pressure
<b>bsfc</b>	: Brake specific fuel consumption
<b>CA</b>	: Crank angle
<b>CDA</b>	: Cylinder Deactivation
<b>CI</b>	: Compression Ignition
<b>CO</b>	: Carbon monoxide
<b>CO<sub>2</sub></b>	: Carbon dioxide
<b>DOC</b>	: Diesel Oxidation Catalyst
<b>DPF</b>	: Diesel Particulate Filter
<b>ECR</b>	: Effective compression ratio
<b>EIVC</b>	: Early intake valve closing
<b>EEVC</b>	: Early exhaust valve closing
<b>EEVO</b>	: Early exhaust valve opening
<b>EGR</b>	: Exhaust Gas Recirculation
<b>EPA</b>	: Environmental Protection Agency
<b>EVC</b>	: Exhaust valve closing
<b>EVO</b>	: Exhaust valve opening
<b>FMEP</b>	: Friction Mean Effective Pressure
<b>HCs</b>	: Hydrocarbons
<b>IMEP</b>	: Indicated Mean Effective Pressure
<b>IVC</b>	: Intake valve closing
<b>IVO</b>	: Intake valve opening
<b>LES</b>	: Lotus Engine Simulation
<b>LIVC</b>	: Late intake valve closing
<b>LIVO</b>	: Late intake valve opening
<b>LNT</b>	: Lean NO <sub>x</sub> Traps
<b>MOP</b>	: Maximum opening point
<b>NO<sub>x</sub></b>	: Nitrogen Oxide
<b>PM</b>	: Particulate Matter
<b>PMEP</b>	: Pumping Mean Effective Pressure
<b>rpm</b>	: Revolution per minute
<b>Re</b>	: Reynolds number
<b>SCR</b>	: Selective Catalytic Reduction
<b>SI</b>	: Spark Ignition
<b>TET</b>	: Turbine Exit Temperature

**TDC** : Top Dead Center  
**VVT** : Variable Valve Timing

## SYMBOLS

<b>A</b>	: Area
<b>B</b>	: Bore
<b>C<sub>p</sub></b>	: Specific heat at constant pressure
<b>D</b>	: Diameter
<b>f</b>	: Friction factor
<b>F</b>	: Force
<b>h</b>	: Enthalpy
<b>k</b>	: Ratio of specific heats
<b>m</b>	: Mass
<b>m<sub>exhaust</sub></b>	: Exhaust mass flow rate
<b>m<sub>f</sub></b>	: Fuel mass flow rate
<b>N</b>	: Engine speed
<b>η<sub>vol</sub></b>	: Volumetric efficiency
<b>η<sub>th</sub></b>	: Brake thermal efficiency
<b>ρ</b>	: Density
<b>P</b>	: Pressure
<b>P<sub>e</sub></b>	: Brake power
<b>Q<sub>LHV</sub></b>	: Lower heating calorific value of fuel
<b>R</b>	: Ideal gas constant
<b>S</b>	: Stroke
<b>t</b>	: Time
<b>T</b>	: Temperature
<b>u</b>	: Velocity
<b>V<sub>d</sub></b>	: Displaced volume
<b>W</b>	: Work
<b>ω</b>	: Angular speed of the engine
<b>Z</b>	: Cylinder numbers
<b>π</b>	: Pi
<b>ε</b>	: Charge cooler effectiveness
<b>μ</b>	: Viscosity
<b>τ</b>	: Torque



## LIST OF TABLES

	<u>Page</u>
<b>Table 2.1</b> : Technical details of the studied Cummins type diesel engine .....	19
<b>Table 4.1</b> : Experimental data for different IVC timings at 2.50 bar engine loading. .....	41
<b>Table 4.2</b> : Nominal valve timings and maximum valve lifts .....	42



## LIST OF FIGURES

	<u>Page</u>
<b>Figure 1.1</b> : Evolution of on-highway emissions criteria.....	3
<b>Figure 1.2</b> : EPA standards for new trucks and buses.....	3
<b>Figure 1.3</b> : NO <sub>x</sub> conversion efficiency change for different SCR catalysts depending on temperatures. ....	4
<b>Figure 1.4</b> : Change of PM combustion efficiency in the presence of NO <sub>2</sub> and O <sub>2</sub> depending on temperatures. ....	5
<b>Figure 1.5</b> : Effect of inlet gas temperature in a DOC system. (a) On the conversion of CO. (b) On the conversion of THCs.....	6
<b>Figure 2.1</b> : LES model of the diesel engine.....	20
<b>Figure 2.2</b> : The schematical steps of LES engine model.....	22
<b>Figure 2.3</b> : Insertion of fuel injection rate data.....	23
<b>Figure 2.4</b> : Boundary conditions of the simulation model.....	24
<b>Figure 3.1</b> : Fluid control volume in duct .....	25
<b>Figure 3.2</b> : Schematic representation of the two-step Lax-Wendroff scheme.....	27
<b>Figure 3.3</b> : An exemplary mass fraction burn variation during combustion period.....	36
<b>Figure 3.4</b> : Effective area variation with valve lift .....	38
<b>Figure 3.5</b> : Compressor efficiency map.....	39
<b>Figure 4.1</b> : Nominal intake & exhaust valve timings on the simulation.....	43
<b>Figure 4.2</b> : Cylinder phase and valve event display of the diesel engine .....	43
<b>Figure 4.3</b> : Advanced and retarded IVC timings .....	44
<b>Figure 4.4</b> : Turbine exit temperature comparison between simulation & experiment .....	45
<b>Figure 4.5</b> : Volumetric efficiency comparison between simulation & experiment.....	46
<b>Figure 4.6</b> : Trapped AFR change along EIVC and LIVC .....	47
<b>Figure 4.7</b> : Exhaust flow rate change with different IVC timings.....	48
<b>Figure 4.8</b> : Fuel injection rate variation along early and late IVC .....	49
<b>Figure 4.9</b> : Brake thermal efficiency change along early and late IVC.....	49
<b>Figure 4.10</b> : IMEP <sub>power</sub> change along EIVC and LIVC .....	50
<b>Figure 4.11</b> : FMPEP and PMEP change along EIVC and LIVC.....	51
<b>Figure 4.12</b> : Experimental pressure-volume diagrams for EIVC timings .....	52
<b>Figure 4.13</b> : Pressure-volume diagrams along the cycle for EIVC with simulation.....	52
<b>Figure 4.14</b> : Maximum pressure change with IVC sweep.....	53
<b>Figure 4.15</b> : Experimental pressure-volume diagrams for LIVC timings .....	54
<b>Figure 4.16</b> : Pressure-volume diagrams along the cycle for LIVC with simulation.....	54
<b>Figure 4.17</b> : TET (°C) change for different engine speeds and engine loadings .....	55
<b>Figure 4.18</b> : Exhaust flow change for different engine speeds and engine loadings.....	56
<b>Figure 4.19</b> : Earlier and later timings of EVC and IVO .....	58
<b>Figure 4.20</b> : TET change for LIVO .....	58
<b>Figure 4.21</b> : Exhaust flow rate change for LIVO .....	59
<b>Figure 4.22</b> : Fuel consumption change for LIVO.....	59

<b>Figure 4.23</b> : TET change for advanced EVC timings.....	60
<b>Figure 4.24</b> : Exhaust flow rate variation with EEVC .....	60
<b>Figure 4.25</b> : Fuel consumption change for EEVC .....	61
<b>Figure 4.26</b> : Advanced EVO timings on the exhaust valve lift profile.....	62
<b>Figure 4.27</b> : TET change for advanced EVO.....	62
<b>Figure 4.28</b> : Exhaust flow rate variation with advanced EVO .....	63
<b>Figure 4.29</b> : Fuel consumption change with EEVO .....	63
<b>Figure 4.30</b> : Pressure-volume diagrams for EEVO .....	64
<b>Figure 4.31</b> : Combined EEVO and EIVC valve lift profiles .....	65
<b>Figure 4.32</b> : Rise of TET (°C) via combined EIVC & EEVO .....	65
<b>Figure 4.33</b> : Exhaust flow rate change along EEVO & EIVC.....	66
<b>Figure 4.34</b> : bsfc change (%) variation compared to nominal valve timings along combined EEVO & EIVC.....	67
<b>Figure 4.35</b> : Higher and lower valve lift profiles of inlet & exhaust.....	68
<b>Figure 4.36</b> : TET and bsfc along higher and lower inlet maximum valve lifts .....	68
<b>Figure 4.37</b> : Exhaust flow rate change for higher and lower inlet max. valve lifts .	69
<b>Figure 4.38</b> : TET and bsfc along higher and lower exhaust maximum valve lifts ..	70
<b>Figure 4.39</b> : Exhaust flow rate change for higher & lower exhaust max. valve lifts .....	70
<b>Figure 4.40</b> : TET (°C) for lower inlet and higher exhaust maximum valve lifts .....	71
<b>Figure 4.41</b> : Exhaust flow rate (kg/min) change for lower inlet and higher exhaust maximum valve lifts .....	72
<b>Figure 4.42</b> : bsfc change (%) variation in comparison to nominal max. valve lifts	73
<b>Figure 4.43</b> : $m_{\text{exhaust flow}} * C_p * TET$ variation for different maximum valve lifts....	73
<b>Figure 4.44</b> : TET (°C) variation on diesel engine performance zone .....	75
<b>Figure 4.45</b> : TET rise (°C) variation with VVT on diesel engine performance zone .....	76
<b>Figure 4.46</b> : Exhaust flow variation with VVT on diesel engine performance zone .....	77
<b>Figure 4.47</b> : Exhaust flow rate reduction compared to nominal valve timings .....	77
<b>Figure 4.48</b> : Variation of thermal power at nominal valve timings .....	78
<b>Figure 4.49</b> : Thermal power change with VVT and low inlet & high exh. max. lifts .....	79
<b>Figure 4.50</b> : Thermal power rise with VVT and low inlet & high exh. max. lifts...	79
<b>Figure A.1</b> : Insertion of main technical specs of the cylinder .....	96
<b>Figure A.2</b> : Friction assumption of the simulation model .....	96
<b>Figure A.2 (continued)</b> : Friction assumption of the simulation model.....	97
<b>Figure A.3</b> : Combustion data inside the cylinders .....	97
<b>Figure A.4</b> : Combustion heat release graph .....	98
<b>Figure A.5</b> : Annand open cycle heat transfer model.....	98
<b>Figure A.6</b> : Annand closed cycle heat transfer model .....	99
<b>Figure A.7</b> : Compressor map data .....	99

# **EFFECTS OF VARIABLE VALVE TIMING ON THE EXHAUST THERMAL MANAGEMENT OF A TURBOCHARGED & INTERCOOLED DIESEL ENGINE**

## **SUMMARY**

Emissions from diesel engines have become recently a significant problem due to their positive effect on global warming and negative effects on human health. Recently, NO<sub>x</sub> and PM emission regulations for diesel engines have become quite strict and the emission limits have decreased to very low numbers.

Engine producers generally use exhaust thermal management systems to reduce the high rates of emissions discharged from diesel engines. Some typical aftertreatment systems are SCR, DPF and DOC. SCR is used to decrease NO<sub>x</sub> emissions, DPF is utilized to reduce PM emissions and DOC is mostly applied in a diesel engine system to diminish unburned hydrocarbons (HCs) and carbon monoxide. Although these aftertreatment systems are indeed effective to meet stringent emission regulations on diesel engines, they have a major drawback. These systems generally require high exhaust gas temperatures in order to have high emission conversion efficiencies. In other words, they are temperature-dependent and mostly need higher than 250°C catalyst temperatures to perform efficiently. However, exhaust gas temperatures are generally lower than 250°C for diesel engines operating at lower engine speed and lower engine loading conditions on the performance map. That not only leads to inefficient aftertreatment systems but also insufficient emission reduction for those engine performance points.

One of the current methods to achieve greater than 250°C exhaust gas temperatures for these lower engine speed and lower engine loading areas is to use VVT. Changing the opening and closing timings of intake and exhaust valves, VVT can be applied to a diesel engine at any speed and at any load. Therefore, the aim of this study is to try to increase the exhaust gas temperatures of a diesel engine above 250°C for different engine speeds and different engine loadings via utilizing VVT. Change of inlet and exhaust maximum valve lifts is also examined in order to rise exhaust temperatures more in the system. The intention is to attain those high exhaust gas temperatures without causing any fuel consumption penalty in comparison to nominal valve timings.

Firstly, a six-cylinder turbocharged and intercooled diesel engine system is modelled to analyze exhaust gas temperatures and also exhaust gas flow rates by using Lotus Engine Simulation (LES) program. The simulation has different elements (cylinders, pipes, ports, valves, turbocharger, intercooler etc.) and these components are explained in a detailed manner with mathematical formulations.

Secondly, validation of the simulation is achieved for earlier and later intake valve closing (IVC) timings on a particular engine speed and engine loading point (1200 rpm and 2.50 bar bmep). The results of the simulation for turbine out temperature

and for volumetric efficiency are generally compatible with the experimental results. It is shown on the validation that advancing IVC timing 65 degrees CA or retarding it 100 degrees CA from nominal timing is adequate in the system to reach 250°C turbine exit temperature (TET). Up to 55° C TET rise is obtained by sweeping IVC timings forward or backward. Also, when effect of IVC on other diesel engine performance parameters is examined, it is seen that advanced and retarded IVC timings results in fuel-saving. However, these timings also cause high exhaust flow rate reduction compared to nominal valve timings in the system. Early IVC (EIVC) leads to more exhaust flow reduction, but it is also found to be more fuel-efficient than later IVC.

Thirdly, other VVT options are searched to combine with EIVC so as to attain higher than 250°C exhaust gas temperatures without causing a substantial reduction on exhaust flow rate. EEVC, LIVO and EEVO are all examined. EEVO is found to be the best option to combine with EIVC. Therefore, combined EIVC&EEVO is applied to the system. IVC is advanced 40 degrees CA from stock IVC timing and EVO is also advanced 70 degrees CA from nominal EVO timing. Although it is successful to satisfy 250°C TET in the system, it also causes a little bit more than 1 % bsfc penalty in comparison to nominal valve timings.

Later, inlet and exhaust maximum valve lifts are analyzed to reduce the fuel penalty on the system. It is seen that when lower inlet and higher exhaust maximum lifts compared to nominal maximum lifts is utilized, not only does it enable the system to acquire greater than 250°C TET, but also it decreases bsfc penalty down to zero percent in comparison to nominal valve timings.

Then, the method is implemented for different engine speeds (1000 rpm to 2000 rpm) and several engine loadings (1.0 bar to 5.0 bar bmep). When it is compared with TET and exhaust flow figures at nominal valve timings calculated on the previous part of the study, it is seen that 250°C target TET line can be decreased to lower engine loadings. For instance, for 1200 rpm engine speed, TET is obtained at only 2.50 bar bmep rather than satisfying the same temperature at 4.50 bar bmep with nominal valve timings and nominal maximum lifts. More importantly, this is achieved without requiring any extra fuel consumption compared to stock valve timings. Also, reduction of exhaust gas flow rates is not as high as the case where only IVC is used to meet the target TET for more efficient exhaust thermal management.

Finally, general evaluation of the study is done by discussing the results achieved in the analysis and the study is concluded on the final part with recommendations for future work. This study is expected to provide insight into the utilization of VVT technique on diesel engines to raise TET particularly on lower engine speed and lower engine loading points of the engine performance map. In this way, more efficient aftertreatment systems can be performed to fullfill the stringent emission criteria.

# DEĞİŞKEN VALF ZAMANLAMASININ TÜRBOŞARJLI & ARASOĞUTUCULU BİR DİZEL MOTORUN EGZOZ ISIL YÖNETİMİ ÜZERİNDEKİ ETKİLERİ

## ÖZET

Dizel motorlar günümüzde dünyada öncü bir rol üstlenmektedir. Endüstri ve sanayiden tarıma, otomotiv araçlarından deniz taşıtlarına kadar hemen her alanda dizel motorlar oldukça yaygın bir şekilde kullanılmaktadır. Ancak bu makinaların hayatımıza kattığı olumlu etkilerin yanı sıra, özellikle son zamanlarda çevremize oldukça olumsuz etkisi söz konusudur. Dizel motorlardan çevreye yayılan yüksek orandaki emisyonlar; küresel ısınmayı arttırıcı etkileri ve insan sağlığına da olumsuz etkileri nedeniyle günümüz dünyasında ciddi bir sorun haline gelmiş bulunmaktadır. Günümüzde dizel motorlar için izin verilen NO<sub>x</sub> ve PM emisyon sınırlamaları çok düşük değerlere düşürülmüştür.

Makina üreticileri dizel makinalardan çevreye yayılan bu yüksek orandaki emisyonları düşürmek için genellikle makina sistemlerinde egzoz ısısı yönetim sistemlerini kullanmaktadırlar. SCR, DPF ve DOC, bu sistemlerin dizel motorlarda en yaygın kullanılan türlerindedir. SCR göreceli olarak NO<sub>x</sub> emisyonlarını düşürmek için daha fazla kullanılırken, DPF yöntemi PM emisyonlarını azaltmakta tercih edilmektedir. DOC yöntemi ise, yanmamış hidrokarbon ve karbonmonoksit oranları için çevre koruma ajanslarınca dizel motorlara konulan sınırlamaların sağlanmasına yönelik bir sistemdir. Her ne kadar bahsi geçen bu ısıl yönetim sistemleri dizel motorlar için belirlenmiş emisyon sınırlarını sağlamak amacıyla kullanılmaktaysa da, pratikte kullanım sırasında her bir egzoz ısıl yönetim sisteminin kendisine has sıkıntıları ve yol açtığı zorluklar bulunmaktadır. Bu sistemlerde, yüksek emisyon dönüşüm verimi sağlayabilmek için genellikle yüksek egzoz gazı sıcaklıklarına ihtiyaç duyulmaktadırlar. Bir başka ifadeyle, bu sistemler sıcaklığa oldukça bağlıdır ve verimli olabilmeleri için katalizör taşıyıcı sıcaklıklarının 250°C'den yüksekte tutulması gerekmektedir. Bu da ancak motordan ısıl yönetim sistemlerine gönderilen egzoz gazı sıcaklığının 250°C'nin üzerinde sürekli bir şekilde seyretmesi ile sağlanabilir. Fakat, dizel motorlarda egzoz gazı sıcaklıkları, dizel motorun çalışma alanında (hıza ve yüke bağlı) özellikle hızın ve yükün nispeten daha düşük seyrettiği durumlarda genellikle 250°C'nin altında kalmaktadır. Düşük egzoz gazı sıcaklığı ile çalışma durumu da, oldukça verimsiz egzoz ısıl yönetimine ve dizel motorun bu koşulda çalıştığı noktalar için yeterli emisyon düşürümünün sağlanamamasına sebep olur. Makina imalatçılarının bu performans noktalarında gereken yüksek egzoz gazı sıcaklıklarına ulaşabilmek için çözümler üretmesi gerekmektedir.

Dizel motorlarda; makina hızının ve makina yükünün nispeten daha düşük olduğu motor performans alanlarında, 250°C'den yüksek egzoz gazı sıcaklığı elde etmek için başvurulan güncel metodlardan birisi de değişken valf zamanlamasıdır (VVT). Emme ve egzoz valflerinin açılma ve kapanma zamanları değiştirilerek, VVT bir

dizel motoruna herhangi bir hız veya herhangi bir yük durumu için uygulanabilir. Bu nedenle; bu çalışmanın amacı, 6 silindirli ve 4 stroklu bir dizel motorunun egzoz gazı sıcaklığının 250°C'nin altında kaldığı performans noktalarında, farklı hız ve farklı yük durumları için VVT yöntemini uygulayarak egzoz gazı sıcaklığını 250°C'nin üstüne çıkarabilmek ve dolayısıyla makina sisteminde daha verimli egzoz ısıl yönetimi elde edebilmektir. Valf açılma ve kapanma zamanlamalarının yanı sıra emme ve egzoz maksimum valf açıklıklarının değişimi de yine egzoz gazı sıcaklığını daha da arttırmak için uygulanmıştır. Çalışmadaki hedef, bu yüksek egzoz gazı sıcaklıklarını elde ederken, başlangıç emme ve egzoz valf açılma ve kapanma zamanlamaları ile başlangıç maksimum valf açıklıklarına kıyasla sistemde herhangi bir yakıt tüketimi artımına sebep olmadan VVT yöntemini birçok farklı hız ve yük durumu için uygulayabilmektir.

Tez çalışmasında öncelikle altı-silindirli türboşarjlı ve arasoğutuculu marinize bir dizel motor sistemi LES motor simülasyon programı kullanılarak, egzoz gazı sıcaklıklarını ve egzoz gazı kütle akış oranlarını incelemek için modellenmiştir. Simülasyon programı, içerisinde marinize dizel motor sistemini oluşturan birçok farklı unsur (silindirler, portlar, valfler, türboşarjer, arasoğutucu, elemanları birbirine bağlayan borular vs.) bulundurmaktadır. Simülasyonu oluşturan bu parçalar toplu olarak bir şekil üzerinde gösterilmiş ve ardından programda kullanılan kabuller ve programa bu elemanlara ait verilerin girişi detaylı bir şekilde gerek metin içinde gerekse de tezin Ek kısmında gösterilmiştir. Ayrıca, bu unsurlarda hesaplamalar için kullanılan matematiksel denklemler de yine ayrıntılı olarak açıklanmıştır.

Tez çalışmasının ilerleyen safhalarında LES programında modellenen marinize dizel motorun 1200 rpm hızında ve 2.50 bar sabit motor yükünde (ortalama efektif basınç) çalıştığı düşünülmüş ve emme valfi kapanma (IVC) zamanlamasının daha erken/geç kapanması durumu açık literatürdeki bir deneysel çalışma ile karşılaştırılmıştır. Yapılan inceleme ve kontroller sonucunda teorik modellemenin literatürdeki baz deney sonuçlarıyla uyumlu olduğu görülmüş, modellemenin kabul edilebilirliği ve doğruluğu anlaşılmıştır. Bilgisayar modellemesi ile hesaplanan türbin çıkış sıcaklığı (TET) ve hacimsel verim değerlerinin literatür deney sonuçları ile uyumlu olduğu gözlenmiştir. Böylece modelleme programının egzoz gazı sıcaklığı hesabında da rahatlıkla kullanılabileceği görülmüştür. Modellemenin doğrulama aşamasında; sabit yük koşulu altında, IVC'nin orijinal kapanma krank açısı (CA) değerinden 65 derece CA geriye ötelenmesi veya 100 derece CA ileriye ötelenmesinin TET değerinin 250°C'den yüksek olması için yeterli olduğu gösterilmiştir. IVC'nin ileri ve geri ötelenmesi ile 55°C'ye varana kadar TET artışı elde edilmiştir. Ayrıca, IVC'nin diğer makina performans parametreleri üzerindeki etkisi incelendiğinde IVC'nin erken ve geç kapanmasının yakıt tüketimini azalttığı gözlenmiştir. Erken kapanma geç kapanmaya kıyasla biraz daha fazla yakıt tasarrufu sağlamaktadır. İleri ve geri ötelenmiş IVC değerlerinin etkileri P-V indikatör diyagramında gösterilmiş, sonuçları orijinal IVC değerleri için açık literatürde ortaya konulan sonuçlarla karşılaştırılmıştır. Karşılaştırmalar sonunda yakıt tasarrufunun sistemdeki pompalama kayıplarının azalmasından kaynaklandığı görülmüştür. Öte yandan, bu erken ve geç kapanma zamanlamaları başlangıç değerine kıyasla, egzoz gazı kütle akış oranında oldukça yüksek düşümlere neden olmaktadır. Erken IVC (EIVC); motorun hacimsel verimini, geç IVC (LIVC) zamanlamasına göre daha fazla düşürdüğü için egzoz gazı kütle akışında daha yüksek oranda azalışa sebep olmaktadır.

Tez çalışmasının ilerleyen safhalarında ise egzoz gazı sıcaklıklarını 250°C'nin yukarısına çıkarmak ve bunu yaparken egzoz gazı akış oranında azalmaya yol açmamak için erken emme valfi düzenlemesine ek başkaca VVT seçenekleri de araştırılmıştır. Erken egzoz valf kapanması, geç emme valfi açılması ve erken egzoz valfi açılması (EEVO) uygulamalarının hepsi ayrı ayrı incelenmiştir. EEVO'nun EIVC ile birleştirilmesinin en iyi seçenek olduğu görülmüştür. Çünkü EEVO; hem egzoz gazı sıcaklığını hızlı bir şekilde arttırmakta, hem de egzoz akış oranı üzerinde olumsuz bir etki yaratmamaktadır. Ayrıca, her ne kadar EEVO yöntemi yakıt tüketimini arttırsa da, EIVC metodunun sistemde sağladığı yakıt tasarrufu ile bu yükseliş en aza indirilebilir ve hatta dengelenerek başlangıçtaki yakıt tüketim değeri korunabilir. Bu nedenle, birleştirilmiş EIVC & EEVO yöntemi sisteme sabit yük altında uygulanmıştır. EIVC başlangıç zamanından sadece 40 derece CA geriye ötelenmiş ve EEVO da başlangıç açılma değerinden 70 derece CA daha önce açılmıştır. Her ne kadar sistemde 250°C'ye oldukça yakın egzoz gazı sıcaklığı elde edilmiş olsa da, birleşik valf zamanlaması metodu başlangıç valf zamanlamasına nazaran 1 %'den biraz daha fazla bir oranda yakıt tüketiminde artışa neden olmuştur.

Sonraki aşamada, emme ve egzoz maksimum valf açıklık değerlerinin değişimi incelenerek simülasyonda oluşan bu % 1'lik yakıt tüketimi artışı giderilmeye çalışılmıştır. Başlangıç valf açıklıklarına kıyasla daha küçük emme valfi maksimum açıklığı ile daha yüksek egzoz valfi maksimum açıklığı kullanıldığında, TET değerinin 250°C'den çok daha yüksek değere ulaşabilmesi sağlanmıştır. Ancak bundan daha da önemli olan sonuç, bu yüksek egzoz gazı sıcaklığı elde edilirken, sistemdeki yakıt tüketiminin başlangıç valf zamanındaki değere düşürülebilmiş olmasıdır. Yöntem, her ne kadar egzoz kütle debisini biraz azaltsa da, TET değerini başlangıç valf maksimum açıklık değerlerine nazaran yeterince arttırdığı için ısı sistemine gönderilen egzoz gazı termal gücü sabit kalabilmektedir.

Son aşamada, yöntemin başarılı olduğunun görülmesi üzerine, metod farklı makina hızlarına (1000 rpm'den 2000 rpm'e) ve birçok farklı makina yük durumuna (1.0 bar'dan 5.0 bar'a) uygulanmıştır. VVT metodu ile, başlangıç valf açılma ve kapanma zamanları ile başlangıç valf maksimum açıklık değerlerine kıyasla, çok daha düşük makina yüklerinde egzoz gazları 250°C TET değerine ulaşabilmektedir. Örneğin, 1200 rpm makina hızı için; dizel motor başlangıç valf değerlerinde, 250°C'nin üstünde egzoz kütle akışını ancak 4.50 bar yüklü durumda sağlayabilirken, VVT ve değişken valf açıklık değerleri ile aynı sıcaklığa 2.50 bar motor yükü durumunda ulaşabilmektedir. Yük durumundaki iyileştirme farklı motor hızlarında farklı değerler olsa da, 250°C egzoz gazı TET eğrisi bu yöntem ile motorun çalıştığı bütün hızlarda daha düşük makina yük durumlarına indirilebilmektedir. Bu da dizel motorun, başlangıç valf durumuna nazaran, çalışma bölgesinin çok daha büyük bir kısmında daha verimli egzoz ısı yönetimine sahip olabilmesi ve emisyon değerlerini izin verilen sınır değerlerde tutabilmesi demektir. Daha da önemli olan sonuç ise, bu sonucun orijinal valf zamanlamasına nazaran fazladan bir yakıt tüketimi gerektirmeden gerçekleşmiş olmasıdır. Ayrıca, her ne kadar egzoz gazı kütle akışında düşüş gözlemlense de; hesaplanan azalma, yalnızca IVC zamanlamasının ileri ve geri ötelenmesi ile 250°C TET değerinin elde edildiği durumdaki kadar yüksek olmamaktadır.

Tezin sonuç kısmında modelleme sonuçları tartışılmış, araştırmanın genel değerlendirilmesi yapılmış ve gelecekte bu yönde çalışma yapacak araştırmacılar için çalışma alan önerileri belirtilmiştir. Bu çalışmayla VVT tekniğinin marine dizel motorların özellikle manevra veya liman içi gibi düşük yükte çalışma durumlarında

egzoz gazı sıcaklıklarının 250°C'nin üzerine nasıl çıkarılabileceđi ortaya konulmuştur. Teorik araştırmanın deneysel araştırmayla desteklenerek gelecekte emisyon azaltımı ile alakalı çalışmalara yöntem bazında fikir vermesi, yol göstermesi ve katkı sağlanması umulmaktadır. Tez bulgularıyla marinize dizel motorların egzoz ısı yönetim sistemleri çok daha verimli hale getirilebilir ve aranan/izin verilen emisyon kriterleri karşılanabilir.

## **1. INTRODUCTION**

The internal combustion engines have a leading role in the world as a power plant for about a century. Thanks to advances in materials, manufacturing, computer analysis and design tools in the current 30 years, the internal combustion engines can attain higher standards of performance. Particularly strict legislations on emissions, fuel scarceness and social and economic factors are bringing new targets for current engine systems for the following years. Therefore, improved diesel engine models via computer simulations will be needed to supply those demands in the future.

Modeling of engine systems have been used for a very long time in the design stage of improved engine models. Numerical simulation of engines has become an appealing choice as it decreases prototyping costs and enable many different parametric and optimization studies to be made on engine models to achieve targeted values. Also, experimental tests cannot measure every detail in engine systems and it is difficult and expensive for different trials. However, once a validated model is acquired; not only is it easier to work the model consecutively, but new targets can also be calculated and examined.

Moreover, new theoretical concepts such as neural network analysis and genetic algorithms which are related to optimization are brought in to use in the area of engine research. Those new concepts will contribute to examine more complicated engine systems. As the more complex components were added to the engines, the capabilities of the simulation tools had to grow and will have to grow due to new regulations set on engine systems.

Recently, emissions from diesel engines have become a significant problem and strict emission limits on diesel engines are expected to be met by engine manufacturers. Therefore, producers try to to create new engine simulations in order to calculate the pollutants discharged from these machines without requiring the experimental tests. Validated simulation models for the strict emission criteria will be the main focus for diesel engines for the forthcoming decades.

In this study, the engine simulated and examined for VVT is a low-load truck diesel engine. However, it can be marinized, converted into a marine diesel engine and can be utilized on small marine vehicles. The diesel engines used as main engines on ships are generally low-speed, large and powerful machines. The reason why a relatively smaller and high-speed diesel engine is preferred to analyze in this thesis is that not only are the technical specifications of the diesel engine known, but also experimental results of the same diesel engine can be obtained from open literature.

Medium and high speed diesel engines are mostly equipped with exhaust thermal management systems in order to reduce the high rate of emissions released into the environment. These exhaust aftertreatment systems require in general higher than 250°C exhaust gas temperatures so as to operate with maximum efficiency. The marinized, high-speed and small diesel engine examined in this thesis discharges exhaust gases below 250°C temperature at idling speed and also at lower engine speed and lower engine loading points of its performance map. In this study, the analysis is limited between 1000 - 1300 rpm engine speeds and 1 bar - 3.50 bar bmep engine loadings. The VVT application is applied for higher engine speeds and higher engine loadings too. However, as stated previously, the main concern for this diesel engine is lower engine speed and lower loading areas. Also, it is assumed on the diesel engine that turbocharger is not out-of-operation on lower engine speeds and the engine inducts air into the compressor at ambient temperature.

## **1.1 Motivation**

Diesel engines today are becoming more efficient and cleaner when compared to previous engines used in transportation, farming or industry. However, nowadays, there is still a significant amount of harmful pollutants such as NO<sub>x</sub> and particulate matter (PM) released by these machines. Although more efficient and more powerful engines are demanded, producers have to achieve this goal by decreasing the emission levels down to the recent emission limits. These emission regulations are needed for both decreasing the air pollution related health problems and minimizing the positive effect of these widely used machines on global warming. As shown on Figure 1.1 below, the emission criteria has become stricter and stricter for heavy-duty diesel engines since 1994 to 2010 [1].

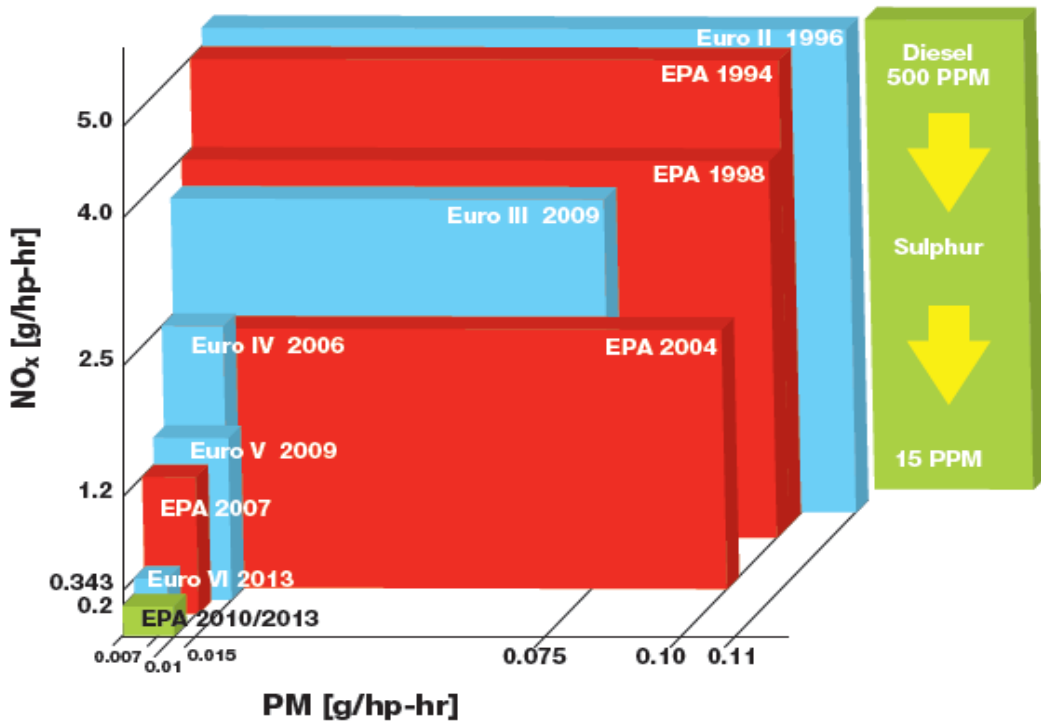


**Figure 1.1 :** Evolution of on-highway emissions criteria [1].

U.S. Environmental Protection Agency (EPA) state on the following Figure 1.2 that PM should not be more than 0.01 g/hp/hr (0.013 g/kWh) and NOx must not be higher than 0.2 g/hp-hr (0.27 g/kWh) for heavy-duty diesel engines used on new trucks and buses [2-4].

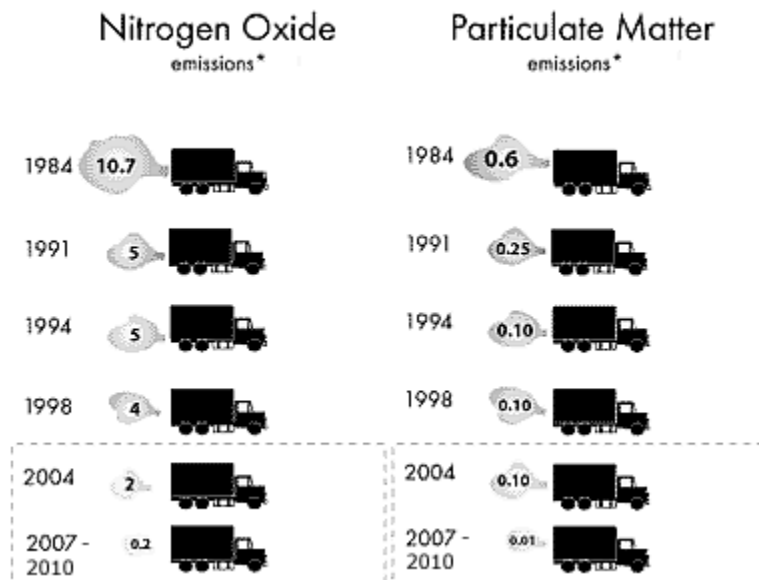


**Figure 1.2 :** EPA standards for new trucks and buses [2].

In order to meet the emission criteria seen above, engine producers must either decrease the amount of harmful pollutants discharged from the engine or utilize

exhaust thermal management systems. Late fuel injection, high pressure fuel injection and exhaust gas recirculation (EGR) have been commonly used to diminish emissions released from diesel engines [5]. Yet, these methods generally have a negative effect on engine efficiency and cannot be practical for the whole engine performance map. Therefore, manufacturers have preferred to use both emission-decreasing techniques and modern exhaust thermal management systems on diesel engines so as to meet the stringent regulations demonstrated on Figure 1.2 above.

Selective catalytic reduction (SCR), lean NOx traps (LNT), diesel oxidation catalyst (DOC) and diesel particulate filter (DPF) are typical exhaust aftertreatment systems. SCR and LNT are both used to lower NOx emissions, DOC is utilized to decrease unburned hydrocarbons (HCs) and carbonmonoxide and DPF is used to reduce PM emissions. These aftertreatment systems are definitely effective at decreasing the emissions down to the limitation levels. However, these systems are mostly temperature-dependent and can be more effective only in a limited temperature range. SCR and LNT have generally effective conversion efficiency of NOx into N<sub>2</sub> and H<sub>2</sub>O, only when catalyst temperature is within 250°C and 450°C limit [3,6-10]. This temperature restriction of aftertreatment systems makes emission reduction difficult for cold start, low speed and low loading cases of diesel engines where engine exhaust temperatures are generally lower than 250°C. When Figure 1.3 below is examined, it is seen that NOx conversion efficiency dramatically goes down as catalyst temperatures are below 250°C [6].

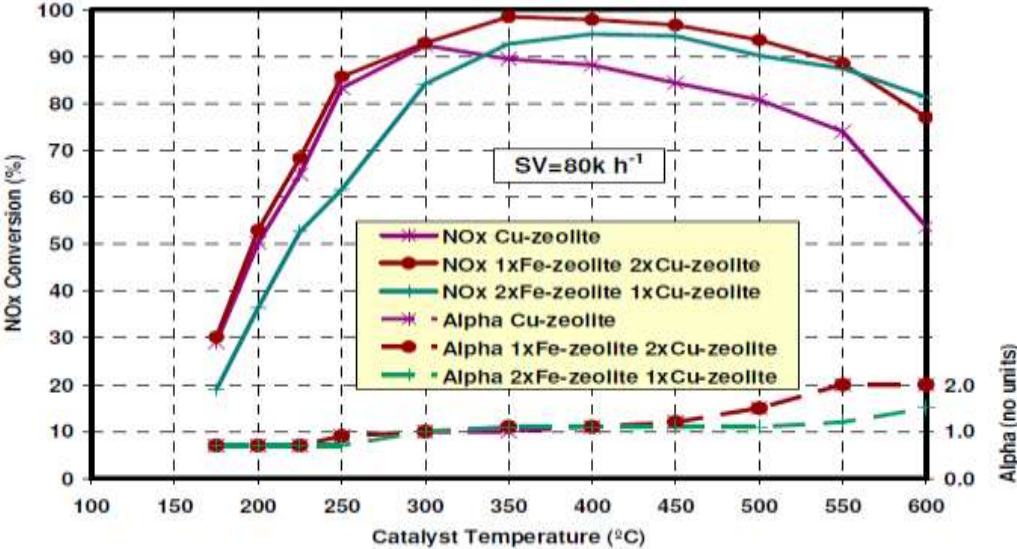


**Figure 1.3 :** NOx conversion efficiency change for different SCR catalysts depending on temperatures [6].

LNT systems also can work effectively in a limited catalyst temperature range. They generally reach their best efficiency between 300°C and 400°C. Above or under these catalyst temperature interval, their NO<sub>x</sub> conversion efficiency sharply drops [7]. It is definite that exhaust gas temperatures must be controlled within a temperature limit in diesel engine systems in order to utilize both SCR and LNT systems in an efficient manner.

In addition to SCR and LNT exhaust thermal management systems, diesel engine today generally utilize DPF so as to collect carbon based soot in the exhaust gas flow. As stated earlier on Figure 1.1, PM emission limitations are decreased to very low levels. This is because these particles are directly affecting human health in a negative manner. They generally cause to respiratory and cardiovascular related health problems [11]. DPF uses a filter to collect the soot particles and these trapped carbon particles are generally oxidized by using oxygen or nitrogen oxide. The combustion of soot particles in oxygen needs very high temperature interval (550°C to 600°C). These temperatures can only be achieved in diesel engines for high speed and high loading cases. However, nitrogen oxide does not require that much high temperatures (250°C to 300°C). On Figure 1.4 below, collected soot combustion efficiency for both NO<sub>2</sub> and O<sub>2</sub> is shown [11,12].

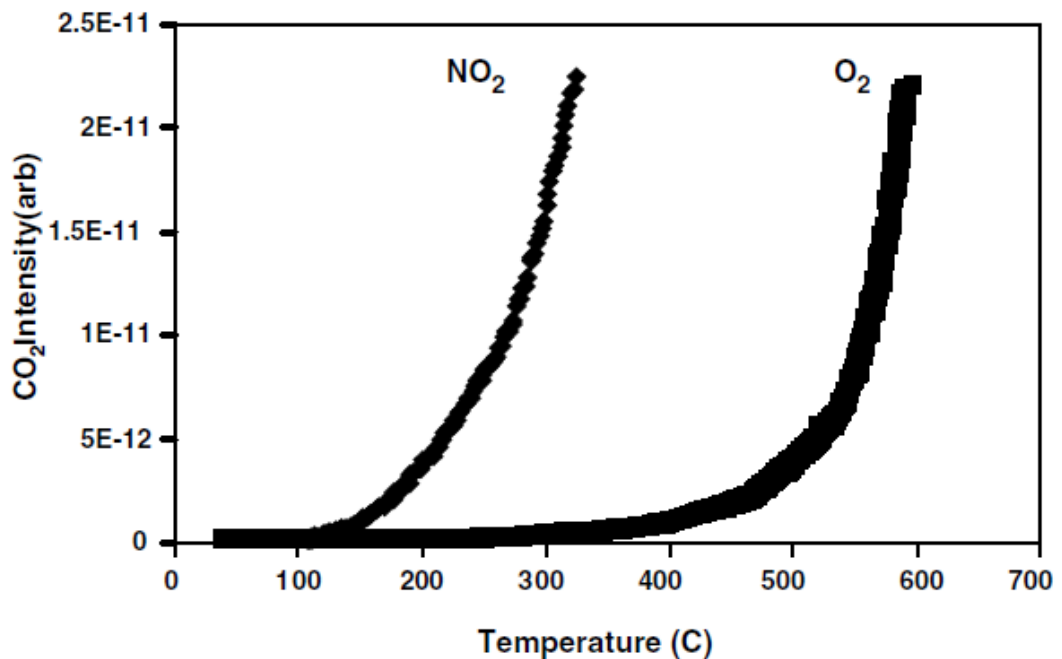


**Figure 1.4 :** Change of PM combustion efficiency in the presence of NO<sub>2</sub> and O<sub>2</sub> depending on temperatures [12].

Moreover, a DOC system is commonly used to oxidize NO to NO<sub>2</sub> and CO to CO<sub>2</sub>. It is also effective at converting HCs into water via oxidization. These systems are temperature-reliant too as SCR, LNT and DPF systems. They generally require greater than 200°C temperatures for efficient performance. [13-15]. As seen on the following Figure 1.5 (a), conversion of CO reaches its maximum efficiency after inlet gas temperatures into the DOC system becomes greater than 200°C. However, when conversion of total hydrocarbons (THCs) is considered on the DOC system, it is shown on Figure 1.5 (b) that 200°C is not sufficient to obtain the maximum conversion efficiency. Just as seen on SCR and DPF, at least 250°C inlet gas temperature is needed to operate DOC with utmost efficiency [15]

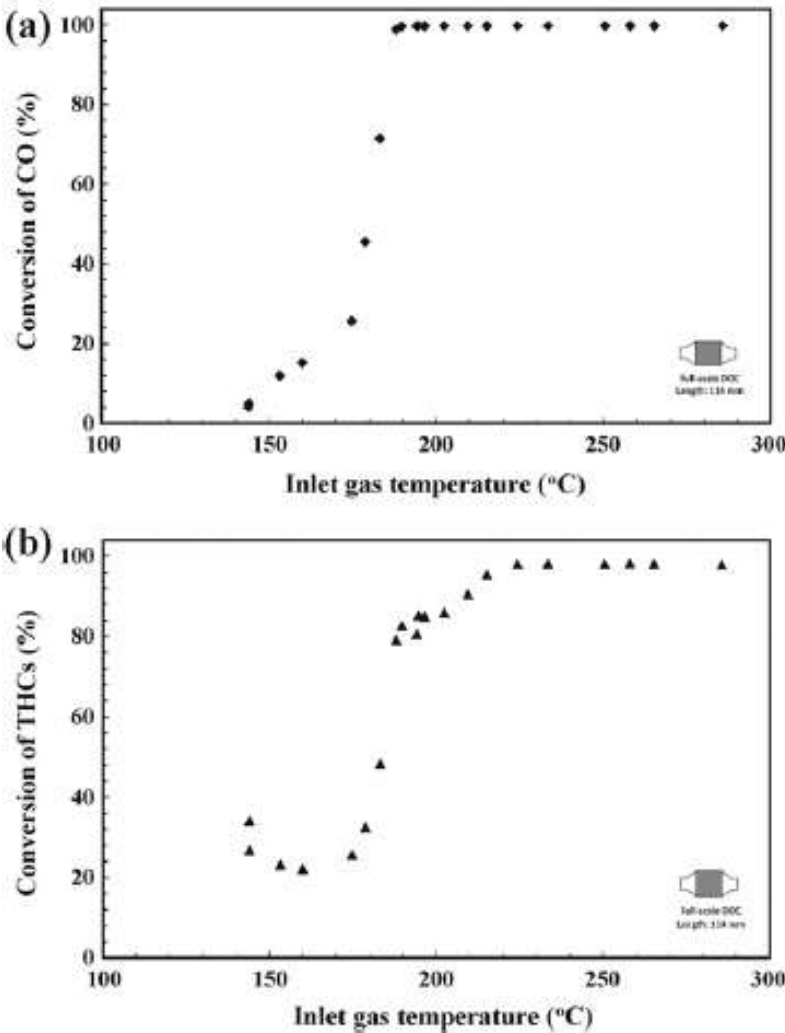


**Figure 1.5 :** Effect of inlet gas temperature in a DOC system. (a) On the conversion of CO. (b) On the conversion of THCs [15].

It can be derived that aftertreatment systems are indeed effective and practical for diesel engines to meet stringent emission regulations. However, they have a serious

drawback. They require exhaust gas temperature range (generally above 250°C in order to perform with higher emission conversion efficiencies. Yet, exhaust temperatures become generally lower than 250°C for diesel engines at low speed and at low engine loading cases. It is also problematic during cold start. Recently, variable valve timing (VVT) has been examined as a method to achieve those greater than 250°C exhaust gas temperatures for exhaust thermal management systems. In the following section, not only are those current studies explained, but also historical background of the effect of VVT on diesel engine and also gasoline engine performance is examined from past studies to the recent analysis on this topic.

## **1.2 Literature Review**

### **1.2.1 VVT effect on gasoline engines**

VVT is one of the solutions for achieving higher torque, brake power, volumetric efficiency and reduced brake specific fuel consumption (bsfc) in both gasoline and diesel engine systems. VVT concept has long ago been searched for gasoline engines. Different VVT techniques on gasoline engines are searched and these methods are classified [16-18]. Practicality of VVT technology and its potential benefits are also examined [19, 20]. Later, effects of intake valve timing on volumetric efficiency [21], engine torque optimization via VVT [22], engine performance improvement via intake valve timing and lift [23], VVT application for better engine performance and low exhaust emissions [24], analysis of early intake valve closing effect on engine performance [25], impact of VVT on SI engine thermal efficiency [26] and optimization of VVT for maximum performance [27] are some of the studies concerning VVT effect on gasoline engines. Hong et al. examined all intake and exhaust valve opening and closing timings on a SI (spark-ignition) engine and P-V diagrams for varied valve timings (50 degrees later or earlier than nominal) are obtained and compared with the nominal engine P-V [28]. In more recent studies, influence of VVT on combustion [29], early intake valve closing effect on performance and emissions [30], VVT for fuel economy improvement [31], engine loading control via utilization of VVT [32], VVT and lift design for performance improvement on a single cylinder gasoline engine [33] are some of the studies where VVT is used on particularly on SI engines. It is seen that

VVT usage on gasoline engines is recently focusing on fuel-efficiency, reduction of emissions and engine performance improvement.

### **1.2.2 VVT effect on diesel engines**

As explained on the earlier section, VVT has been searched for gasoline engines thoroughly. However, VVT has not been documented well for diesel engines [17, 20]. One of the reason is that inlet air isn't throttled in diesel engines as done in gasoline engines. That doesn't let diesel engines have a great pumping loss reduction using VVT as can be achieved in gasoline engines. Another reason is that diesel engines have high compression ratios and the distance between piston and valves at top dead center is relatively smaller when compared to spark-ignition engines. [17, 20]. Therefore, application of VVT is limited for inlet valve opening (IVO) and exhaust valve closing (EVC) timings in order to prevent piston-valve strike. But same restriction is not valid for inlet valve closing (IVC) and exhaust valve opening (EVO) timings. Also, compression ratio of medium speed diesel engines are not as high as high-speed ones. Changing one of these timings when others are constant or changing inlet and exhaust phases and lifts in particular engine speeds or for a specified engine speed interval can help improve torque, brake power, volumetric efficiency and also bsfc reduction. The following paragraphs will explain the studies concerning the effects of VVT on diesel engines.

Endo et al. investigated the impact of rising intake and exhaust valve opening areas on a high boosted diesel engine [34]. It is shown in the study that larger valve opening areas are indeed effective at decreasing the pumping losses and at improving fuel consumption especially at higher engine speeds and higher engine loading cases.

Leonard et al. examined the application of VVT to a turbocharged diesel engine [35]. Effect of parametric investigation of valve overlap on reverse flow is studied and it is found that decreasing the valve overlap at part load contributes to decrease the backflow of exhaust gases into the inlet manifold. At 25 percent fuelling level and with a 40° variable phasing system, residual gases can be diminished from 3.9 percent to 0.12 percent.

Özsoysal et al. searched the effect of VVT on a high speed turbocharged marine diesel engine [36]. The study particularly considers how the intake valve timing affects the diesel engine in order to decrease the reverse flow at intake valve at low

engine loading conditions. It is shown in the study that there is fuel consumption improvement when one of the intake valve timings is retarded or when intake valve timing duration is increased close to 30 degrees CA in comparison to nominal intake duration. However, advancing the timings of inlet valves while exhaust timings are fixed results in lower efficient engine performance.

Özsoysal et al. also tried to observe the effect of different number of valves on a marine diesel engine performance [37]. A thermodynamic-based simulation is modeled and the impact of 2, 4 and 6 valve cases on the engine pressure is calculated.

Stone et al. analyzed VVT system on a highly turbocharged diesel engine [38]. It is shown that phasing the inlet valve timings or decreasing the inlet valve lift and period is useful methods to reduce the exhaust backflow to the cylinder and to the inlet manifold. Effect of change of IVO on ignition delay, averaged exhaust gas temperature, air flow rate and scavenge ratio are also studied.

Benajes et al. examined the impact of intake valve pre-lift on a 6-cylinder diesel engine utilizing wave action model [39]. The study asserts that intake valve pre-lift is definitely beneficial so as to obtain higher internal EGR. It also suggests that fuel delivery adjustments or turbocharger modifications should be considered for greater internal EGR.

Lancefield et al. modeled a modern European 2.15 L 4-cylinder 4 valve diesel engine with VVT using Ricardo's "Wave" program [40]. It is demonstrated in the study that brake specific fuel consumption (bsfc) can be reduced up to approximately 2.3 % via early IVC and up to around 1 % by using late IVC. Furthermore, at low speeds, torque can be raised up to 15.4 % for 1600 rpm and up to 16.4 % for 1000 rpm by optimizing both IVC and EVO timings.

Tai et al. investigated a 2.7 L, V6 4 valves/cylinder, direct injected, common rail turbocharged diesel engine with camless valvetrain so as to observe the effects of IVC and EVO timings [41]. It is asserted that optimizing IVC timing with constant exhaust valve timing leads up to 6.2 % torque increase at low and medium speeds; while fuel consumption change is not affected significantly. Also, it is claimed that when both IVC and EVO are optimized, torque improvements can go up to 45.9 % again at low and medium speeds, however, fuel consumption raises. Internal EGR

examination to improve vehicle transient operation, effect of changing intake valve lift, lift profile and valve timing on in-cylinder swirl, effect of advancing IVC timing on peak cylinder pressure are the future work suggestions in the study.

Lancefield tried to identify the impacts of variable valve actuation (VVA) on the fuel economy of a part loaded light-duty diesel engine [42]. Retarding and advancing intake valve closing timings by 33 degrees CA from the nominal value, up to 19 % and up to 5 % bsfc reduction are achieved at part load condition. Also, for the studied part loaded diesel engine, bsfc can be decreased to a minimum value by late opening of the exhaust valve up to 11 degrees CA from the nominal timing.

Parvate-Patil studied VVT and its effects on a single cylinder diesel engine [43]. VVT effects on gasoline and diesel engines are explained individually by retarding the timings. Fuel injection is taken constant and also change of valve timing for all 8 different valve opening and closing situations is fixed, 50 degrees CA earlier or later than their nominal values. It is suggested in the study that reduction of exhaust pumping losses with VVT, internal EGR via early IVO and late EVC for decreasing NO<sub>x</sub> emissions, effects of valve opening and closing with variable lift and duration and also effects of VVT on gas dynamics should be examined for future studies.

Murata et al. tried to obtain premixed combustion by using VVT in a direct injected single cylinder water cooled diesel engine [44]. It is reported that late IVC (LIVC) at medium engine speed can be used to decrease combustion temperatures. Therefore, NO<sub>x</sub> and smoke can be decreased significantly in the system.

Nevin et al. tested a Caterpillar 3401 direct injected single cylinder oil test engine using variable IVC to obtain premixed charged compression ignition (PCCI) [45]. It is concluded in the study that CO and PM rates are reduced by 70 % via LIVC and NO<sub>x</sub> emissions are decreased by more than 50 % at low load case with constant fueling by delaying the IVC timings.

Sugiyama et al. used early intake valve closing (EIVC) in order to control volumetric efficiency and effective compression ratio [46]. EIVC leads to fuel-efficient engine performance, but the decrease in fuel consumption goes down at lower loading cases. He also showed that when variable compression ratio is combined with advanced intake valve opening (IVO), in-cylinder combustion can be improved and in-cylinder temperature can be increased.

He et al. utilized LIVC so as to control the emissions in a single cylinder research engine [47]. It is claimed in the study that 25 % to 50 % NO<sub>x</sub> decrease can be achieved at different operating conditions with LIVC. Also, LIVC is effective in reducing soot emissions and enables less EGR to be used for constant NO<sub>x</sub> emissions.

Yang and Keller also studied LIVC in a diesel engine system for decreasing the emissions [48]. They used 1-D GT Power model in their study and showed that retarding IVC has the potential to diminish NO<sub>x</sub> emissions by 24 % and to improve bsfc 1 % in comparison to nominal IVC timing. They also noted that their simulation results should be validated with experiments.

Deng and Stobart examined a Caterpillar C6.6 heavy duty diesel engine with variable valve timing [49]. The study investigates the bsfc improvement for different engine speeds and torque. Early and late EVO with constant EVC results in increased bsfc, early and late IVC with constant IVO leads up to 6 % decreased bsfc. Delayed inlet and exhaust valve timings can reduce the bsfc up to 4 % and also changing exhaust valve phasing enables up to 1 % bsfc improvement and altering inlet valve phasing results in 4 % bsfc diminution. No bsfc benefit can be gained when IVO and EVO are both advanced the same angle.

Dembinski investigated the Miller-cycle (EIVC and LIVC) effect on efficiency, emissions and exhaust temperatures on a diesel engine [50]. He found that NO<sub>x</sub> emissions were decreased and brake thermal efficiency of the engine rised for both EIVC and LIVC cases. He also stated that when higher compression ratios are combined with Miller-cycle method on the diesel engine; not only can exhaust temperatures be rised, but also greater brake thermal efficiencies can be achieved.

Tomoda et al. analyzed the effects of VVT and valve lift so as to increase the thermal efficiency of a diesel engine [51]. Using variable phase for both intake and exhaust valves and also variable intake lift, NO<sub>x</sub> emission is decreased more than 40 % and also 4 % fuel consumption reduction is obtained.

Modiyani et al. applied variable intake valve closing timings on a turbocharged multi-cylinder diesel engine and studied the effects of these changings on gas exchange and effective compression ratio (ECR) [52]. They state that ECR is directly

linked to the both early and late IVC timings. ECR goes down for both advanced and retarded IVC timings and so does volumetric efficiency.

Kitabatake et al. tried to decrease fuel consumption and exhaust emissions by utilizing fully flexible variable valve actuation (VVA) [53]. They searched the optimum intake and exhaust valve profiles for different engine performance cases in order to obtain fuel saving and to reduce emissions. They applied cylinder deactivation for lower engine loading cases so as to achieve more fuel saving. They also investigated internal EGR by changing the valve overlap timings as an option to external EGR.

### **1.2.3 VVT effect on the exhaust thermal management of diesel engines**

On the previous section, VVT impact on the performance of diesel engines were investigated. It is observed that VVT is definitely beneficial for diesel engines. It can be utilized to control air intake, fuel consumption, backflow of exhaust gases and also exhaust gas temperatures for aftertreatment systems. On this section, recent studies which particularly examine the methods for more efficient exhaust thermal management systems are explained. Particularly, effect of VVT on thermal management is broadly investigated.

There is an ongoing search for strategies to improve aftertreatment systems. These methods generally include using fuel additive Cerium in combination with an engine control system to raise the exhaust gas temperatures [54], applying different fuel injection timing, boost pressure and EGR rate [55], throttling the air inlet flow at the same time with the fuel flow [56], developing an actively regenerating DPF which uses atomized fuel addition to the upstream of the regeneration to rise exhaust temperature [57, 58], excess fuel injection early and late in the combustion to manage the temperature of a DPF system [59], developing a control-oriented model to particularly examine the effect of post-injection timing and post-injection rate on the temperature dynamics of the exhaust thermal management [60]. One of the current methods to obtain higher exhaust temperatures for more effectual aftertreatment systems is to utilize VVT on diesel engine systems [61]. Recent works focusing on the impact of VVT on aftertreatment management are listed on the following paragraphs below.

Fessler and Genova searched the effect of an electro-hydraulic VVA system on a 3.0 liter diesel engine [62]. It is shown in the study that when different VVA methods are applied together, high exhaust gas temperatures for efficient aftertreatment systems can be achieved at low loads. Particularly, early exhaust valve opening has a considerable impact on exhaust temperatures, however, this method results in fuel penalty.

Bohac and Assanis examined different exhaust valve opening and closing timings on a spark-ignition engine [63]. They primarily applied earlier opening of exhaust valves (by 60° degrees CA) and showed that a significant exhaust temperature rise can be achieved. But HC emissions and fuel consumption rises too. Secondly, earlier EVO is combined with earlier EVC (by 40° CA) and HC emissions decreased by 27%. Yet they conclude that there is a definite fuel consumption penalty to be considered with this method.

De Ojeda studied the impact of VVT on diesel combustion [64]. He pointed out with experiments on a medium duty V8 6.4L diesel engine that earlier closing of intake valve timing results in fuel-saving and also reduction in PM emissions.

Schwoerer et al. explored the effect of different VVA methods on diesel exhaust thermal management systems [61]. It is stated in the study that advanced or retarded closing of intake valve is generally applied for achieving the desired effective compression ratio, advanced opening of exhaust valves is implemented to high exhaust gas temperatures to support aftertreatment systems. Negative valve overlap (NVO) is also an option to obtain internal EGR to obtain sufficient exhaust temperatures to operate exhaust thermal management effectively.

Honardar et al. investigated the effects of different ways (exhaust valve timing phase, main injection variation, post injection variation and throttle valve variation) to improve the exhaust temperature management on emissions, bsfc rise and external EGR requirements on diesel engines [65]. It is asserted in the study that when exhaust valve phasing is advanced, exhaust temperature can be increased up to approximately 40°C, but there is also 11 % bsfc growth in the system.

Wickström studied the use of VVA for improving the thermal management of exhaust gases especially at low load conditions in diesel engines [66]. Different VVT strategies are tested in different engine loads on a single-cylinder research engine.

Loading is kept constant while VVT is implemented. Early and late IVC result in higher exhaust temperatures with lower NO<sub>x</sub> emissions, but greater fuel consumption (up to 11 %). Exhaust and intake valve phase shifts are also rising the exhaust temperature and cause a NO<sub>x</sub> fall of up to 8 g/kWh, however, bsfc growth can go up to 25 g/kWh.

Ehleskog et al. tried to utilize early and late IVC on a heavy duty single cylinder AVL 501 diesel engine so as to drop NO<sub>x</sub> emissions [67]. The variation of IVC timings was applied for cases both with and without using exhaust gas recirculation (EGR). They also searched the effect of different swirl ratios. They found that decreased engine-out emissions can be achieved without fuel consumption rise and higher exhaust gas temperatures via EIVC. LIVC with EGR also led to lower PM emissions with reduced NO<sub>x</sub> emissions without rising the fuel consumption.

Garg et al. investigated the effects of early and late intake valve closing timings (EIVC&LIVC) on exhaust thermal management of a six-cylinder turbocharged&intercooled diesel engine [68, 69]. The engine loading is kept constant in the study and it is shown that turbine exit temperature (TET) can be increased to 250°C (more than 60°C TET rise) for a low loading and low engine speed condition both with EIVC&LIVC timings. It is seen that TET is inversely proportional with the volumetric efficiency for either advanced or retarded IVC timings. It is also demonstrated in the study that EIVC&LIVC result in fuel-saving condition in comparison to nominal IVC timing due to the increase in open-cycle efficiency. However, this method causes to reduction in exhaust flow rate and it decreases the heat transfer from the exhaust flow to the catalyst substrate.

Gehrke et al. tested a single cylinder MAN D20 research engine in order to investigate the potential benefits of VVA on exhaust thermal management [70]. When early IVC is applied, there is up to 60°C exhaust temperature rise. But Particulate Matter (PM) and CO increase in the system and also a slight bsfc growth is seen. Same exhaust temperature rise and emission increase are observed for late IVC too. For the negative valve overlap (crank angle between IVO and EVC) case; although exhaust gas temperature gain can become up to 70°C, bsfc and PM can go up rapidly for the high negative overlap values. Finally, for the earlier EVO, greater bsfc, PM and CO emissions are the penalties so as to raise the exhaust gas temperature more than 60°C.

Roberts et al. searched the effect of early EVO on exhaust temperature and fuel consumption growth for a constant torque operation in a turbocharged, charge cooled, exhaust gas recirculated (EGR) six cylinder Cummins diesel engine [71, 72]. The analysis claims that the method results in lower (max. 5 % decrease) brake thermal efficiency, BTE, (therefore, higher fuel consumption) for low speeds and high loads in order to increase the turbine out temperature. However, for high speeds and low loads, a lower (about 2 % decrease) BTE is required to raise the turbine exit temperature. In the study, 30°C to 100°C exhaust temperature increase is obtained by advancing EVO 90 CA from the nominal position and that proves early EVO as a useful method for exhaust thermal management.

Zammit et al. researched the impact of advanced closing of inlet valve and cylinder disablement on fuel consumption and emissions on a 4 cylinder common rail direct injection diesel engine [73]. In the study, at first, IVC is closed 60° degrees CA earlier than nominal and secondly, two cylinders were disabled when working on nominal IVC timing. These two methods rised the exhaust gas temperature in the system. IVC timing advancement is more effective for degrees more than 30° CA from nominal. At light loads, cylinder disablement is more beneficial than earlier IVC for both reducing emissions and also reaching higher exhaust gas temperatures which enable more effective aftertreatment performance.

Magee used cylinder deactivation (CDA) and late IVC (LIVC) in order to raise the exhaust gas temperature above 250°C for efficient thermal management in a diesel engine for different load cases [74]. It is shown in the study that when CDA and LIVC are applied together, exhaust temperature values at low loads can become higher than 250°C for various operating speeds of the diesel engine. Lower NOx levels are yielded, however, brake thermal efficiency can not be increased significantly in the system.

Zhang et al. also examined the impact of LIVC and rebreathing valve methods on the performance and emissions of a DI diesel engine for 1 to 5 bar gross IMEP engine loading cases [75]. LIVC is compared with extra opening of intake valve during the exhaust process and also extra opening of exhaust valve during the intake process. It is shown that those additional openings during exhaust and intake processes are more effective at increasing the exhaust gas temperature than LIVC for different EGR rates. The same is valid for different engine loadings too. Extra exhaust valve

opening is the most effective method to rise exhaust gas temperatures, decreasing the NO<sub>x</sub> emissions the most in comparison to additional intake valve opening and LIVC.

Ding et al. searched the cylinder deactivation effect on exhaust thermal management at loaded and lightly loaded idle conditions of a six-cylinder turbocharged&intercooled diesel engine [76, 77]. 75 °C turbine out temperature (TOT) rise without fuel consumption rise for lightly loaded idle and 120°C TOT raise with 2 % fuel consumption penalty for loaded idle is achieved with the combination of cylinder deactivation, intake/exhaust valve throttling and LIVC.

Bharath et al. explored the effect of EEVO both with a cam phaser and with a fully flexible variable valvetrain and also cylinder deactivation on a multi-cylinder light duty engine [78, 79]. GT-Power and KIVA programs are utilized for the simulation of the engine. It is stated in the study that EEVO (32° degrees CA earlier than nominal) method enables the adequate exhaust gas temperature increase in the system to achieve more effective DOC where UHC and CO conversion efficiency reaches more than 90 %. However, there is a fuel consumption penalty due to the poorer expansion stroke. Also, they found that cylinder deactivation can be the most preferable option for engine operation conditions close to idle since this method is fuel-saving compared to nominal engine condition.

### **1.3 Purpose of Thesis**

As the recent studies on exhaust thermal management systems are evaluated on previous sections, it can be derived that these works generally concentrate on strategies to increase the engine-out exhaust gas temperatures for improving the conversion efficiency of these aftertreatment systems. However, in these studies, whenever VVT is utilized, either more fuel is required to manage constant engine loading with EEVO or exhaust gas flow rate decreases with early or late IVC. Moreover, valve timings and maximum lifts are not applied in these works in a combined manner. Therefore, the intention in this study is to utilize VVT and also variable inlet and exhaust maximum valve lifts for different engine speeds and engine loading cases so as to rise turbine exit temperature (TET) above 250°C on a turbocharged and intercooled diesel engine without more fuel injection requirement in comparison to nominal valve timings. Early IVC is combined with EEVO to obtain higher than 250°C TETs. Also, effect of variation of maximum valve lifts is

examined. When these valve timing and valve lift combination is implemented together, it seen that same greater than 250°C exhaust gas temperatures can be achieved without fuel consumption penalty and without decreasing the exhaust flow rate compared to the case where only EIVC is used to reach above 250°C exhaust temperatures for low loaded areas of the diesel engine.

The study focuses on the thermal power of the exhaust gases leaving the turbine instead of just concentrating on the increase of the temperature of these gases above 250°C. Temperature of catalyst substrates on aftertreatment systems are generally needed to be greater than 250°C in order to perform high emission conversion efficiencies. This is achieved via the heat transfer from the exhaust gases to the catalyst substrates. However, heat transfer depends on both temperature and exhaust flow rates of these gases. Therefore, obtaining exhaust gases with higher than 250°C temperatures may be insufficient if the method used to provide this results in dramatic exhaust flow rate reductions on the system. This is particularly seen when only IVC is advanced further backward or retarded further forward to reach greater than 250°C temperatures for low loading points. This can obviously be problematic for low loading or cold-start cases of diesel engines. Catalysts can not reach higher efficiencies on time even though the temperature going directly to the exhaust thermal management system is above 250°C. The method used in the study seems to be promising to keep thermal power at higher rates. It can be a solution for these engine loading points by validating it on some specific engine speed and engine loading cases in the future.

The study with the main intention explained above includes six sections. Firstly, specifications of the diesel engine studied are explained and the simulation model built by using Lotus Engine Simulation (LES) program is demonstrated. Steps of LES engine model is given on a graph. Model built for selected turbocharged&intercooled diesel engine are explained with figures from the program. Assumptions taken, the specifications inserted into the program, boundary conditions are all expressed with related figures. Since there are several figures to shown, these graphs are put on the appendice section. Secondly, mathematical formulations utilized in the simulation are expressed. One dimensional flow of gas inside the pipes, combustion model, in-cylinder calculations, heat transfer from the cylinder, friction model of the diesel engine, turbocharger model are all explained in

this part. Thirdly, diesel engine simulation is validated with the experimental results of the same diesel engine for different IVC timings using LES at 1200 rpm engine speed and constant 2.50 bar bmep engine loading. Then TETs at nominal valve timing condition for different engine speeds and engine loadings are calculated and shown in a graph. It is once again seen in the study that low TET is generally a problem for low engine speed and low engine loading cases. Then, different VVT methods are implemented on the system to observe the effects on TET and exhaust flow rate. The best option to raise those two engine performance parameters is found to combine EEVO and EIVC on the system. Although TET is yielded very close to 250°C with this combination, it also results in 1 % bsfc rise in comparison to nominal valva timings. After, inlet and exhaust maximum valve lifts are examined to decrease that fuel injection rise down to zero. EIVC and EEVO combination and low inlet and high exhaust maximum lifts is found to be a promising option for achieving higher thermal power while keeping the fuel consumption fixed in the system. Later, general evaluation of the study is made and finally, the study is concluded and recommendations for the future studies are given on the last section of the study.

## 2. DIESEL ENGINE SPECIFICATIONS AND THE SIMULATION MODEL

On this section of the study, diesel engine used is explained with detailed specifications and also the simulation model of the diesel engine is explained.

### 2.1 Diesel Engine Specifications

The engine used for the study is Cummins type 6 cylinder turbocharged and intercooled diesel engine. The detailed specifications are given on Table 2.1 below. The same engine is utilized in Garg's study for increasing the turbine out temperatures above 250°C for more effective exhaust thermal management [68]. The validation of the simulation via LES will be shown in the fourth section by using the experimental results Garg achieved in his study [68]. These experiments were made for different early and late IVC timings at 1200 rpm engine speed and engine loading is kept constant while closing timings are changed.

**Table 2.1 :** Technical details of the studied Cummins type diesel engine.

<b>No of cylinders</b>	6
<b>Bore (mm)</b>	107
<b>Stroke (mm)</b>	124
<b>Connecting-Rod Length (mm)</b>	192
<b>Displacement (L)</b>	6.7
<b>Compression ratio</b>	17.3
<b>Firing order</b>	1-5-3-6-2-4
<b>Fuel System/Type</b>	Direct Injection / Diesel
<b>Calorific Value of Fuel (kJ/kg)</b>	42700
<b>Intake Method</b>	Turbocharged & Air-Air Intercooled

As shown above on Table 2.1, diesel engine direct-injected, turbocharged and also it has a firing order starting from the first cylinder ending in fourth one. When the simulation model is prepared, these specifications are considered in LES. However, some other required data to construct whole diesel engine simulation is defined

appropriately on the simulation in order to obtain the experimental performance values of the same diesel engine which were achieved by Garg [68].

### 2.2 The Simulation Model

In this study, Lotus Engine Simulation (LES) program is used for the simulation of the studied turbocharged&intercooled diesel engine [80]. The simulation model is shown on Figure 2.1 below.

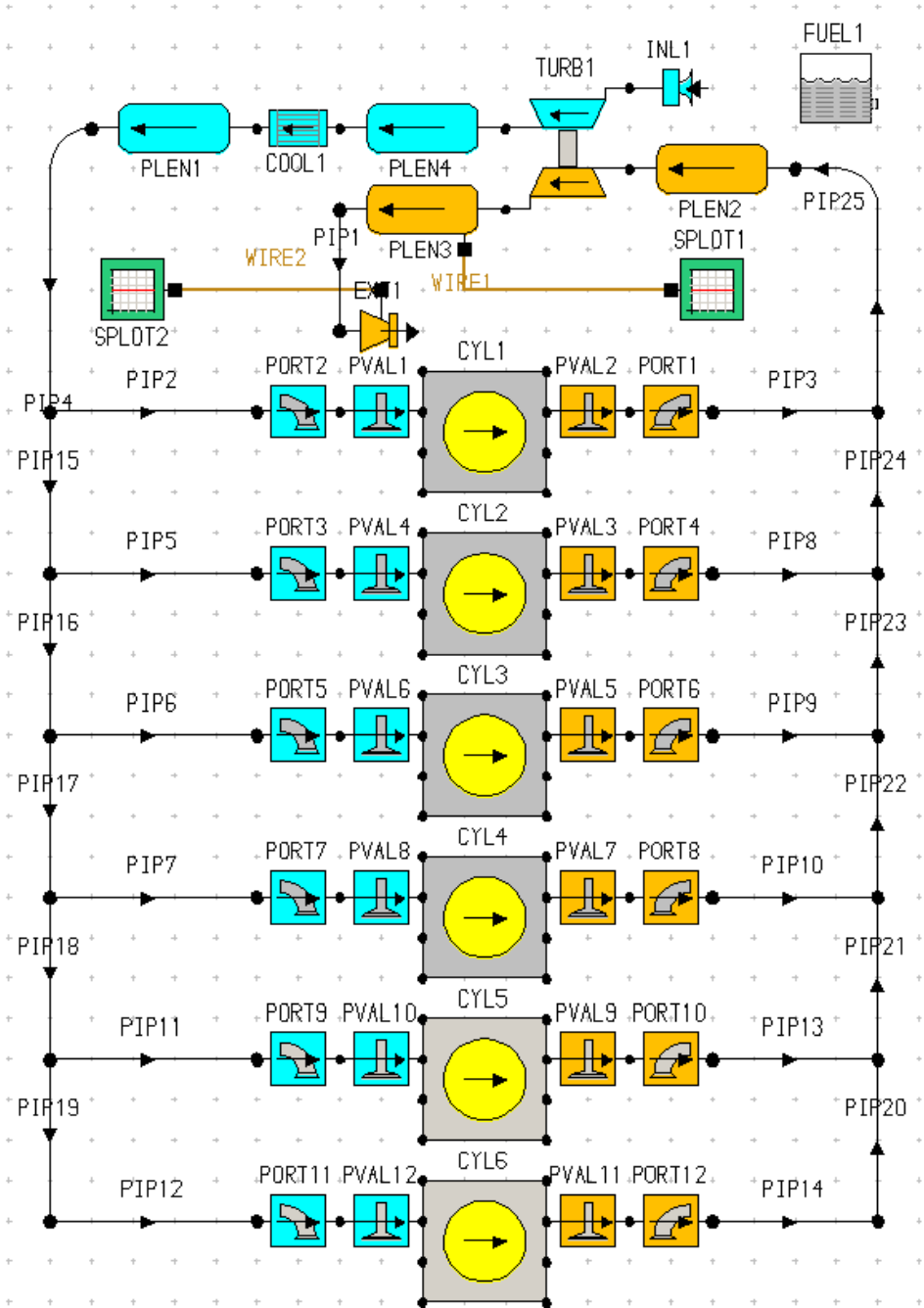


Figure 2.1 : LES model of the diesel engine.

As demonstrated on Figure 2.1 above, every component of the system can be easily seen. Cylinders, valves, ports, intercooler, turbocharger, plenums, sensors (seen on the figure as SPLOT1 and SPLOT2) and also pipes connecting these elements are all individually shown on the figure. Sensor SPLOT 1 is used to measure the exhaust gas temperatures leaving the turbine. These temperatures are intended to increase above 250°C for different engine speeds and various engine loadings in the study. Sensor SPLOT2 is utilized to obtain the exhaust gas flow rates for different engine performance points. Fueling system is pictured separately from the system. As mentioned on Table 2.1 before, it is direct-injected and diesel fuel is utilized in the study.

Exhaust thermal management system is not shown in the system seen above on Figure 2.1. In the study, it is assumed that exhaust gases released from the turbine go directly into the aftertreatment system. The study focuses on the temperature and exhaust gas flow rate of the exhaust gases leaving the turbine which have an important role on the conversion efficiency of the exhaust thermal management. Sensors SPLOT1 and SPLOT2 will be helpful to obtain these two critical data as mentioned previously.

The mathematical formulations for the elements above and for combustion, friction and heat transfer of the diesel engine are explained in a detailed manner in the following section. On this section, it is intended to show the basics of the diesel engine studied and also elements combined on LES to simulate the diesel engine. Intake and exhaust valve timings, valve maximum lifts and change of lifts between opening and closing timings both for intake and exhaust will be expressed on the validation of the model part. The intended VVT application will be implemented to the model after it is validated with the experimental results on Garg's work [68].

### **2.2.1 Steps of LES engine model**

On the following Figure 2.2, the schematical steps of engine model built in LES are shown [81]. As it is seen explicitly, after every step, the program checks the validity of the built engine model or inserted data, specifications. Finally, when the operating conditions are determined to be true, then the simulation is run at the specified engine speed to achieve the demanded engine loading with the fuel injection rate inserted.

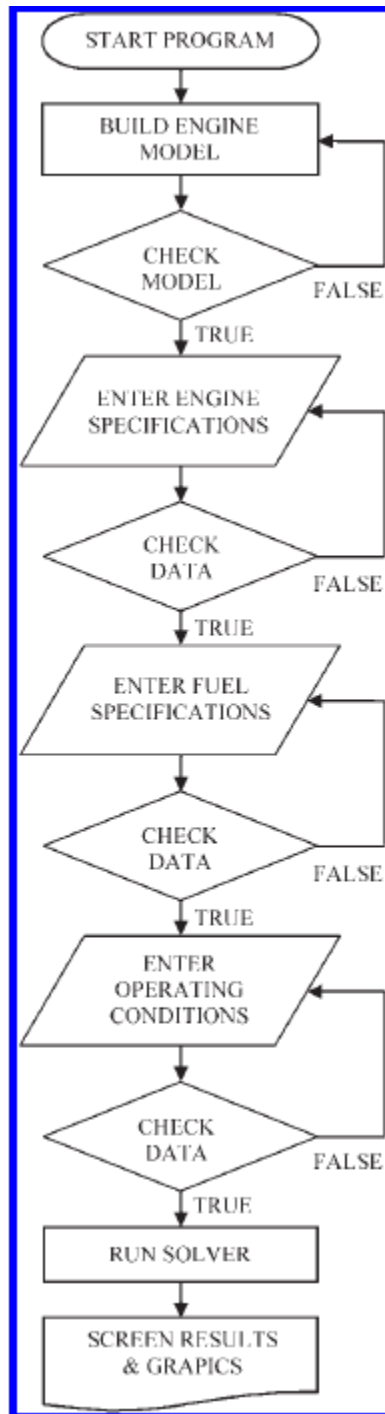


**Figure 2.2 :** The schematical steps of LES engine model [81].

### 2.2.2 LES engine model data insertion

The general specifications of the turbcharged and intercooled six-cylinder diesel engine were given on Table 2.1. Although these technical details are really significant for the simulation, these specs are not sufficient to have a reliable model of the engine. There are other specs to be determined and assumption to be taken in order to run a simulation model on LES.

On this part, only fuelling and boundary conditions figures will be shown below. Other figures related with the program (combustion, friction, heat transfer etc.) are put into the Appendices section on Appendix A. On the following Mathematical Formulations section, the equations used to build these particular elements of the whole model and assumptions taken in those components are explained in a detailed manner.

Figure 2.3 below points out the fuelling injection rate ( $\text{mm}^3/\text{inj}$ ) for different engine speeds changing from 1000 rpm to 2000 rpm at 2.50 bar bmep engine loading condition. As expected, injection rate is increasing as the engine speed rises in the system. Heywood states that combustion efficiency is generally higher than 95 % in diesel engines [82]. Therefore, as shown on the figure, it is taken as 0.98 in order to keep the engine loading constant at 2.50 bar bmep. For other engine loadings (from 1.0 bar bmep to 5.0 bar bmep), this value is not changed. Instead fuelling injection rate is varied to alter the loading of the system on the same speed. Also, injection rate is same for all six cylinders in the system as seen particularly for 1200 rpm on the figure below.

Test Point	Speed (rpm)	Combustion Option	Combustion Efficiency (0-1)	Maldistribution Factor	Fuelling Option	Cylinder Data	Cylinder No.	Trapped Air/Fuel Ratio	Equivalence Ratio	Fuelling Rate ( $\text{mm}^3/\text{inj}$ )
1	1000	Combustion Efficiency	0.9800		Fuelling Rate	Common	All			25,700
2	1100	Combustion Efficiency	0.9800		Fuelling Rate	Common	All			26,300
3	1200	Combustion Efficiency	0.9800		Fuelling Rate	Individual	1			26,950
							2			26,950
							3			26,950
							4			26,950
							5			26,950
							6			26,950
4	1300	Combustion Efficiency	0.9800		Fuelling Rate	Common	All			27,750
5	1400	Combustion Efficiency	0.9800		Fuelling Rate	Common	All			28,500
6	1500	Combustion Efficiency	0.9800		Fuelling Rate	Common	All			29,300
7	1600	Combustion Efficiency	0.9800		Fuelling Rate	Common	All			30,250
8	1700	Combustion Efficiency	0.9800		Fuelling Rate	Common	All			31,250
9	1800	Combustion Efficiency	0.9800		Fuelling Rate	Common	All			32,350
10	1900	Combustion Efficiency	0.9800		Fuelling Rate	Common	All			33,650
11	2000	Combustion Efficiency	0.9800		Fuelling Rate	Common	All			35,100

**Figure 2.3 :** Insertion of fuel injection rate data.

Moreover, boundary conditions assumed on the simulation are demonstrated on the following Figure 2.4. Ambient air pressure and inlet boundary pressure, exit boundary pressure are taken as 1 bar. Ambient air temperature and inlet boundary temperature are assumed 20° C in the system.

Test Point	Speed (rpm)	Humidity Option	Specific Humidity (kg/kg)	Relative Humidity (R-1)	Ambient Air Pressure (bar-abs)	Ambient Air Temperature (C)	Inlet No.	Inlet Boundary Pressure	Inlet Boundary Temperature (C)	Exit No.	Exit Boundary Pressure (bar-abs)	Exit Temp Initialisation
1	1000	Specific Humidity (kg/kg)	0.0130000	0.8745018	1.00000	20.00	1	1.00000	20.00	1	1.00000	Use Cyl 1 at EVO
2	1100	Specific Humidity (kg/kg)	0.0130000	0.8745018	1.00000	20.00	1	1.00000	20.00	1	1.00000	Use Cyl 1 at EVO
3	1200	Specific Humidity (kg/kg)	0.0130000	0.8745018	1.00000	20.00	1	1.00000	20.00	1	1.00000	Use Cyl 1 at EVO
4	1300	Specific Humidity (kg/kg)	0.0130000	0.8745018	1.00000	20.00	1	1.00000	20.00	1	1.00000	Use Cyl 1 at EVO
5	1400	Specific Humidity (kg/kg)	0.0130000	0.8745018	1.00000	20.00	1	1.00000	20.00	1	1.00000	Use Cyl 1 at EVO
6	1500	Specific Humidity (kg/kg)	0.0130000	0.8745018	1.00000	20.00	1	1.00000	20.00	1	1.00000	Use Cyl 1 at EVO
7	1600	Specific Humidity (kg/kg)	0.0130000	0.8745018	1.00000	20.00	1	1.00000	20.00	1	1.00000	Use Cyl 1 at EVO
8	1700	Specific Humidity (kg/kg)	0.0130000	0.8745018	1.00000	20.00	1	1.00000	20.00	1	1.00000	Use Cyl 1 at EVO
9	1800	Specific Humidity (kg/kg)	0.0130000	0.8745018	1.00000	20.00	1	1.00000	20.00	1	1.00000	Use Cyl 1 at EVO
10	1900	Specific Humidity (kg/kg)	0.0130000	0.8745018	1.00000	20.00	1	1.00000	20.00	1	1.00000	Use Cyl 1 at EVO
11	2000	Specific Humidity (kg/kg)	0.0130000	0.8745018	1.00000	20.00	1	1.00000	20.00	1	1.00000	Use Cyl 1 at EVO

Figure 2.4 : Boundary conditions of the simulation model.

### 3. MATHEMATICAL FORMULATIONS

In this section, equations and assumptions behind the theory of the diesel engine simulation are explained. Governing equations of gas flow in pipes, cylinders, heat transfer and combustion modeling, ports, valves, turbocharger, charge cooling and engine dynamics are individually described.

#### 3.1 Governing Equations of Gas Flow

In the diesel engine simulation, one-dimensional model of pipe gas dynamics are applied for the gas flow in pipes. At each time step (crank angle), conservation equations for mass, momentum and energy are solved for calculating the conditions within the pipe elements.

The flow of a compressible fluid through an infinitesimal section of pipe is shown below in Figure 3.1. When the area variation is small, the fluid properties can be taken uniform across any cross-section and can be considered as functions of  $x$  and time only. Therefore, the flow can be assumed as quasi-one-dimensional [83, 84]. The related properties are pressure, density, velocity of flow and cross-sectional area in order.

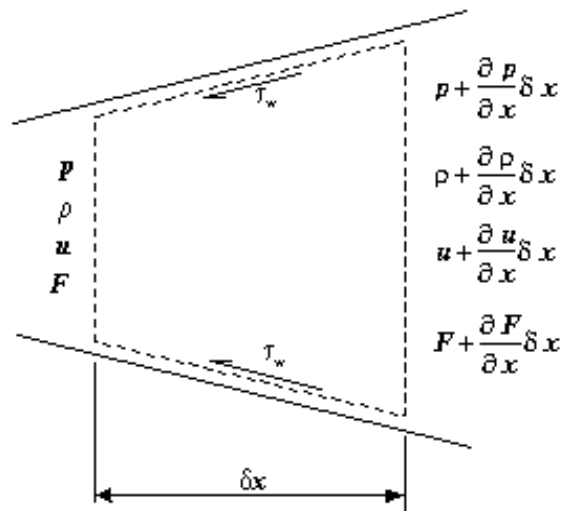


Figure 3.1 : Fluid control volume in duct [83].

The governing equations (continuity, momentum and energy equations in order) for the 1-dimensional flow of a compressible fluid in a pipe with area variation, wall friction and heat transfer are [83]:

$$\frac{\partial(\rho F)}{\partial t} + \frac{\partial(\rho u F)}{\partial x} = 0 \quad (3.1)$$

$$\frac{\partial(\rho u F)}{\partial t} + \frac{\partial(\rho u^2 + p)F}{\partial x} - p \frac{dF}{dx} + \frac{1}{2} \rho u^2 f \pi D = 0 \quad (3.2)$$

$$\frac{\partial(\rho e_0 F)}{\partial t} + \frac{\partial(\rho u h_0 F)}{\partial x} - q \rho F = 0 \quad (3.3)$$

In the equations above  $p$ ,  $f$ ,  $D$ ,  $e_0$ ,  $h_0$  and  $q$  represent pressure, pipe wall friction coefficient, diameter of the duct, specific stagnation internal energy, specific stagnation enthalpy and rate of heat transfer per unit mass. The equations can also be shown in vector form as:

$$\frac{\partial W}{\partial t} + \frac{\partial F(W)}{\partial x} + C = 0 \quad (3.4)$$

where,

$$W = \begin{bmatrix} \rho F \\ \rho u F \\ \rho e_0 F \end{bmatrix} \quad (3.5)$$

$$F(W) = \begin{bmatrix} \rho u F \\ (\rho u^2 + p)F \\ \rho u h_0 F \end{bmatrix} \quad (3.6)$$

$$C = \begin{bmatrix} 0 \\ -p \frac{dF}{dx} \\ 0 \end{bmatrix} + \begin{bmatrix} 0 \\ \rho G f \\ -q \rho F \end{bmatrix} \quad (3.7)$$

This representation of the equations is called the '*conservation law*' form as the equations can be obtained directly from the integral conservation equations of mass, momentum and energy applied to the fixed control volume.

The two-step Lax-Wendroff (Richtmyer) is used to solve the governing equations above. This numerical method is a space-centred scheme based on the computational stencil shown below on Figure 3.2 [84]. The detailed formulations are given below the figure.

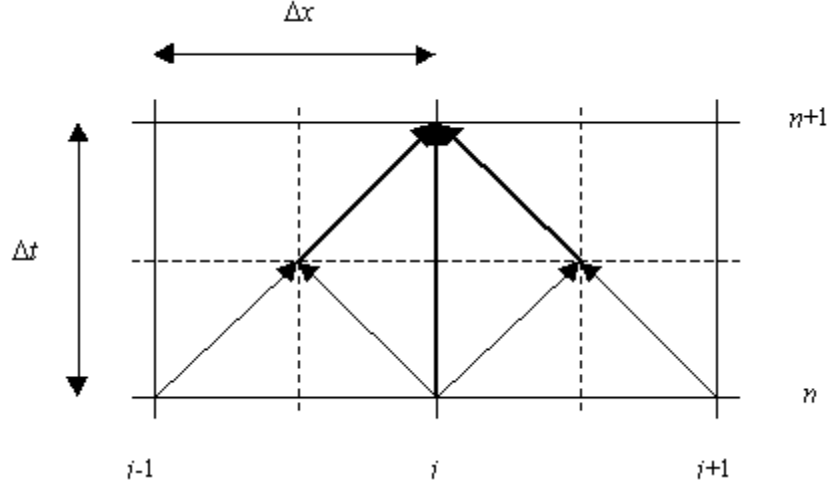


**Figure 3.2 :** Schematic representation of the two-step Lax-Wendroff scheme.

This scheme can be modified to include the source terms and can be expressed with the following formulas:

$$W_{i+1/2}^{n+1/2} = \frac{1}{2}(W_{i+1}^n + W_i^n) - \frac{\Delta t}{2\Delta x}(F_{i+1}^n - F_i^n) - \frac{\Delta t}{4}(C_{i+1}^n + C_i^n) \quad (3.8)$$

$$W_{i-1/2}^{n+1/2} = \frac{1}{2}(W_i^n + W_{i-1}^n) - \frac{\Delta t}{2\Delta x}(F_i^n - F_{i-1}^n) - \frac{\Delta t}{4}(C_i^n + C_{i-1}^n) \quad (3.9)$$

$$W_i^{n+1} = W_i^n - \frac{\Delta t}{\Delta x}(F_{i+1/2}^{n+1/2} - F_{i-1/2}^{n+1/2}) - \frac{\Delta t}{2}(C_{i+1/2}^{n+1/2} + C_{i-1/2}^{n+1/2}) \quad (3.10)$$

### 3.2 Calculation of the Engine Performance Parameters

Diesel engine performance parameters in LES are calculated with the following equations below [82, 85]:

The brake mean effective pressure (bmep) of the diesel engine is found with:

$$bmep = imep_{cycle} - fmep \quad (3.11)$$

Sandoval&Heywood engine friction model [86] is used to obtain friction mean effective pressure (fmep) shown in formula above. This friction model is explained in a detailed manner in the following 3.3 subsection.

The indicated mean effective pressure ( $imep_{cycle}$ ) in equation (3.11) is calculated with:

$$imep_{cycle} = W_c/V_d \quad (3.12)$$

In the equation (3.12) above,  $W_c$  (kJ) represents the net indicated work per cycle and  $V_d$  shows the cylinder displacement volume.

$W_c$  is defined as:

$$W_c = \int p dV \quad (3.13)$$

Displaced volume,  $V_d$ , is obtained with the following equation:

$$V_d = S(\pi B^2/4) \quad (3.14)$$

where  $S$  and  $B$  are the stroke and cylinder bore.

The brake power,  $P_e$  (kW), and torque,  $\tau_e$  (Nm), are calculated with the equations given:

$$P_e = \left( bmep V_d N Z / n_r 60 \right) \quad (3.15)$$

$$\tau_e = \left( 10^3 P_e / \omega \right) \quad (3.16)$$

$N$  is the engine speed (rpm) and  $Z$  is the cylinder number in the equations (3.15) and (3.16) above.

Also,  $n_r$  is the revolution per cycle and is taken as 2 for four stroke engines. Angular speed of the engine,  $\omega$  (rad/s), in equation (3.16) is defined as:

$$\omega = 2\pi N / 60 \quad (3.17)$$

The brake specific fuel consumption, bsfc (g/kWh), is calculated with the following formula below:

$$bsfc = \dot{m}_f / P_e \quad (3.18)$$

$P_e$  is found with the formula (3.15) for (3.18) and  $\dot{m}_f$  shows the fuel mass flow rate (g/h).

The brake thermal efficiency of the system,  $\eta_{th}$ , can be calculated with:

$$\eta_{th} = \frac{3600 P_e}{\dot{m}_f Q_{LHV}} \quad (3.19)$$

where  $Q_{LHV}$  represents lower heating calorific value of fuel (kJ/kg).  $P_e$  and  $\dot{m}_f$  are specified in earlier equations.

Finally, volumetric efficiency is found out with the given equation below:

$$\eta_{vol} = \left( \frac{2\dot{m}_{ia}10^3}{60\rho_{ia}V_dN} \right) \quad (3.20)$$

where  $\dot{m}_{ia}$  is inlet air mass flow rate (g/h) and  $\rho_{ia}$  is inlet air density (kg/m<sup>3</sup>). Inlet air density is calculated with:

$$\rho_{ia} = 10^3 p_{ia} / RT_{ia} \quad (3.21)$$

### 3.3 Calculation of Diesel Engine Friction

The friction model in the simulation depends on the equations from the Sandoval&Heywood engine friction model [86]. It is an updated version of the equations in Patton, Nitschke and Heywood engine friction model [87]. The update by Sandoval&Heywood is that the impact of changing oil viscosity is considered for the redefinition of the friction results. A function of engine oil viscosity is determined and the variation of hydrodynamic friction's share with respect to this function is investigated for each four basic friction parts: rotating, reciprocating, valvetrain and auxiliary friction. The total engine friction is calculated by adding up those four sections. Before explaining these main sections, hydrodynamic scaling is defined as:

$$\mu_{scaling} = \sqrt{\frac{\mu(T)}{\mu_0(T_0)}} \quad (3.22)$$

where  $\mu_0(T_0)$  is the viscosity of the oil from the test engine and  $\mu(T)$  is the viscosity of the engine that the friction calculation is aimed for. The four main friction sections can now be expressed in detailed.

#### 3.3.1 Rotating friction

This friction part has three sections; main bearing seal friction, main bearing hydrodynamic lubrication friction and turbulent dissipation to pump fluids. Total of these three parts gives the definite rotating friction.

Main bearing seal friction (kPa) concerns the front and rear main bearing seal friction and can be calculated with:

$$Seal\ FMEP = 1.22 * 10^5 * \frac{D_b}{B^2 S n_c} \quad (3.23)$$

$D_b$ ,  $B$ ,  $S$  and  $n_c$  represent the main bearing diameter, bore, stroke and the number of cylinders.

Main bearing hydrodynamic lubrication friction (kPa) is found with:

$$Lub\ FMEP = 3.03 * 10^{-4} * \sqrt{\frac{\mu}{\mu_0}} * \left( \frac{RPM * D_b^3 * L_b * n_b}{B^2 S n_c} \right) \quad (3.24)$$

RPM,  $L_b$  and  $n_b$  show engine speed, length of main bearing and number of main bearings.

Turbulent dissipation to pump fluid (kPa) considers the losses owing to the transfer of oil through the bearings and can be calculated with the following equation:

$$Turb\ FMEP = 1.35 * 10^{-10} * \left( \frac{D_b^2 * N^2 * n_b}{n_c} \right) \quad (3.25)$$

Therefore, total rotating friction can be found with:

$$Total\ Rotating\ Friction = (Seal\ FMEP + Lub\ FMEP + Turb\ FMEP) \quad (3.26)$$

### 3.3.2 Reciprocating friction

This part involves also three elements: piston friction under hydrodynamic and mixed friction, piston ring friction due to gas loading and connecting rod hydrodynamic friction values.

The first one, piston friction (kPa) is found with summing the two equations given below:

$$Piston\ FMEP_{hydrodynamic} = 1.05 * 10^3 * \sqrt{\frac{\mu}{\mu_0}} * \left( \frac{S_p}{B} \right)^2 \quad (3.27)$$

$$Piston\ FMEP_{mixed} = 4.06 * 10^4 * \left( 1 + \frac{500}{N} \right) * \left( \frac{1}{B} \right)^2 \quad (3.28)$$

where  $S_p$  and  $B$  values are the mean piston speed and cylinder bore.

The second subsection, Piston ring friction (kPa) involves the friction due to gas loading. Friction owing to gas loading can be obtained with the application of the formula below:

$$Ring\ FMEP_{gas\ loading} = C * 6.89 * \frac{P_i}{P_a} * \left[ 0.088 * \sqrt{\frac{\mu}{\mu_0}} * r_c + 0.182 * r_c^{(1.33 - 0.056 S_p)} \right] \quad (3.29)$$

where  $P_i$ ,  $P_a$  and  $r_c$  are intake and ambient pressures and compression ratio.  $C$  value is the Lotus adjustment coefficient which is derived from the experimental data [85].

Connecting rod friction (kPa) is found out with the formula given below:

$$\text{Con Rod FMEP} = 3.03 * 10^{-4} * \sqrt{\frac{\mu}{\mu_0}} \left( \frac{rpm.D_b^3 L_b n_b}{B^2 S n_c} \right) \quad (3.30)$$

Therefore, total reciprocating friction is the aggregate of the piston, total ring and connecting rod frictions.

### 3.3.3 Valve train friction

This friction component has three main parts. These are camshaft bearing friction, cam and follower friction and finally oscillatory valvetrain friction. The coefficients used in the formulations are chosen from Patton-Heywood friction model [87].

Camshaft bearing friction is defined as:

$$\text{Camshaft FMEP} = 244 * \sqrt{\frac{\mu}{\mu_0}} * \left( \frac{RPM * n_b}{B^2 * S * n_c} \right) \quad (3.31)$$

Cam follower friction can be found by one of the two methods. The method chosen relies on the fact that valve train has flat followers or roller followers.

For flat follower:

$$\text{Cam follower FMEP}_{\text{flat}} = \left[ C_{ff} \left( 1 + \frac{500}{rpm} \right) \frac{n_v}{S n_c} \right] \quad (3.32)$$

$$\text{Cam follower FMEP}_{\text{roller}} = \left[ C_{rf} \left( \frac{rpm * n_v}{S n_c} \right) \right] \quad (3.33)$$

where coefficients  $C_{ff}$  and  $C_{rf}$  are obtained from Patton-Heywood friction model [87].

Valve train oscillatory friction is computed in two sub-sections. These parts are ‘oscillating hydrodynamic friction’ and ‘oscillating mixed lubrication friction’. These two sections are found with:

$$\text{Oscillating hydrodynamic FMEP} = C_{oh} \sqrt{\frac{\mu}{\mu_0}} \left[ \frac{(L_v^{1.5}) * (RPM^{0.5}) * n_v}{(B * S * n_c)} \right] \quad (3.34)$$

$$\text{Oscillating mixed lubrication FMEP} = C_{om} \left( 1 + \frac{500}{RPM} \right) \left[ \frac{L_v * n_v}{(S * n_c)} \right] \quad (3.35)$$

where  $L_v$  is valve lift and  $C_{oh}$  and  $C_{om}$  are oscillating hydrodynamic constants determined by valvetrain type from Patton-Heywood friction model [87].

Therefore, total valvetrain friction is the sum of the camshaft bearing friction, cam follower friction, valve train oscillatory frictions.

### 3.3.4 Auxiliary friction

This is the last friction term and is found by a Lotus altered type of the updated Sandoval&Heywood auxiliary friction formula which depends on a function of engine speed [80]:

$$\text{Aux FMEP} = A * [8.32 + (1.86 * 10^{-3} * RPM) + (7.45 * 10^{-7} * RPM^2)] \quad (3.36)$$

Finally, total engine friction is calculated with the aggregate of the four main parts as follows:

$$\text{TOTAL FMEP} = \text{FMEP}_{\text{rotating}} + \text{FMEP}_{\text{reciprocating}} + \text{FMEP}_{\text{valvetrain}} + \text{FMEP}_{\text{auxiliary}} \quad (3.37)$$

## 3.4 Pipe Wall Friction and Heat Transfer

The pipe wall friction factor,  $f$ , is defined as [83, 84]:

$$f = \frac{\tau_w}{(1/2)\rho u^2} \quad (3.38)$$

In this equation above,  $\tau_w$  represents the shear stress in pipe walls. Generally, pipe wall friction factor is taken as constant in the region where Re number is between 0.004-0.01. However, for Re numbers in the range  $5*10^3 - 10^8$ , a different formula can be used:

$$f = \frac{0.25}{\left[ \log_{10} \left( \frac{k}{3.7D} + \frac{5.74}{Re^{0.9}} \right) \right]^2} \quad (3.39)$$

The heat transfer term,  $q$ , in the governing equations represent the simple convective heat transfer in the radial direction from the gas to the pipe. An approximate approach for convective heat transfer is applied [88]. The assumption is that heat and momentum transfer in steady flow can be extended to non-steady flow. The heat transfer rate per unit mass is:

$$q = \frac{4h}{\rho D} (T_w - T_g) \quad (3.40)$$

where  $h$  is the convective heat transfer coefficient and  $T_w$  and  $T_g$  are the temperatures of the pipe inner wall and gas. If  $h$  is taken as  $\left(\frac{f}{2}\rho u c_p\right)$  and the fluid is assumed to be the ideal gas, then;

$$q = \frac{2fu}{D} \frac{kR}{k-1} (T_w - T_g) \quad (3.41)$$

where  $k$  and  $c_p$  are the ratio of specific heats and specific heat at constant pressure.

### 3.5 In-cylinder Calculations

The conditions within cylinders are calculated at each crank angle by solving the energy equation [88]:

$$\frac{\partial Q}{\partial t} + \frac{\partial B}{\partial t} - \frac{\partial W}{\partial t} = \frac{\partial E}{\partial t} + \sum \delta H \quad (3.42)$$

In the equation above,  $Q$  is the net rate of heat energy transfer into the system,  $B$  is the heat release due to combustion,  $\delta H$  is the enthalpy change due to gas flows.  $W$  and  $E$  represent the displacement work and the internal energy.

Firstly, change in cylinder pressure due to energy and volume changes is estimated:

$$\delta p = p_{cyl} \left( \frac{\delta Q + \delta B + \delta H}{m_{cyl} c_v T_{cyl}} - k \frac{\delta V}{V_{cyl}} \right) \quad (3.43)$$

Then, using  $\delta p$  value, displacement work is estimated and that value is used to estimate the temperature difference:

$$\delta W = \delta V (p_{cyl} + 0.5 \delta p) \quad (3.44)$$

$$\delta T = \frac{\delta Q + \delta B - \delta W}{c_v} \quad (3.45)$$

New temperature and pressure values in the system are calculated as:

$$T_{new} = T_{cyl} + \delta T \quad (3.46)$$

$$p_{new} = \frac{m_{cyl} R_{cyl} T_{new}}{V_{new}} \quad (3.47)$$

As there is a new  $\delta p$  value (difference between  $p_{new}$  and  $p_{cyl}$  values), displacement work can be recalculated given the formula (3.44) above. Also, heat transfer is

calculated dependent on mean gas temperature during increment. Therefore, energy change due to this temperature difference is found with using formula (3.42) as:

$$\frac{\partial E}{\partial t} = \frac{\partial Q}{\partial t} + \frac{\partial B}{\partial t} - \frac{\partial W}{\partial t} - \sum \delta H \quad (3.48)$$

Internal energy change in the cylinder can also be calculated with:

$$\delta E_2 = E_{new} - E_{cyl} \quad (3.49)$$

The error in temperature due to the mismatch between these two formulations above is:

$$\delta T = \frac{E_1 - E_2}{c_v} \quad (3.50)$$

If temperature difference,  $dT$ , is above 0.01 K value; calculations are redone. When convergence is achieved, all the values withing the cylinder are calculated for the final case.

The gas property model is based on polynomial curve fits to the thermodynamic data for each species ( $H_2$ ,  $O_2$ ,  $N_2$ ,  $H_2O$ ,  $CO_2$ ,  $NO$ ,  $C_{12}H_{26}$ ). For each species  $i$  at temperature  $T$ , the enthalpy ( $h$ ) and the internal energy ( $u$ ) are given by:

$$h = C(1, i) + C(2, i)T + C(3, i)T^2 + C(4, i)T^3 + C(5, i)T^4 + C(6, i)T^5 \quad (3.51)$$

$$u = C(1, i) + (C(2, i) - 8.3143)T + C(3, i)T^2 + C(4, i)T^3 + C(5, i)T^4 + C(6, i)T^5 \quad (3.52)$$

The specific enthalpy and internal energy values are calculated by multiplying the equations above with the mass fraction for the related species. The constants for the polynomials are obtained from Heywood [82].

### 3.6 Combustion System

A single zone heat release model is applied to the system. Therefore, the heat released is used to heat the whole combustion space during combustion. The empirical heat release functions are derived from the Wiebe equation and adapted to diesel combustion characteristics by the addition of a pre-mixed combustion phase [89].

The Wiebe function define the mass fraction burned as:

$$m_{frac} = 1.0 - \exp^{-A\left(\frac{\theta}{\theta_b}\right)^{M+1}} \quad (3.53)$$

in which, A and M are coefficients in Wiebe equation.  $\theta$  is actual burn angle (after start of combustion),  $\theta_b$  is the total burn angle (0-100% burn duration) [89].

In two-part Wiebe equation, total combustion period includes two periods: premixed combustion period and diffusion combustion period. The mass fraction burned in the premixed combustion is given as:

$$m_{frac,premixed} = 1.0 - \left[1 - \left(\frac{\theta}{\theta_b}\right)^{C_1}\right]^{C_2} \quad (3.54)$$

and for diffusion combustion period, it is:

$$m_{frac,diffusion} = 1.0 - \exp^{-A\left(\frac{\theta-\Delta}{\theta_b-\Delta}\right)^{M+1}} \quad (3.55)$$

Finally, mass fraction value is calculated with the following formula for two-part Wiebe:

$$m_{frac} = \beta[Pre - mixed] + (1 - \beta)[Diffusion] \quad (3.56)$$

In the equations above,  $C_1$  and  $C_2$  are coefficients in Watson&Pille equation.  $\beta$  and  $\Delta$  are the fraction of premixed combustion to total combustion and delay angle between premixed and diffusion combustion values. In the study, these coefficients are taken as  $A=6.0$ ,  $M=0.1$ ,  $C_1 = 2.5$ ,  $C_2 = 2500$ ,  $\beta=0.05$  and  $\Delta=0.0$  in order to replicate the experimental results of the turbocharged&intercooled DI diesel engine.

Combustion duration is defined as the number of crank degrees before or after TDC at which combustion starts. In this study, it is taken as 3 degrees CA after TDC. The combustion period can be calculated with the following formula which is obtained from experiments by Lotus [80].

$$0 - 100\% (degree) = 30.0 + \left(\frac{50.0}{Trapped\ AFR*0.06691*0.7}\right) \quad (3.57)$$

where AFR represents the air-fuel ratio of the gas mixture inside the cylinder. An exemplary combustion period is shown on Figure 3.3 where SOC shows start of combustion, A50% represents the 50 % mass fraction burned CA and EOB states the end of burning. [80].

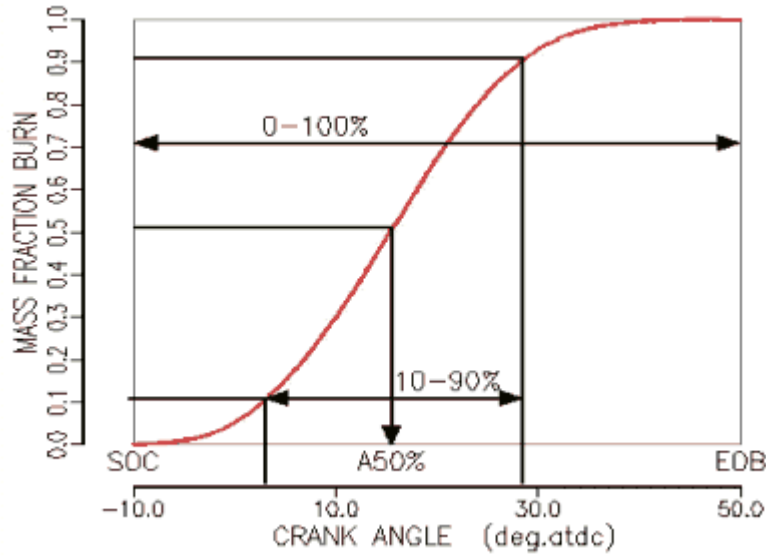


**Figure 3.3** : An exemplary mass fraction burn variation during combustion period [80].

### 3.7 Cylinder Heat Transfer

In LES, heat transfer can be modelled with different heat transfer formulations such as Annand, Woschni and Eichelberg [80]. Annand heat transfer model is chosen in the simulation for the cylinders. This is because when studies using LES as engine modelling are examined, Annand heat transfer model is generally preferred in order to calculate the heat transfer from cylinders [81,90,91].

The connective heat transfer model defined by Annand can be stated as [92]:

$$\frac{hD_{cyl}}{k} = ARe^B \quad (3.58)$$

In (3.58);  $h$  is heat transfer coefficient ( $W/m^2K$ ),  $k$  is thermal conductivity of gas in the cylinder ( $W/mK$ ),  $D_{cyl}$  is cylinder bore,  $Re$  is Reynolds number and  $A$  and  $B$  are Annand open or closed cycle coefficients which are taken for open cycle as 1.1 and 0.7 and for closed cycle as 0.15 and 0.8. The heat transfer per unit cylinder area can be calculated with:

$$\frac{dQ}{A} = h(T_{gas} - T_{wall}) + C(T_{gas}^4 - T_{wall}^4) \quad (3.59)$$

where  $A$  is area,  $T$  is temperature and  $C$  is Annand closed cycle coefficient, taken as  $4.29 \times 10^{-9}$ .

### 3.8 Charge Cooler

Charge coolers are used for removing heat from the gas in the engine simulation model. Pressure loss, coolant temperature and effectiveness verses mass flow rate data constitute the main characteristics of the charge cooler. In the simulation, the mass flow in the charge cooler is calculated for the instantaneous pressure drop. The same procedure is also true for coolant temperature and effectiveness data [80].

The charge cooler effectiveness is described as:

$$\varepsilon = \frac{T_{charge,in} - T_{charge,out}}{T_{charge,in} - T_{coolant,in}} \quad (3.60)$$

where  $T_{charge,in}$  and  $T_{charge,out}$  represent charge cooling inlet and outlet temperatures,  $T_{coolant,in}$  shows the cooling inlet temperature.

### 3.9 Cylinder Scavenging

The cylinder scavenging operates charge gas mixing with the gas already in the cylinder before the cylinder gas is removed from the cylinder. Perfect mixing model is used in the simulation.

The assumption in this model is that any charge gas entering the cylinder is instantaneously, homogeneously mixed with the gas currently in the cylinder. Thus the subsequent transfer of gas to the exhaust will cause some of the charge gas to be removed from the cylinder [93].

The scavenging terms in the simulation are:

$$\eta_{scav} = \frac{m_{air}}{m_{air} + m_{resid}} \quad (3.61)$$

$$\Lambda = \frac{m_{air\ supplied}}{m_{air} + m_{resid}} \quad (3.62)$$

$$\eta_{ch} = \frac{m_{air}}{(m_{bdc})_{ref}} \quad (3.63)$$

$$\eta_{trap} = \frac{m_{air}}{m_{air\ supplied}} \quad (3.64)$$

These equations above represent scavenging efficiency, scavenging ratio, charging efficiency and trapping efficiency consecutively.

### 3.10 Flow Through Valves and Ports

A simple one-dimensional model for flow through a valve or port using the analogy of an orifice, having an equivalent flow area (an area that produces the same flow rate under the same upstream and downstream pressures) is used. Applying the energy equation from upstream to the valve throat for isentropic steady flow, and assuming that the inlet velocity is negligible, gives [94]:

$$\frac{dm}{dt} = A_2 P_1 \sqrt{\left\{ \left( \frac{2k}{k-1} \right) \frac{1}{RT_1} \left[ \left( \frac{P_2}{P_1} \right)^{2/k} - \left( \frac{P_2}{P_1} \right)^{(k+1)/k} \right] \right\}} \quad (3.65)$$

This mass flow equation may seem working well in theory. But in practice, secondary flow effects, boundary layer separation, friction, etc. leads to the mass flow rate being less than that calculated from equation (3.65) above. A discharge coefficient is used for this practical difficulty. Therefore, it is rewritten as:

$$\frac{dm}{dt} = C_d A_2 P_1 \sqrt{\left\{ \left( \frac{2k}{k-1} \right) \frac{1}{RT_1} \left[ \left( \frac{P_2}{P_1} \right)^{2/k} - \left( \frac{P_2}{P_1} \right)^{(k+1)/k} \right] \right\}} \quad (3.66)$$

The value of the discharge coefficient ( $C_d$ ) or effective area ( $A_2$ ) is established from steady flow tests at varying valve lifts and pressure ratios. It is shown in Figure 3.4 below that the effective area ( $C_d A_2$ ) is a function of valve lift and pressure ratio. The effect of the pressure ratio is small when compared to the valve lift [94].

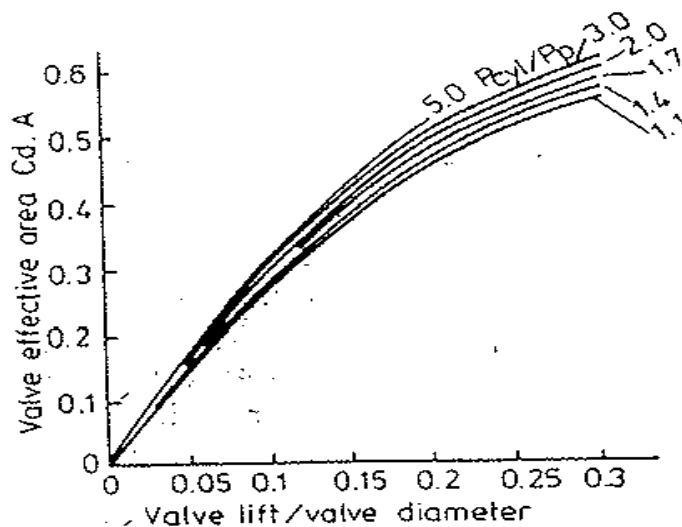
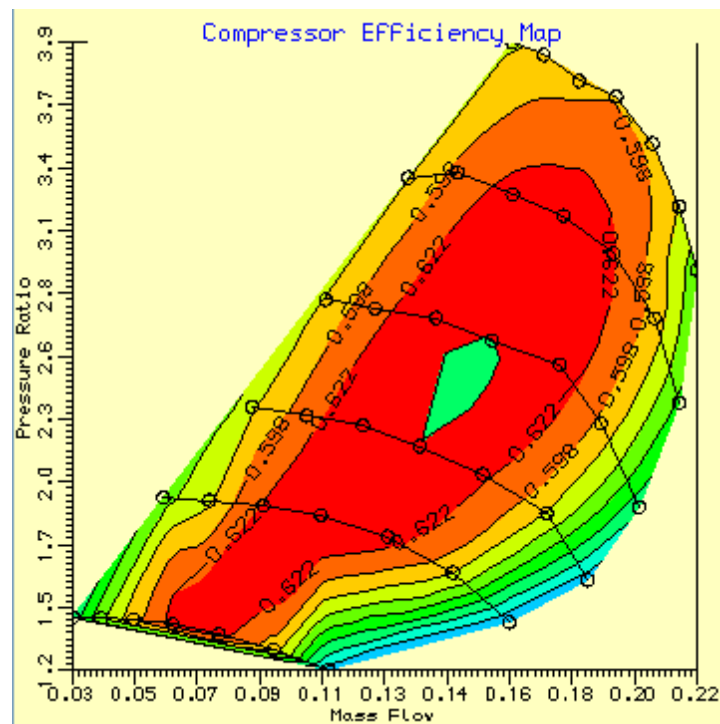


Figure 3.4 : Effective area variation with valve lift [94].

### 3.11 Turbocharger

Turbocharger is modelled as compressors and turbines on a common free spinning (or compounded) shaft. The non-dimensionalised characteristic maps of compressor and turbine are used to obtain the instantaneous performance of these elements. For a given engine application; mass flow, pressure ratio, speed and efficiency scaling factors are used to state a particular compressor/turbine map. The accurate simulation of free spinning turbochargers demands that the simulation converge on a shaft speed that provides an exact work balance between compressors and turbines.

Compressor maps must be defined as a series of constant speed lines defining mass flow, pressure ratio and efficiency. Compressor map used in the simulation is seen below in Figure 3.5 [80].



**Figure 3.5 :** Compressor efficiency map [80].

At each crank angle increment; the mass flow rate and efficiency of the compressor are calculated from the current corrected shaft speed and the instantaneous pressure ratio across the device. The calculation procedure is to interpolate a constant speed line from the map data. (see above). From this line the mass flow and efficiency defined by the current pressure ratio are interpolated.



#### 4. VVT APPLICATION ON THE SYSTEM

Diesel engine specifications were given with details on the second section of the study. Also, simulation of the diesel engine with LES was demonstrated with detailed elements. On this section, the proposed VVT application on the system will be implemented to achieve higher than 250°C exhaust gas temperatures. However, at first, the simulation model must be validated with experimental results in order to utilize a reliable model while using VVT. Then, the intended VVT method can be applied to the system.

##### 4.1 Validation of the Model

The simulated diesel engine was also studied by Garg [68]. That was mentioned before on section 2. The engine speed was 1200 rpm and engine loading was taken as 2.50 bar in that study. The same is valid in this study too.

The experimental results taken from [68] for volumetric efficiency and turbine exit temperature (TET) are shown on Table 4.1 below. These experimental data for the diesel engine at 1200 rpm engine speed and at 2.50 bar engine loading is used for the validation of the simulation model.

**Table 4.1** : Experimental data for different IVC timings at 2.50 bar engine loading.

IVC Timing (CA)	Volumetric Efficiency (%)	TET (°C)
-65	63,00	254,5
-50	72,30	232,0
-40	78,00	220,5
-20	88,50	206,5
0	93,60	198,0
20	94,50	195,0
50	89,60	203,0
70	82,30	217,0
90	74,20	235,0
100	69,30	249,0

As seen on Table 4.1 above, volumetric efficiency and TET values vary when IVC timings is closed earlier or later than its nominal timing. 0 CA denotes the nominal IVC timing above. Negative numbers show the advanced and positive ones demonstrate the retarded closing timing of the intake valve. The aim of the simulation will be to calculate these engine performance values as close as those experimental data above.

Also, nominal intake and exhaust opening&closing timings, inlet and exhaust maximum valve lifts are listed on Table 4.2 below. Only intake valve closing timing is altered, other opening and closings timings and valve lifts are kept constant for the validation.

**Table 4.2 :** Nominal valve timings and maximum valve lifts.

<b>Intake Valve Opening (CA)</b>	20 CA BTDC
<b>Intake Valve Closing (CA)</b>	25 CA ABDC
<b>Exhaust Valve Opening (CA)</b>	20 CA BBDC
<b>Exhaust Valve Closing (CA)</b>	20 CA ATDC
<b>Inlet Maximum Valve Lift (mm)</b>	8.50
<b>Exhaust Maximum Valve Lift (mm)</b>	9.90

As it is shown on Table 4.2 above, intake valve opens 20 Crank Angle (CA) before top dead center (BTDC) and closes 25 CA after bottom dead center (ABDC). Opening timing of the exhaust valve is 20 CA before bottom dead center (BBDC) and closing timing is 20 CA after top dead center (ATDC). Valve lifts given above are fixed in the validation.

The simulation model was shown previously in the second part of the study on Figure 2.1. The specifications given on Table 2.1 are used in the simulation in order to simulate the diesel engine at 1200 rpm and 2.50 bar engine loading. However, some other required data is defined appropriately on the simulation in order to obtain the experimental results seen on Table 4.1. Some of the engine parameters assumed are explained on the previous mathematical formulations part's subsections.

It is easy to define opening and closing timings on the simulation. Nominal intake and exhaust timings are shown on Figure 4.1 below.

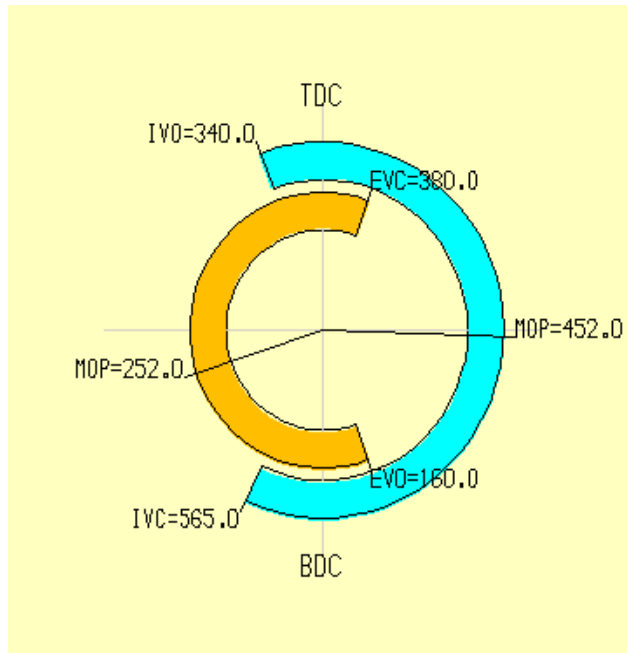


**Figure 4.1 :** Nominal intake & exhaust valve timings on the simulation.

On Figure 4.1, the blue part shows the intake valve timing interval, the yellow part demonstrates the CA interval between opening and closing timings of exhaust. MOP on the figure points out the maximum opening point (CA degree after opening for both intake and exhaust). As mentioned on Table 4.2, MOP goes to 8.5 mm valve lift for intake and 9.9 mm valve lift for exhaust.

Also, there is a firing-order which is mentioned before on Table 2.1. It starts with no 1 cylinder and ends with no 4. This can be explicitly seen on Figure 4.2 below.

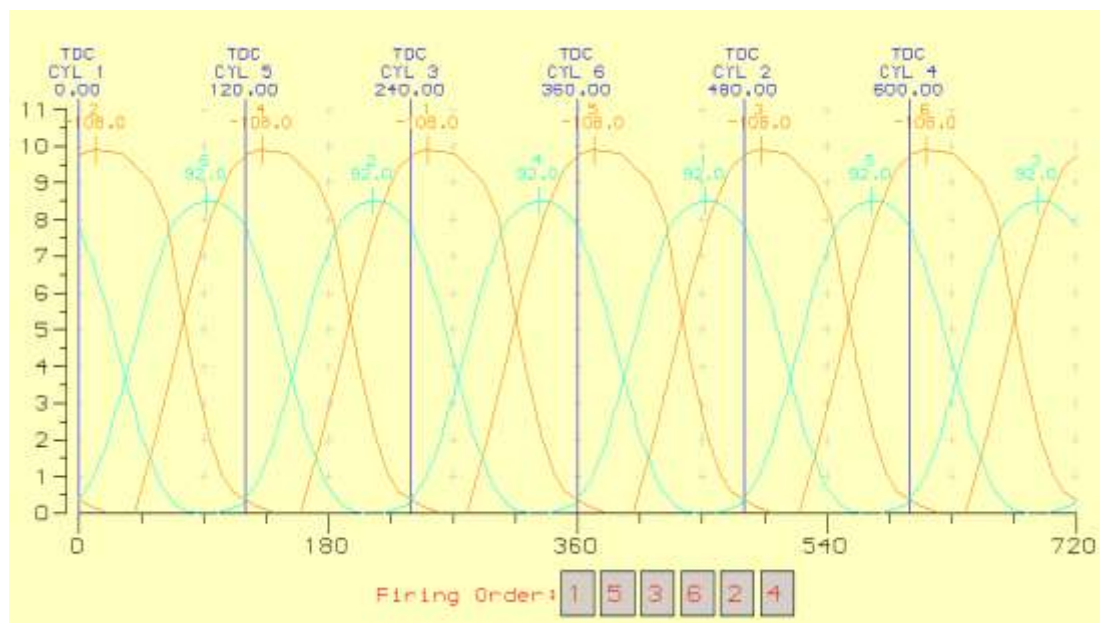


**Figure 4.2 :** Cylinder phase and valve event display of the diesel engine.

As there are six cylinders and one cycle in diesel engines takes 720 CA, there is 120 CA degrees phase between cylinders. All cylinders have the same valve timings and lifts specified on Figure 4.1. This is also seen on Figure 4.2 too.

The nominal IVC timing is 25 CA ABDC. The first intention is to alter this timing forward and backward and to observe the effect on TET and volumetric efficiency. The experimental results on Table 4.1 are yielded via changing IVC timings as shown on Figure 4.3 below.

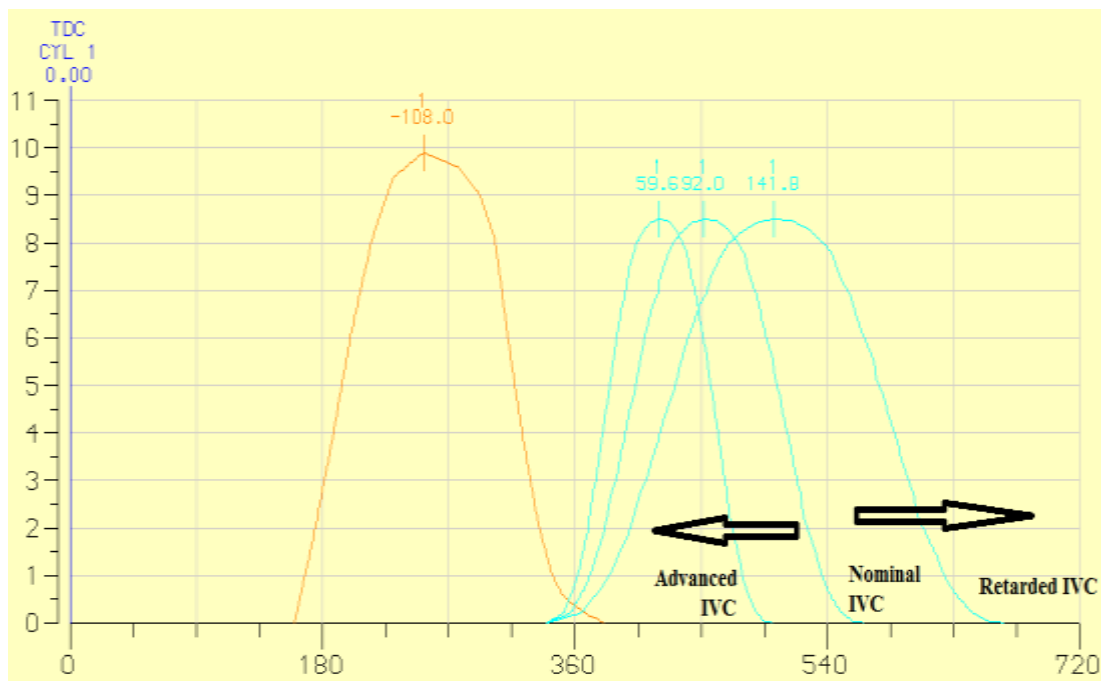


**Figure 4.3 :** Advanced and retarded IVC timings.

The changing on IVC timing is shown for cylinder no 1 on Figure 4.3 above. This is indeed valid for all other 5 cylinders in the system too. While changing IVC timings, especially for advanced IVC timings, valve lift values get higher and higher at TDC. This high lifts at TDC can result in piston-valve crash for very high intake valve lift values at this point. In Garg's study, the distance between valve lift and piston is shown as 1 mm at TDC [68]. Therefore, the same restriction is binding in this study too. VVT is applied to the system under this limitation so as to prevent a piston-valve crash.

While changing the closing timings of intake, engine loading which is taken as bmep is managed constant at 2.50 bar in order to compare the effect of variable IVC on a fixed loaded engine. Therefore, fuel injection rate is altered for every specific IVC timing so as to hold engine loading constant. Only nominal IVC (25 CA ABDC) is

closed later or earlier when all other valve timings and maximum valve lifts are kept constant.

By using the engine specifications on Table 2.1, assumptions and mathematical expressions stated on previous section, the validation graphs of the simulation are yielded for TET on Figure 4.4 and for volumetric efficiency on Figure 4.5.

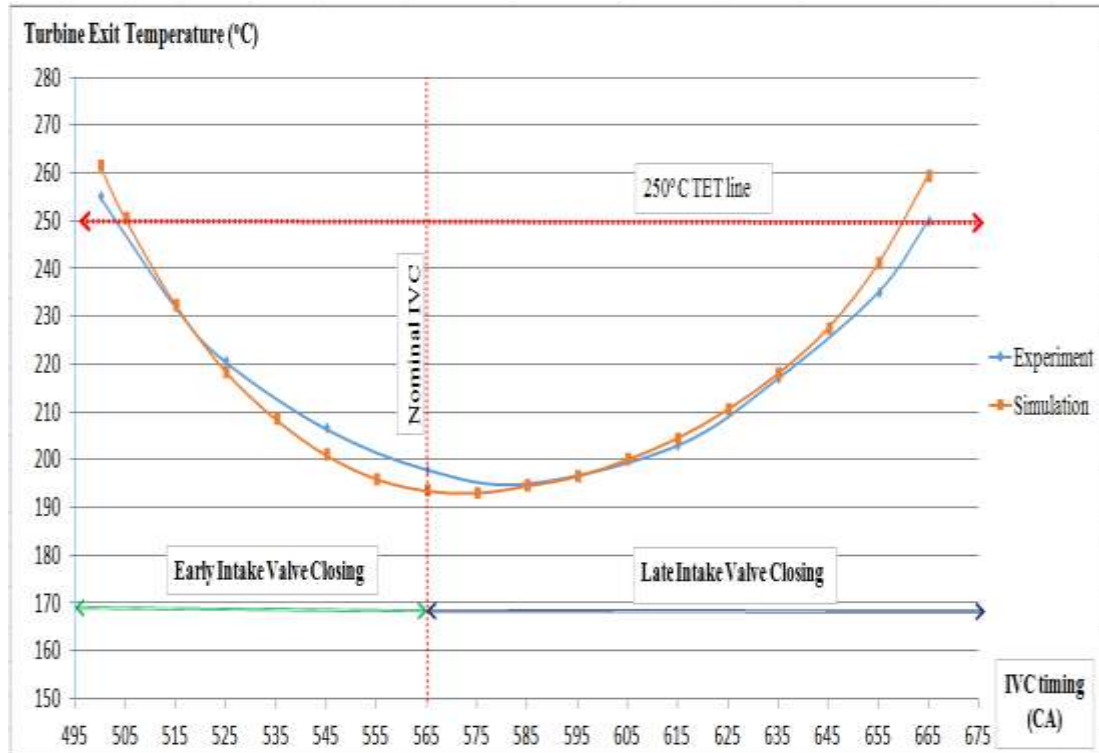


**Figure 4.4 :** Turbine exit temperature comparison between simulation&experiment.

As it is shown from Figure 4.4 above, simulated and experimental TET values are compared. It is seen that the calculated results are generally compatible with the experimental TET data. As seen, changing IVC timing is very useful for rising TET from 195 °C nominal value to higher than 250°C which is determined as a limit temperature for more effective exhaust thermal management. Early and late IVC are both beneficial. Advancing IVC timing 65 CA (40 CA BBDC) from the nominal value can result in 60°C TET increase at 1200 rpm and 2.50 bar bmep. However, for the same TET rise, IVC timing must be retarded 100 CA (125 CA ABDC) from the nominal closing timing. Therefore, earlier closing affects faster than later closing. However, sweeping closing timing in both ways has the similar effect on exhaust gases leaving the turbine. It can be derived that variation of closing timing has positive effect on TET. It is particularly important for a low loading point (2.50 bar

bme<sub>p</sub>), since nominal exhaust temperature is 195°C for this point and it is much lower than 250°C.

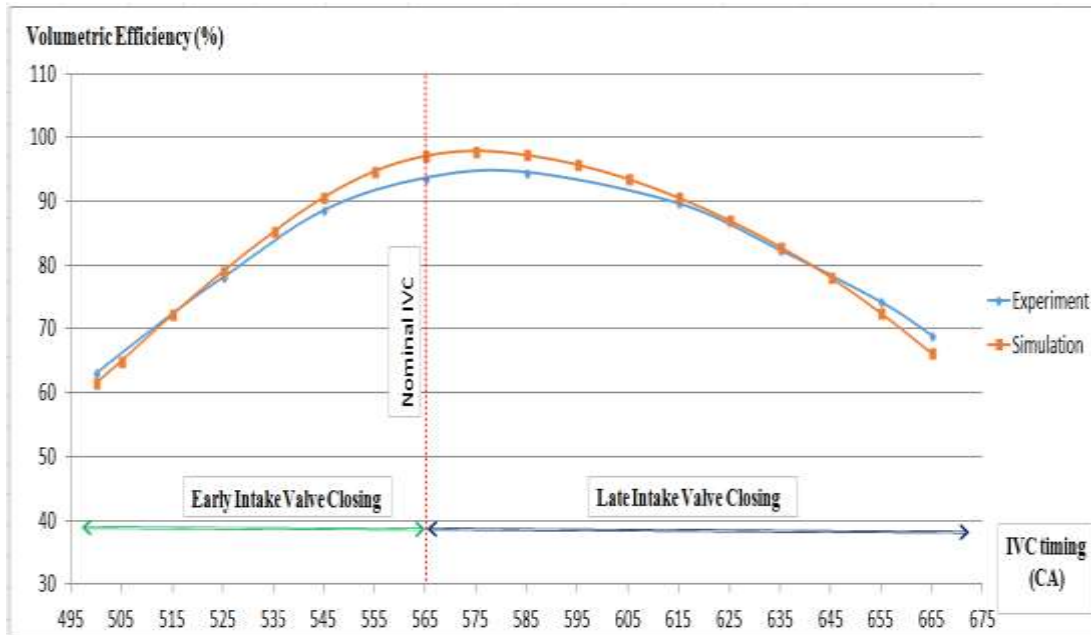


**Figure 4.5 :** Volumetric efficiency comparison between simulation&experiment.

Effect of changing IVC timing on volumetric efficiency is demonstrated on Figure 4.5 above. The simulation results are relatively close to experimental results as achieved on TET. As seen from the experimental and simulation results, volumetric efficiency decreases in both directions in comparison to nominal IVC timing. Earlier and later closing timings affect volumetric efficiency negatively. It drops sharply with EIVC and sufficient retardation of IVC causes the same volumetric efficiency reduction in the system. EIVC shortens the air inlet time and LIVC pushes some of the air out of the cylinder by extending the intake valve duration.

It is important to notice that although advanced and retarded IVC lead to dramatic reductions of volumetric efficiency, it also enables the system to achieve greater than 250°C exhaust temperatures going directly to the aftertreatment systems. It can be stated that whenever the volumetric efficiency goes down, TET gets higher than nominal timing. For the same engine loading case, it is obvious that TET is inversely proportional with the volumetric efficiency. This is valid when IVC is swept either earlier or later than the stock valve timing.

It can also be derived that simulation model has promising results with VVT. The results are not far-fetched from the experimental results for both TET and volumetric

efficiency. It can be asserted that the simulation model is reliable and can be used to predict the TET values for different engine speed and engine loading cases.

#### 4.2 Examining the Effect of IVC on Diesel Engine Performance

As explained on the previous subsection that earlier and later IVC timing is definitely practical for reaching higher than 250°C TET and hence more efficient exhaust thermal management. However, as seen on Figure 4.5 volumetric efficiency is decreasing dramatically for both EIVC and LIVC cases. It goes down less than 70 % with LIVC and even lower than 65 % with EIVC. The same reduction effect is also seen on trapped air to fuel ratio (AFR) on the system as shown on Figure 4.6 below.

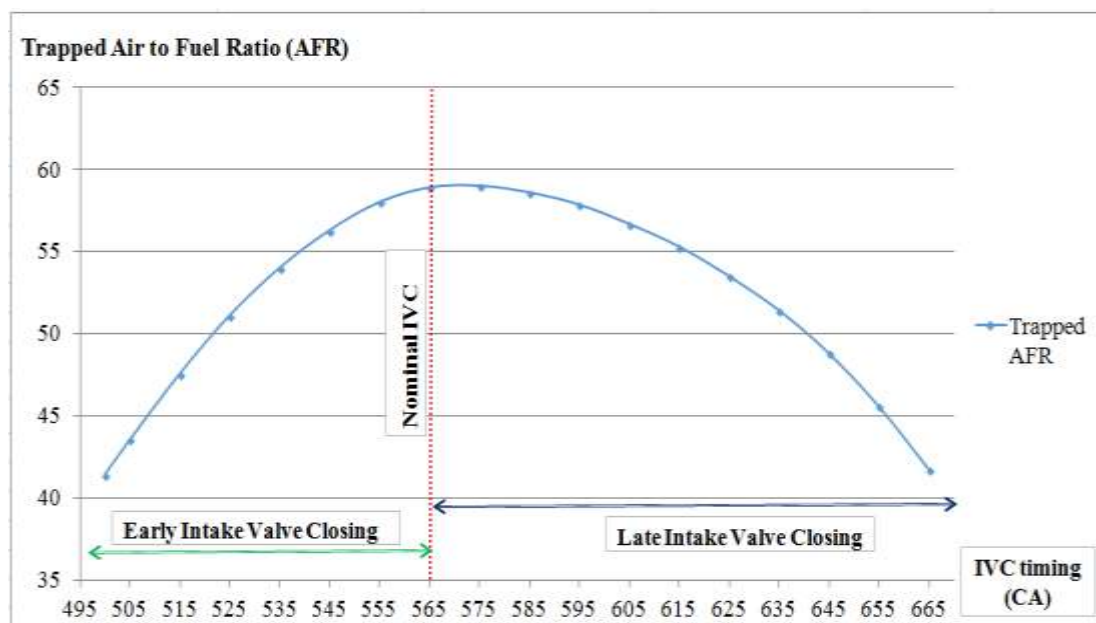


**Figure 4.6 :** Trapped AFR change along EIVC and LIVC.

The decrease in AFR also stems from the reduction of volumetric efficiency along EIVC and LIVC. Less air is inducted into the system compared to nominal case and only fuel injection rates are adjusted for different IVC timings to keep engine loading constant at 2.50 bar bmep.

It can be deduced that those extra air close to nominal IVC timing causes a decrease on TET. As the closing timing is advanced or retarded, volumetric efficiency decreases and lower air is used to achieve same engine loading and TET increases. TET is reciprocally proportional with the volumetric efficiency. The lower the volumetric efficiency is, the higher the TET becomes. Effect of IVC timing on other engine performance parameters are examined below.

### 4.2.1 Exhaust flow rate

Volumetric efficiency has a critical role for obtaining higher exhaust gas temperatures and enables exhaust thermal management systems to perform more effectively. As explained on the previous section, having lower volumetric efficiency at constant engine loading via sweeping IVC timings causes an abrupt rise on TET. However, it also has a negative effect. It leads to reduction on exhaust flow rate shown on Figure 4.7 below.

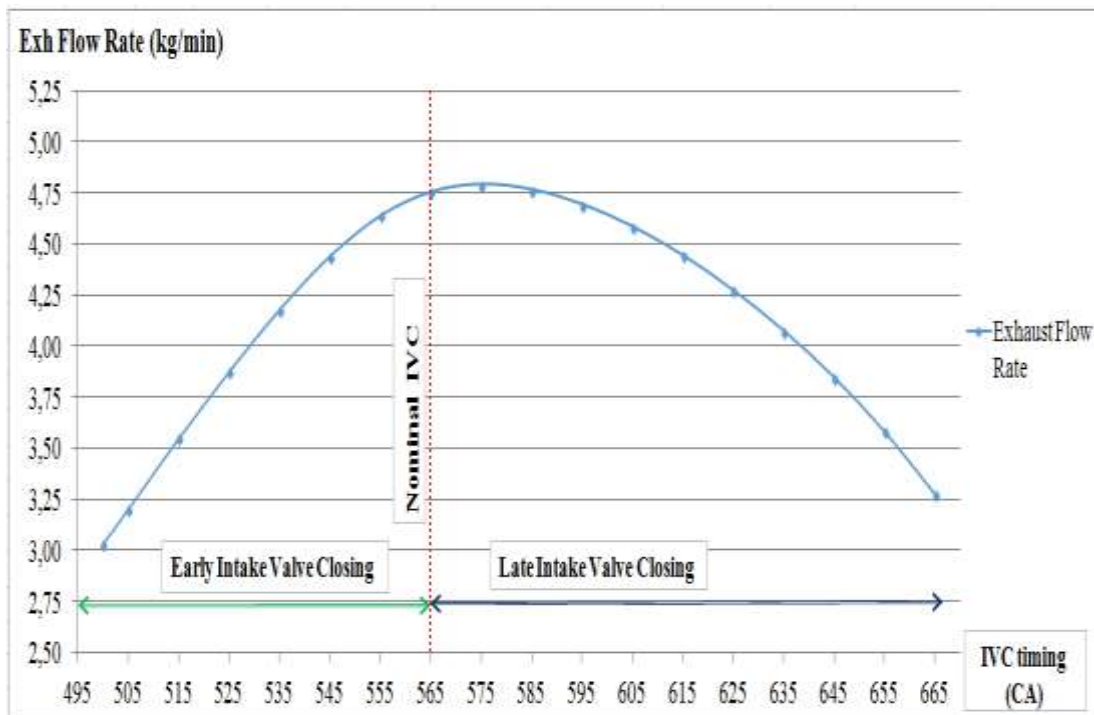


**Figure 4.7 :** Exhaust flow rate change with different IVC timings.

There is no doubt that increasing TET greater than 250°C is significant for more effectual aftertreatment systems. This is definitely necessary in order to achieve catalyst temperatures higher than 250°C on exhaust thermal management systems. But, decreased exhaust flow rate reduces the catalyst temperature change rate. This is because heat transfer to the catalyst substrates does not only rely on exhaust gas temperatures, but also exhaust gas flow rates. Therefore, diminishing exhaust flow rate decreases the heat transfer rate from the exhaust gases leaving turbine to the catalyst substrates on thermal management systems. As explained on the purpose of the study part, in this study, the search is to find out appropriate VVT on the diesel engine system to both reach higher than 250°C exhaust temperatures, but also to achieve this without a dramatic exhaust flow rate reduction on the system.

## 4.2.2 Fuel injection rate

Although this method results in decrease in exhaust flow which is significant for the heat transfer from exhaust gases to the catalyst substrate, it also has another positive effect. As demonstrated on Figure 4.8 below, fuel injection rate goes lower than the nominal injection rate for either EIVC or LIVC for constant engine loading cases.

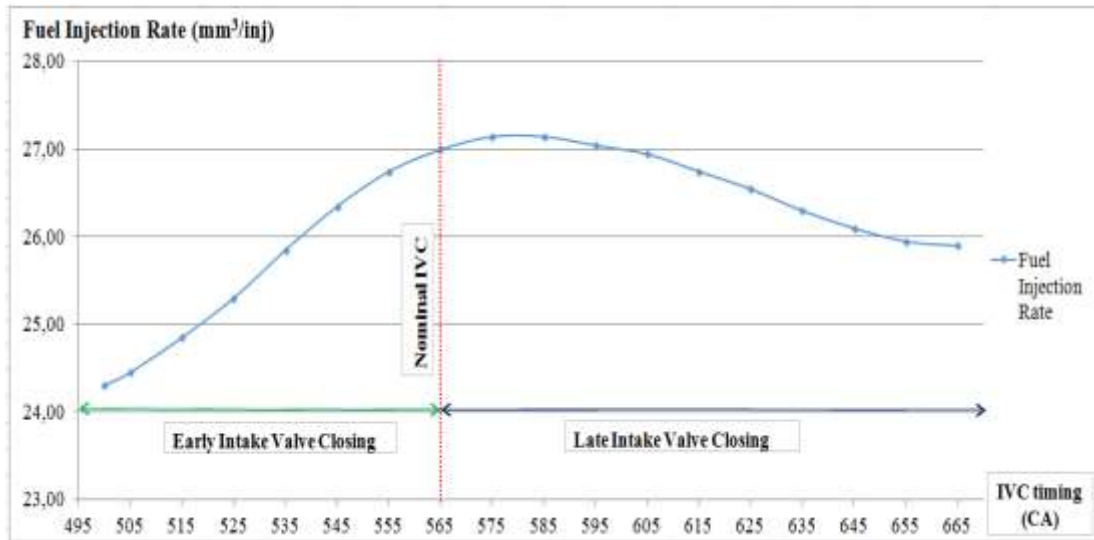


**Figure 4.8 :** Fuel injection rate variation along early and late IVC.

When the figure above is examined, less fuel is required to manage the same engine loading for both advanced and retarded closing timings of intake. It can be derived that not only does the method sufficiently raise the exhaust temperatures to the desired 250°C temperature limit, but also it results in fuel-saving diesel engine performance. This positive effect can also be seen on Figure 4.9 below with the increase on brake thermal efficiency.

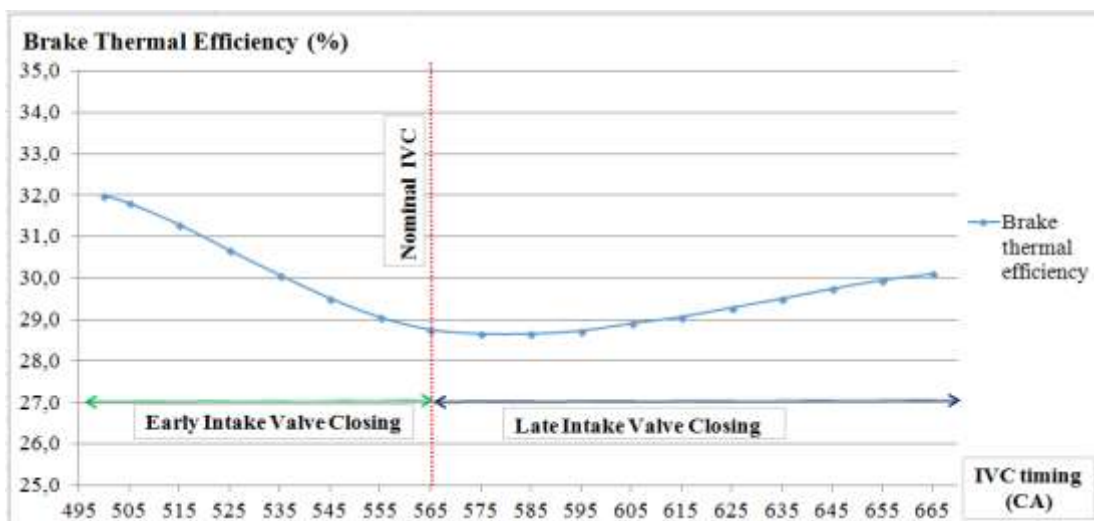


**Figure 4.9 :** Brake thermal efficiency change along early and late IVC.

As the fuel consumption drops for forward and backward sweeping of IVC, brake thermal efficiency of the system increases as expected compared to nominal IVC timing. In order to understand the reason behind this thermal-efficient performance of the diesel engine along EIVC and LIVC, Friction mean effective pressure (FMEP), pumping mean effective pressure (PMEP) and indicated mean effective pressure of the power phase ( $IMEP_{power}$ ) values should be examined. In section 3, bmp was defined as the difference between indicated mean effective pressure of the whole diesel cycle ( $IMEP_{cycle}$ ) and diesel engine FMEP.  $IMEP_{cycle}$  is calculated with the following formula below [82]:

$$IMEP_{cycle} = IMEP_{power} + PMEP \tag{4.1}$$

**4.2.3 FMEP, PMEP and  $IMEP_{power}$  variation along IVC sweep**

As the  $IMEP_{power}$  change along advanced and retarded closing timings shown in Figure 4.10 below is examined, it is seen that less power is needed to obtain same 2.50 bar bmp in the system. The results found are compatible with the Figure 4.8 and Figure 4.9 where earliest IVC timing is more fuel-efficient than the latest IVC timing.

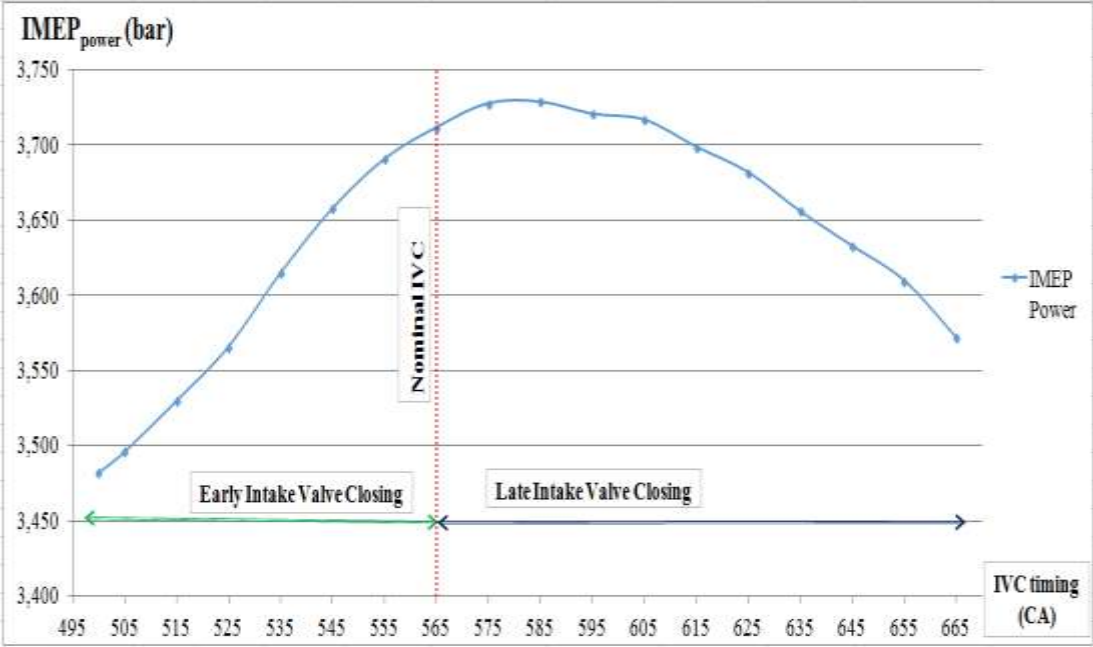


**Figure 4.10 :**  $IMEP_{power}$  change along EIVC and LIVC.

The decrease in  $IMEP_{power}$  in the system is an expected result since fuel injection rate is reducing through EIVC and LIVC as shown previously on Figure 4.8. However, FMEP and PMEP should be further investigated in order to grasp where the fuel-

saving effect comes from. FMEP and PMEP variation for different IVC timings are demonstrated on Figure 4.11 below.

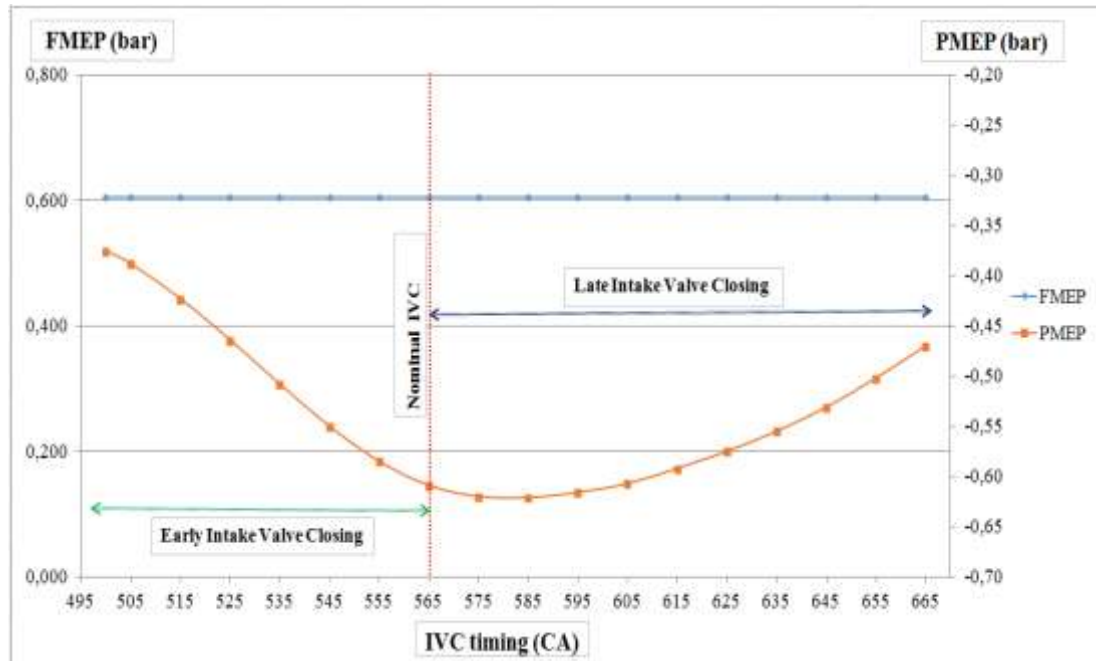


**Figure 4.11** : FMEP and PMEP change along EIVC and LIVC.

It is seen that FMEP does not alter significantly when IVC is changed, it is more or less the same. However, PMEP is decreasing as IVC goes earlier or later than the stock IVC timing. This may stem from the reduction of volumetric efficiency as obtained on Figure 4.6. Because decreasing air induction along EIVC and LIVC results in lower pumping losses in the system.

It can be concluded that lower PMEP enables the system to perform with lower  $IMEP_{power}$ . Therefore, less fuel is demanded in the system to hold the engine loading constant. In order to comprehend the reduction in PMEP in a detailed manner, change of pressure behaviour for EIVC and LIVC sweeps should be examined.

#### 4.2.4 Pressure-volume diagrams

As demonstrated on the previous section, the effect of fuel-efficiency is due to the reduction in PMEP in the system. Change of PMEP can be observed by investigating the change of pressure behaviour along the cycle while IVC is advanced or retarded in the system. The experimental results for EIVC and LIVC from Garg's study [69] are shown on the following Figures 4.12 and 4.15. Simulation results are put below the Garg's results in order to compare for both EIVC and LIVC. At first, pressure-volume diagrams for earlier IVC timings are compared on Figures 4.12 and Figure

4.13. Experimental results are given in PSI and in<sup>3</sup> for pressure and volume in Garg's study (Figures 4.12 and 4.15). In ITU studies, SI units are generally taken for graphical results. Therefore, these units are converted into bar and cm<sup>3</sup> for pressure and volume. The simulation results are in bar and cm<sup>3</sup> units for pressure and volume too (Figures 4.13 and 4.16).

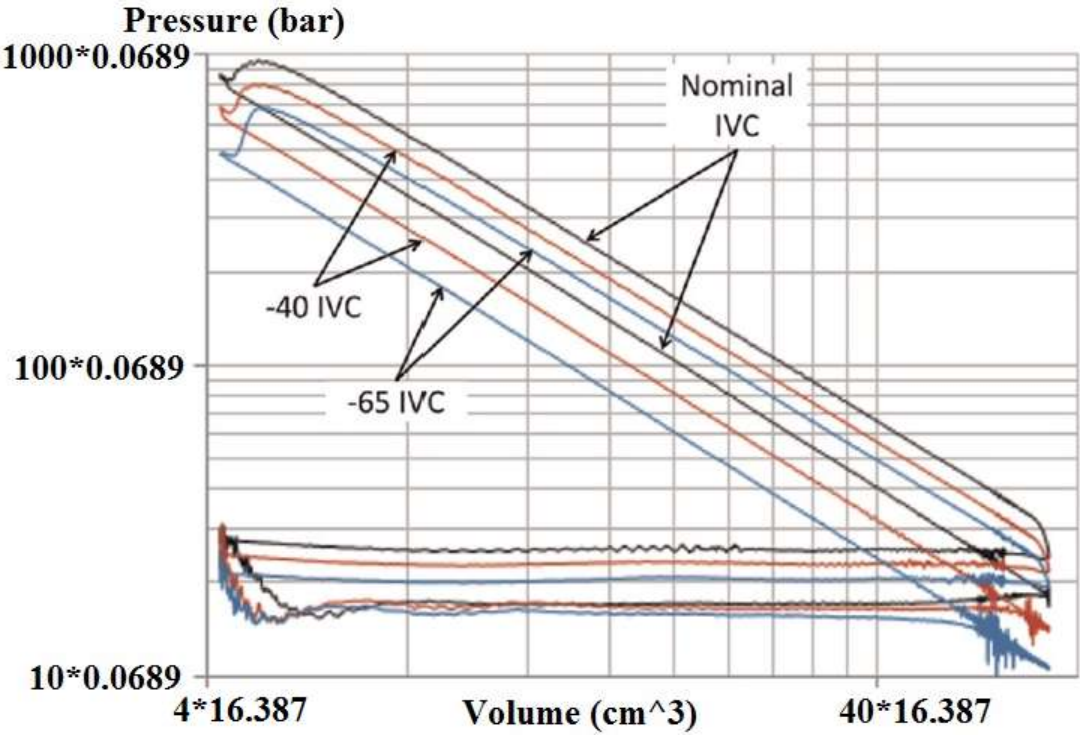


Figure 4.12 : Experimental pressure-volume diagrams for EIVC timings [69].

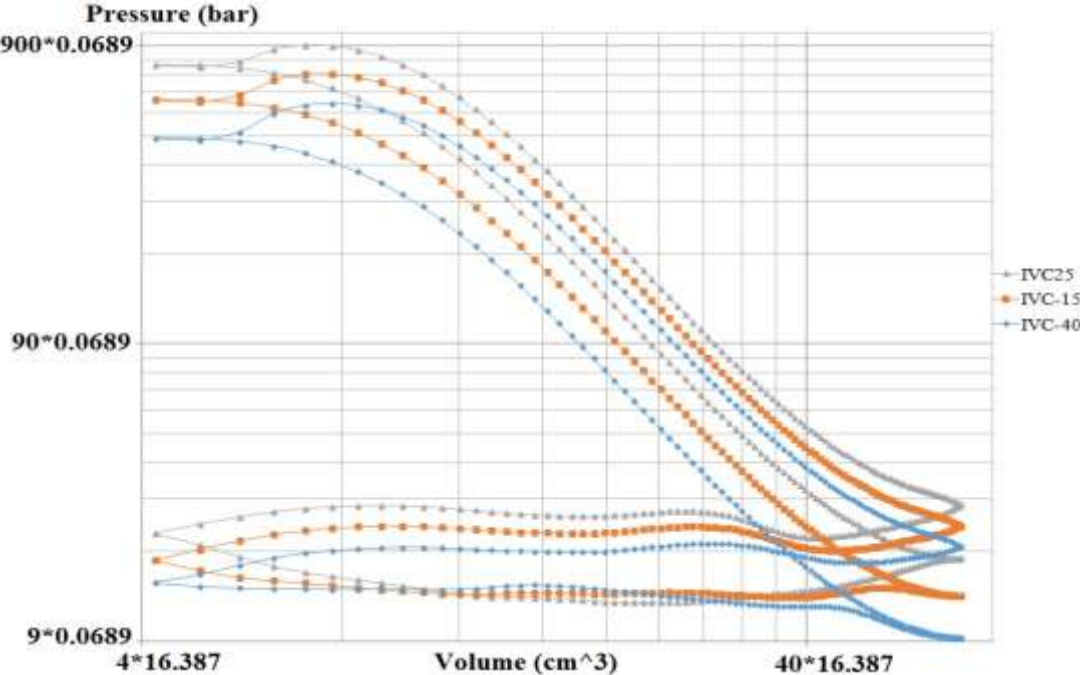
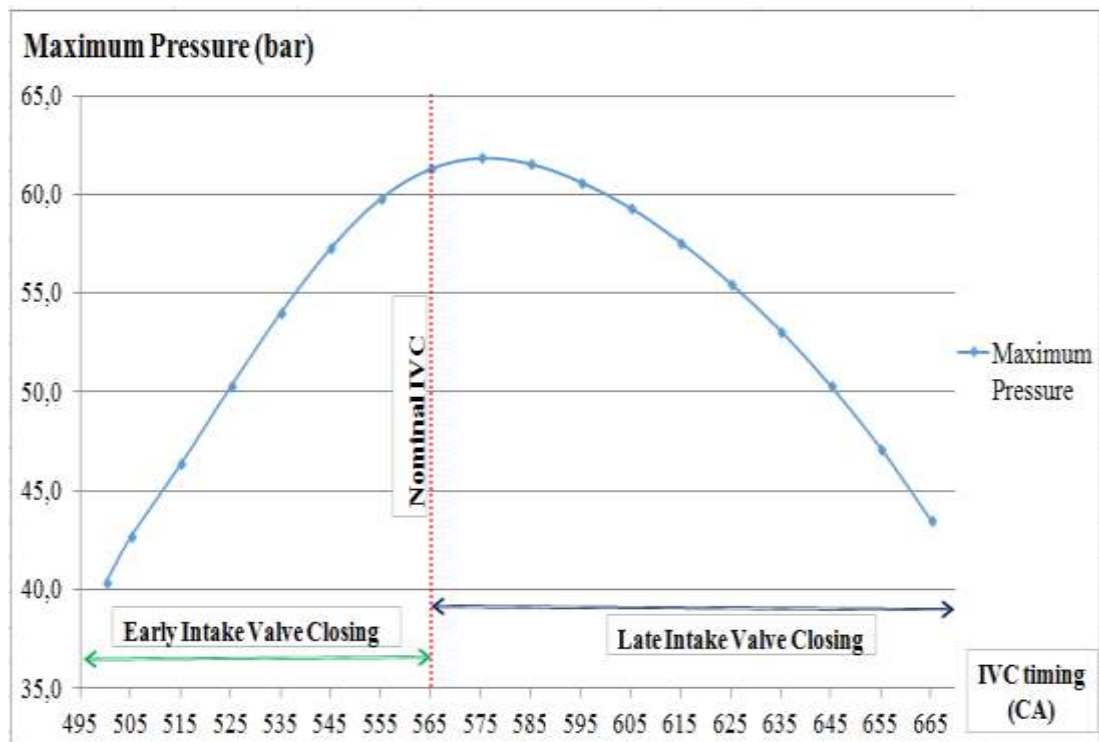


Figure 4.13 : Pressure-volume diagrams along the cycle for EIVC with simulation.

On Figure 4.13 above, IVC25 shows the nominal IVC timings which was also specified on Table 4.2 and Figure 4.1. IVC-15 is the 40 CA advanced timing and IVC-40 also points out 65 CA advanced IVC timing. As the pressure variation along the cycle is analyzed on the diagram, it is seen that when IVC is closed earlier than nominal, maximum pressure ( $P_{max}$ ) decreases. That leads to decreased pressure at the end of power and expansion phases and lower pumping loops (lower PMEPs) are needed for advanced IVC timings. Change of  $P_{max}$  can also be seen in a detailed manner on Figure 4.14 below.



**Figure 4.14 :** Maximum pressure change with IVC sweep.

The same situation is valid for retarded closing timings of intake too. The experimental results are seen on the following Figure 4.15 and simulation results for the same case are demonstrated on the following Figure 4.16 below. Unlike Figure 4.13, on this case, IVC is closed 70 CA later at first seen on the figure with IVC95 and it is also closed 100 CA later than the nominal with IVC125. Maximum pressure drops with IVC95 and decreases further with IVC125 (this case is also demonstrated on Figure 4.14). Lower pressure takes place at the end of power and expansion and lower pumping losses are required (similar to Figure 4.13) along the cycle for LIVC. When Figure 4.14 and Figure 4.5 are compared, it is definite that both  $P_{max}$  and PMEP are directly proportional with the volumetric efficiency.

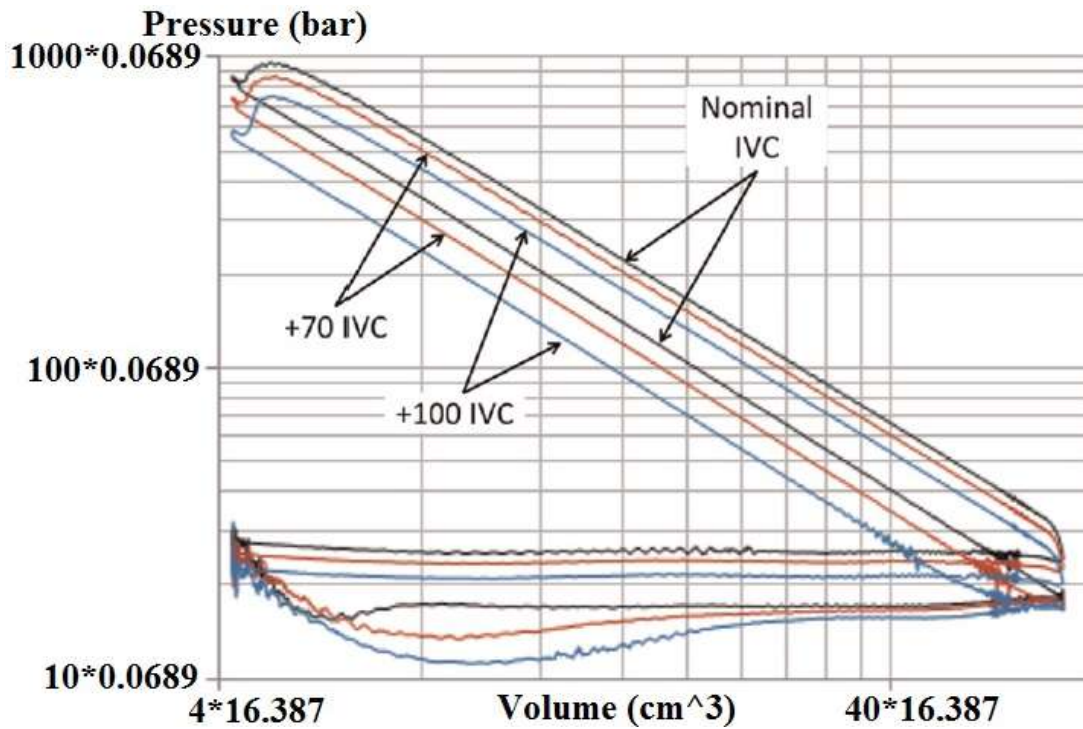


**Figure 4.15 :** Experimental pressure-volume diagrams for LIVC timings [69].

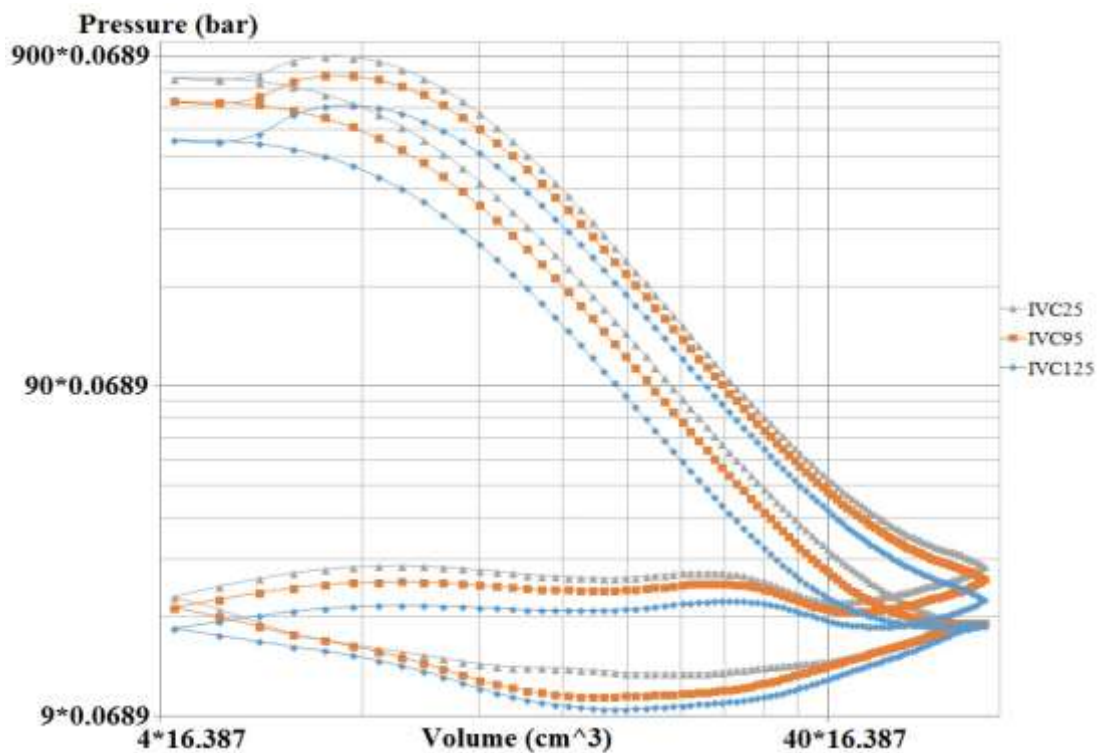


**Figure 4.16 :** Pressure-volume diagrams along the cycle for LIVC with simulation.

It can be derived from Figures 4.13 and 4.16 that decrease in volumetric efficiency and air flow into the system results in reduced pumping losses and hence lower PMEPs. Therefore, lower  $IMEP_{power}$  is needed for constant 2.50 bar bmep and lower fuel injection into the system is sufficient to manage engine loading fixed. The

reason to prefer EIVC rather than LIVC in the study is that this method decreases PMEPs more than LIVC as shown on Figure 4.11. More efficient method can be an advantage while combining different VVT strategies to achieve greater than 250°C exhaust temperatures.

### 4.3 TET and Exhaust Flow Diagrams for Different Engine Speeds and Engine Loadings

The simulation model of LES is used for a particular engine speed (1200 rpm) and a particular engine loading case (2.50 bar bmep) and it is seen that reliable results for exhaust gas temperatures can be attained by utilizing it. The case examined is a low speed and low engine loading point. As expressed on earlier sections, diesel engines generally have lower than 250°C TET values at low engine speeds and low engine loading points. At this specific point, TET was calculated as 195°C with nominal valve timings. However, diesel engine can work at lower&higher engine speeds and lower&higher engine loadings. TET will be higher and lower than that number for different performance zones of the diesel engine. Therefore, it is intended to observe the TET change for different engine speeds and engine loadings at nominal valve timings and maximum valve lifts. Valve timings on Figure 4.1 are not changed. Only fuelling rate is altered in order to manage constant bmep for different engine speeds. TET change is demonstrated on Figure 4.17 below.

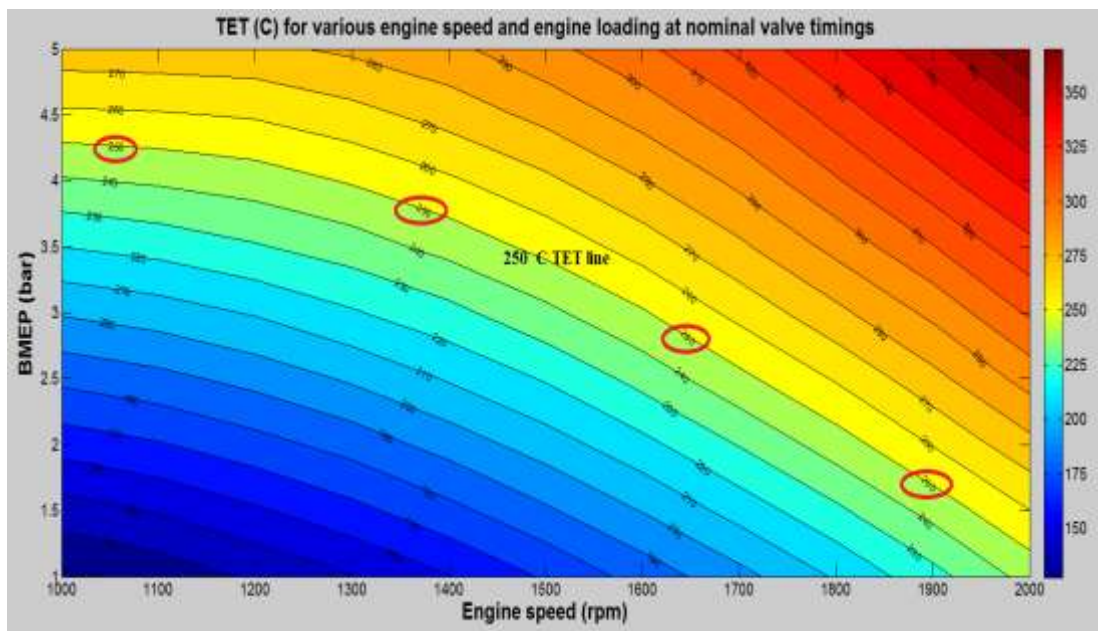


**Figure 4.17 :** TET (°C) change for different engine speeds and engine loadings.

As it is seen on the figure above, change of TET is examined for engine speed from 1000 rpm to 2000 rpm and for engine loading 1 bar to 5 bar. Engine loading is taken as bmep. It is shown on the engine performance zone that TET is lower than 250°C under the yellow line between 1000 rpm and 2000 rpm engine speeds. At low loading and low engine speeds TET is much lower than 250°C and that causes to lower efficient exhaust thermal management on those parts. High TET rises are required on those areas in order to reach greater than 250°C exhaust gases. However, as seen on the figure, high engine speed zones have temperatures closer to 250°C and thus low TET rises will be sufficient for those areas to obtain turbine out temperatures above 250°C. In comparison to the calculations done on earlier section, less advanced or less retarded IVC timings can be adequate for greater than 250°C TETs for higher engine speeds.

It is proved on previous section that alteration of IVC timings for fixed bmep is definitely beneficial for TET rise. Not only does it increase TET, but also it enables a fuel-saving engine system. However, there is an abrupt reduction on exhaust flow rate due to the decrease in volumetric efficiency and this is not useful for the heat transfer to the catalyst substrate on exhaust thermal management. As mentioned before, heat transfer from the exhaust gases to the catalyst substrate depends on both TET and also exhaust gas flow rate. Therefore, exhaust gas flow should also be considered to achieve more effective aftertreatment systems. Exhaust flow rate at nominal valve timings is seen below on Figure 4.18.

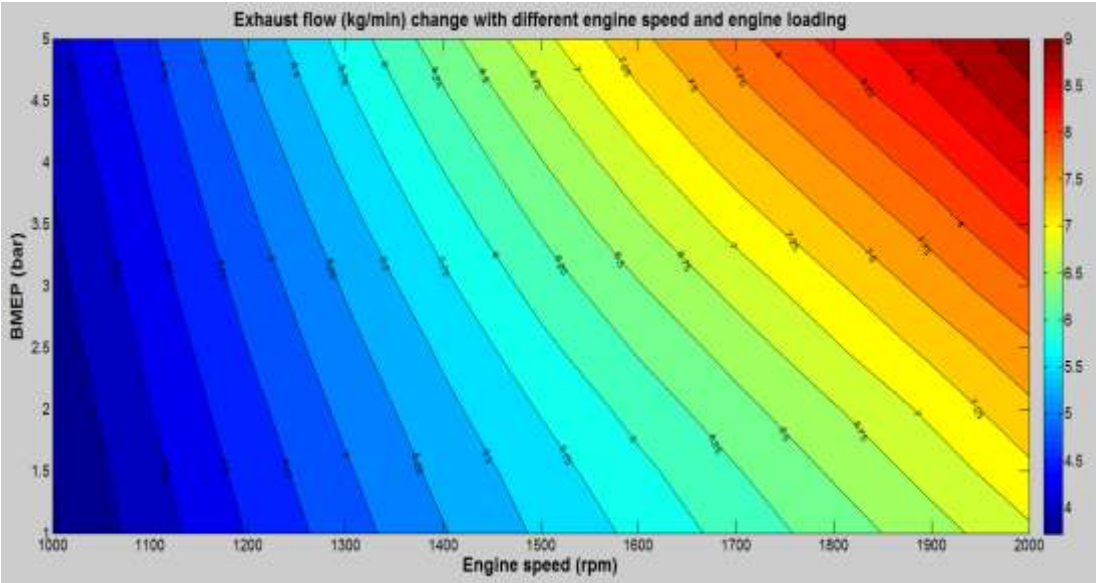


**Figure 4.18 :** Exhaust flow change for different engine speeds and engine loadings.

On the figure above, it is shown that low loading and low engine speed points have lower exhaust flow rates in comparison to high speed and high loading parts. This makes those zone especially important since it is known from Figure 4.17 that those points also have TETs much lower than 250°C. As it is obtained previously on Figure 4.7, exhaust flow rate reduces almost 36 % compared to nominal valve timing at 1200 rpm and 2.50 bar engine loading in order to exceed 250°C TET limit via EIVC. It can be derived that high exhaust flow rate reduction is a penalty for those points when only EIVC is utilized to rise TET above 250°C. Therefore, the aim of this study is to use EIVC in combination with other VVT methods and change of inlet&exhaust max. valve lifts so as to decrease the TET line shown on Figure 4.17 to lower engine loadings. This is intended to be achieved without allowing a dramatic exhaust flow rate reduction and without permitting a fuel injection rate rise compared to nominal valve timing case.

#### **4.4 Effects of Other VVT Methods on the System**

Other than IVC timing, intake valve opening (IVO), exhaust valve closing (EVC) and exhaust valve opening (EVO) timings can be investigated for exhaust flow change and higher TETs in the system. The first goal is to find out the appropriate option from those VVT methods to combine with EIVC. Afterwards, the effect of change of inlet and exhaust maximum valve lifts will be considered.

Changing IVO and EVC is restricted with the movement of the piston close to the Top Dead Center (TDC) area. As shown on Figure 4.19 below, for early IVO (EIVO) and late EVC (LEVC) valve lifts are getting greater than 1mm at top dead center (TDC). On the validation of the simulation section, this 1 mm distance is specified as a limit for different VVT options. Because it can lead to piston-valve crash which is not allowed during the cycle. Therefore, primarily, late IVO (LIVO) and early EVC (EEVC) which are safer (valve lifts lower than 1 mm at TDC) are examined in the system to be beneficial to both TET and exhaust flow rate. After analyzing these two options, EVO will be examined in a separate subsection. As it is known from the literature review, early EVO (EEVO) is indeed effective for obtaining higher TETs although it results in fuel consumption penalty [71, 72]. However, similar TET rise should be calculated with LES too in order to consider EEVO as a strategy to combine with EIVC.

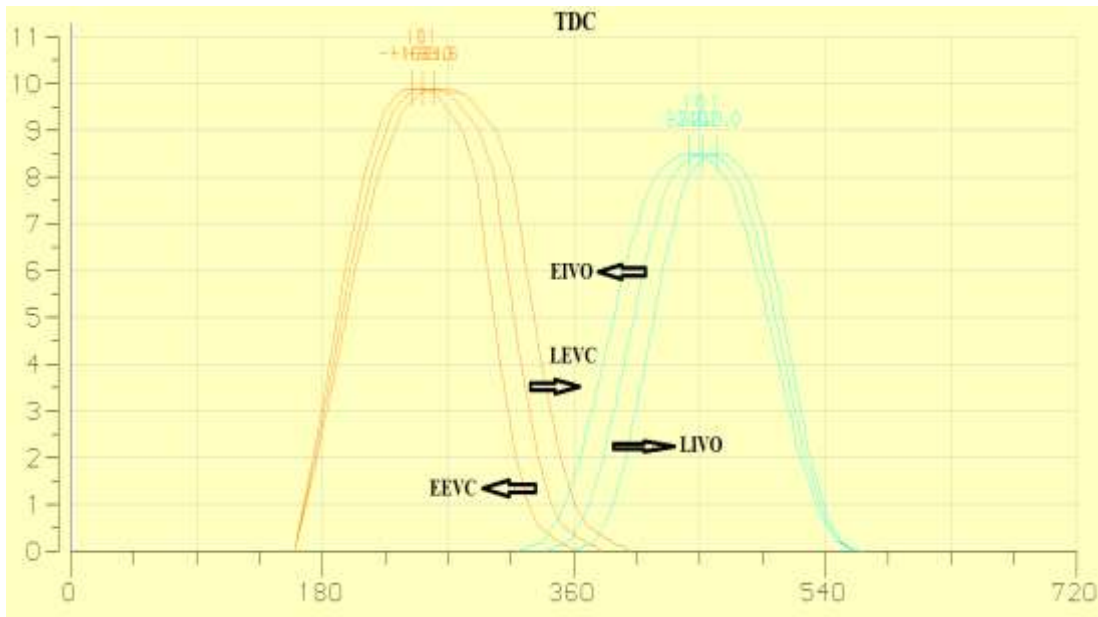


**Figure 4.19** : Earlier and later timings of EVC and IVO.

#### 4.4.1 Late intake valve opening

Exhaust gas temperature change is shown below on Figure 4.20 for LIVO. Also, change of exhaust flow rate is seen on Figure 4.21 for retarded opening timings of intake.

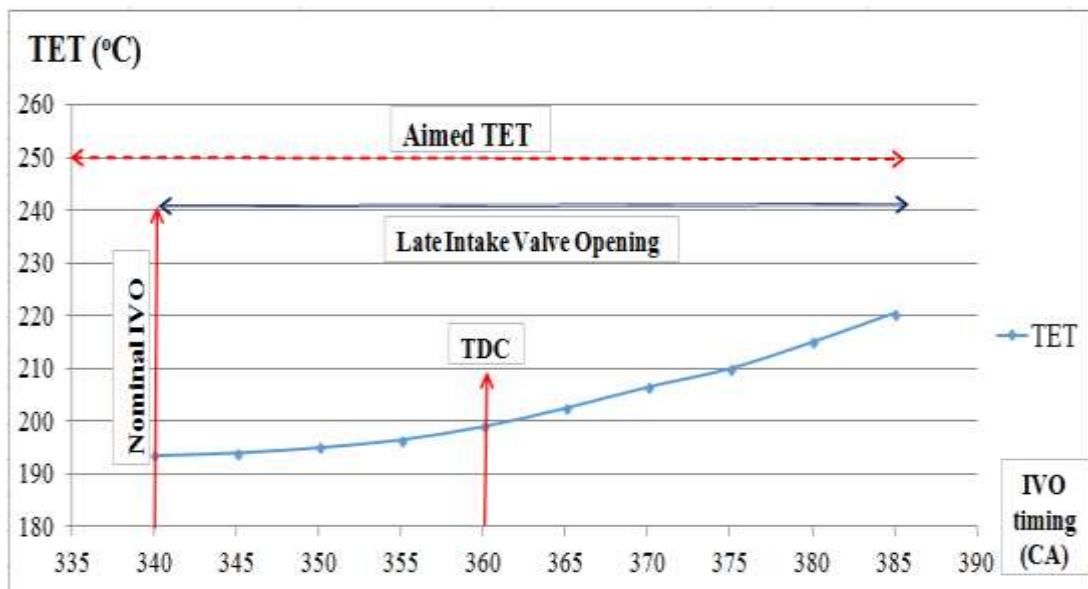


**Figure 4.20** : TET change for LIVO.

The nominal opening timing of the intake is 20 degrees CA BTDC as shown on Figure 4.20. As the opening is swept towards TDC and even retarded more until 25 degrees CA ATDC, there is not a significant TET rise in the system. Although up to 25°C TET increase is obtained by decreasing the overlap time (degree between IVO

and EVC) and allowing more residual gases in the cylinder, exhaust flow rate decreases for the most retarded case as seen on Figure 4.21 below. Because LIVO causes volumetric efficiency to drop when it is applied ATDC.

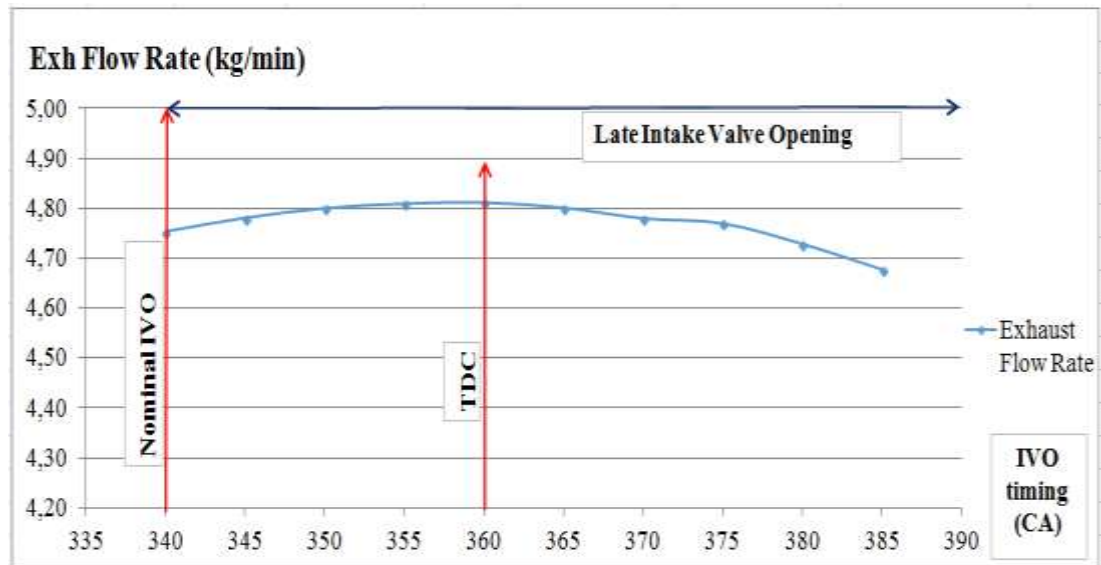


**Figure 4.21 :** Exhaust flow rate change for LIVO.

Not only is the reduction in exhaust flow rate a problem for this case, but also there is high fuel consumption penalty as demonstrated on Figure 4.22 below. As this method increases the pumping losses in the system [28], more fuelling rate is required to hold engine loading constant at 2.50 bar. It can be derived that this VVT method is not appropriate to combine with EIVC to achieve higher than 250°C TETs.

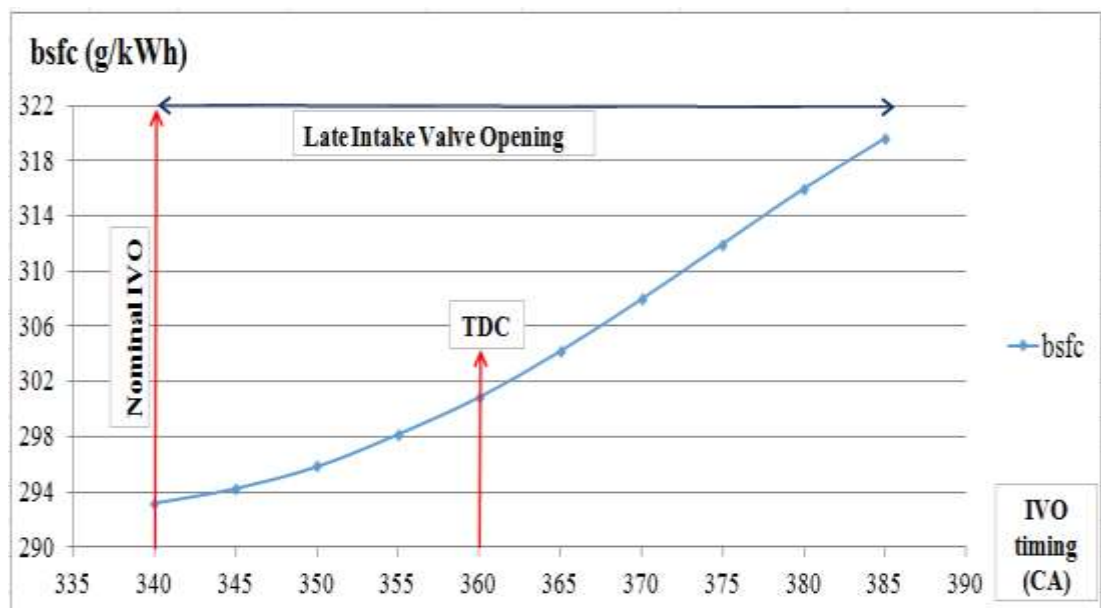


**Figure 4.22 :** Fuel consumption change for LIVO.

#### 4.4.2 Early exhaust valve closing

Nominal EVC timing is 20 degrees CA ATDC as shown on Figure 4.23. EVC timing is advanced until 15 degrees CA BTDC. It is seen that EEVC is indeed effective for high TETs. TET becomes even more than 250°C for the most advanced EVC case.

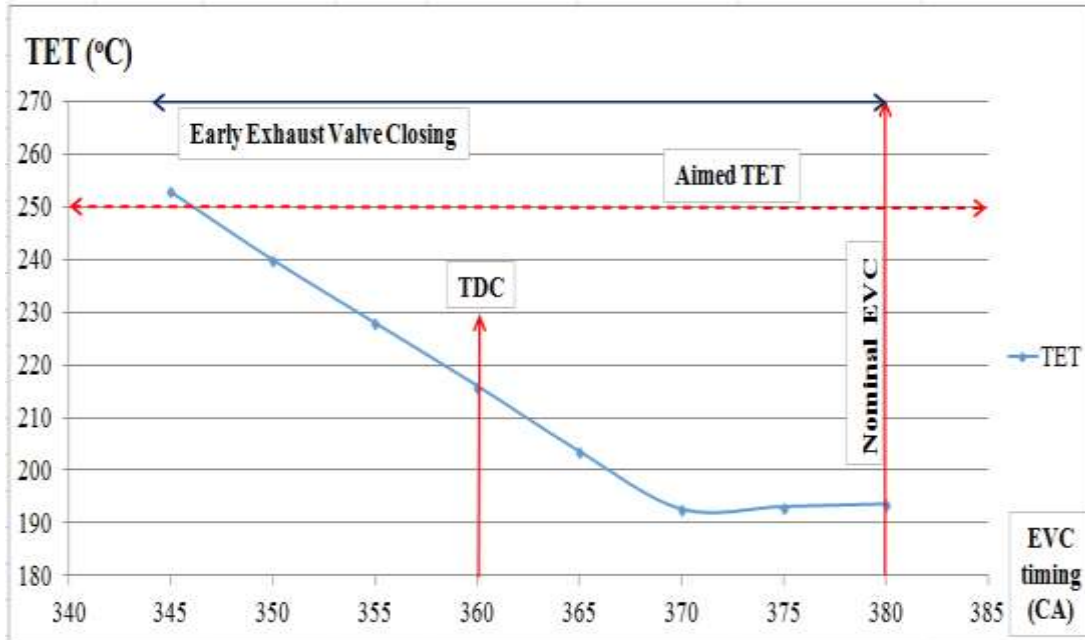


Figure 4.23 : TET change for advanced EVC timings.

However, when Figure 4.24 below is examined, it is seen that EEVC leads to an abrupt exhaust flow reduction. It is very similar to the case when EIVC is applied to the system.

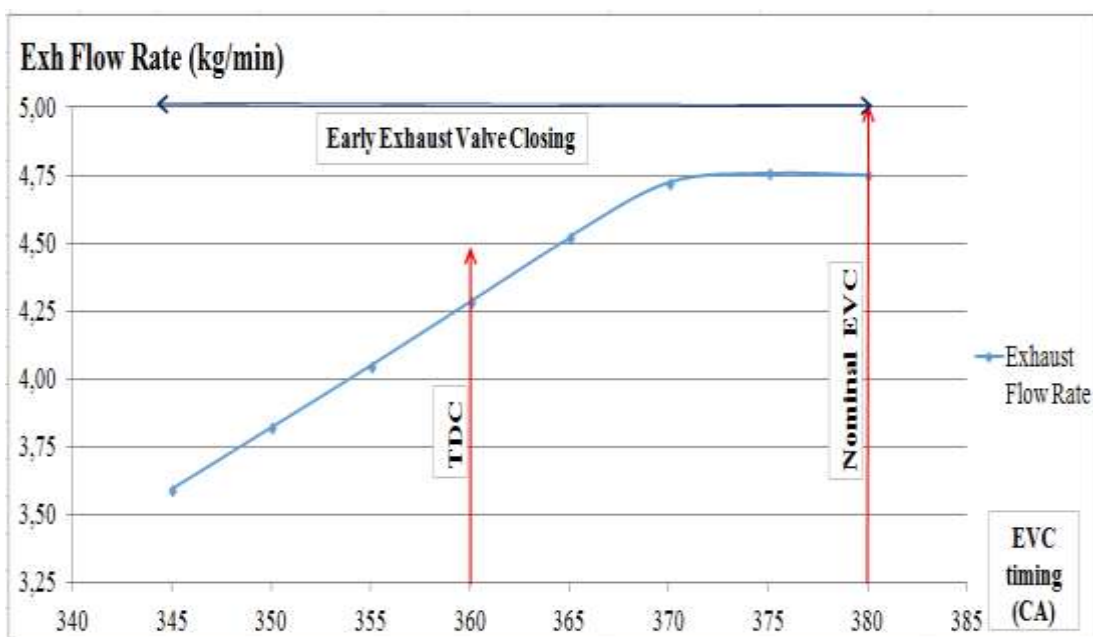
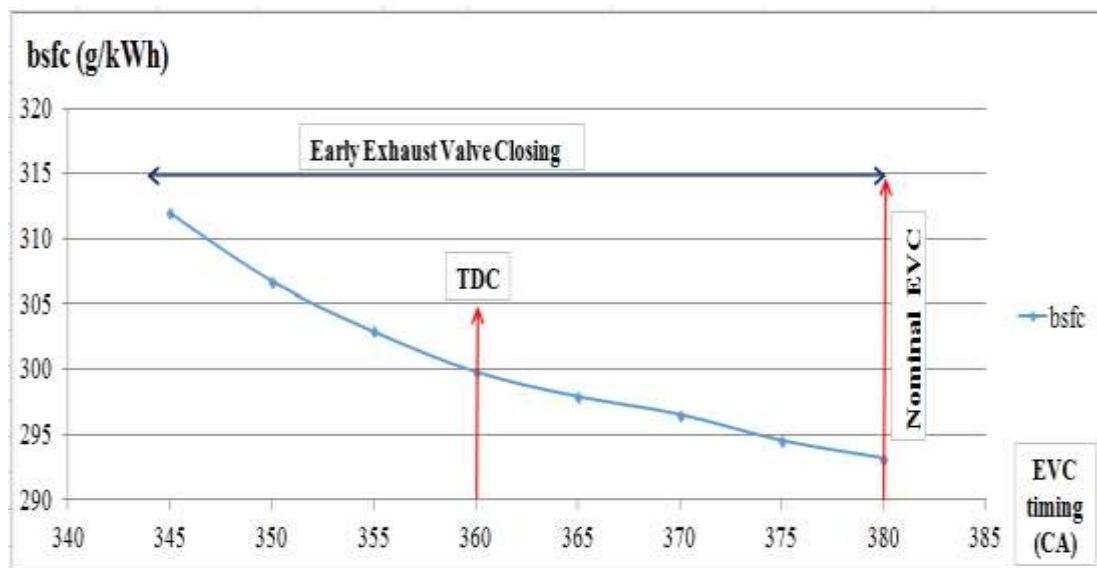


Figure 4.24 : Exhaust flow rate variation with EEVC.

The reason behind this sharp exhaust flow rate decrease is that when EVC timing is advanced, not all of the exhaust gases can be discharged from the cylinder through exhaust ports. Because exhaust timing duration is shortened to complete that release. Some of the exhaust gases flow back to the intake port, some of the gases stay in the cylinder and mix with the fresh charge. Although this situation increases the TET via rise in the residual gases, it also needs more fuel consumption in the system as shown on Figure 4.25. Since having more residual gases in the next cycle decreases the combustion efficiency, fuel injection rate should be increased to compensate this.



**Figure 4.25 :** Fuel consumption change for EEVC.

EEVC also becomes impractical to combine with EIVC due to the negative effect on exhaust flow rate. However, it is definite that it can be an option to reach higher than 250°C for high speed and low loading points where exhaust flow is already at high rates.

#### 4.4.3 Early exhaust valve opening

Nominal EVO timing is 20 degrees CA BBDC as shown on Figure 4.26 below. On this section the intention is to open EVO much earlier than BDC in order to increase exhaust gas temperatures in the system. As examined on the literature review section, EEVO has a great potential to rise turbine out temperatures, particularly for high engine speed and high engine loading cases [71, 72, 78]. In order to observe the same effects in LES, EVO is advanced from 20 degrees CA BBDC to 105 degrees CA BBDC. All other valve timings and valve lifts are kept constant. Also, engine loading is managed fixed at 2.50 bar bmep as done previously on other VVT methods.

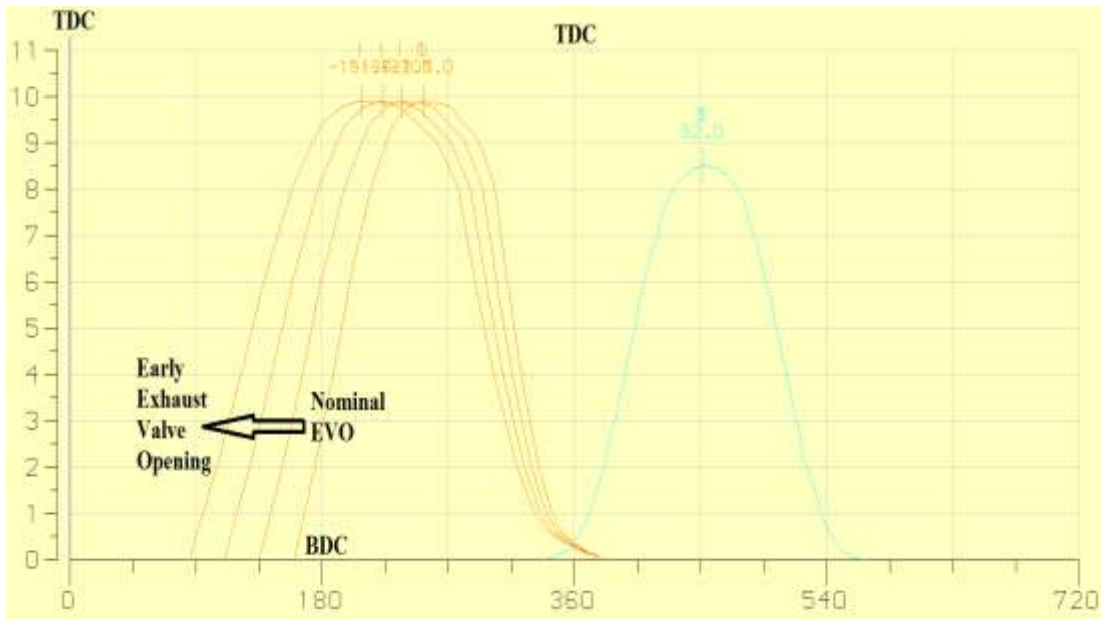


**Figure 4.26 :** Advanced EVO timings on the exhaust valve lift profile.

The results for TET for earlier swept EVO timings are seen on Figure 4.27 below. As timing is getting further from the BDC, TET is rising rapidly in the system. The reason behind this sharp increase in TET comes from the fact that the diesel engine starts to release the exhaust gases from the cylinder earlier than nominal case. At earlier valve timings, these gases have higher pressures and higher temperatures since EVO timing is closer to combustion phase. Therefore, exhaust gases with higher temperatures go into the turbocharger and leave the turbine with greater temperatures in comparison to nominal EVO timing.

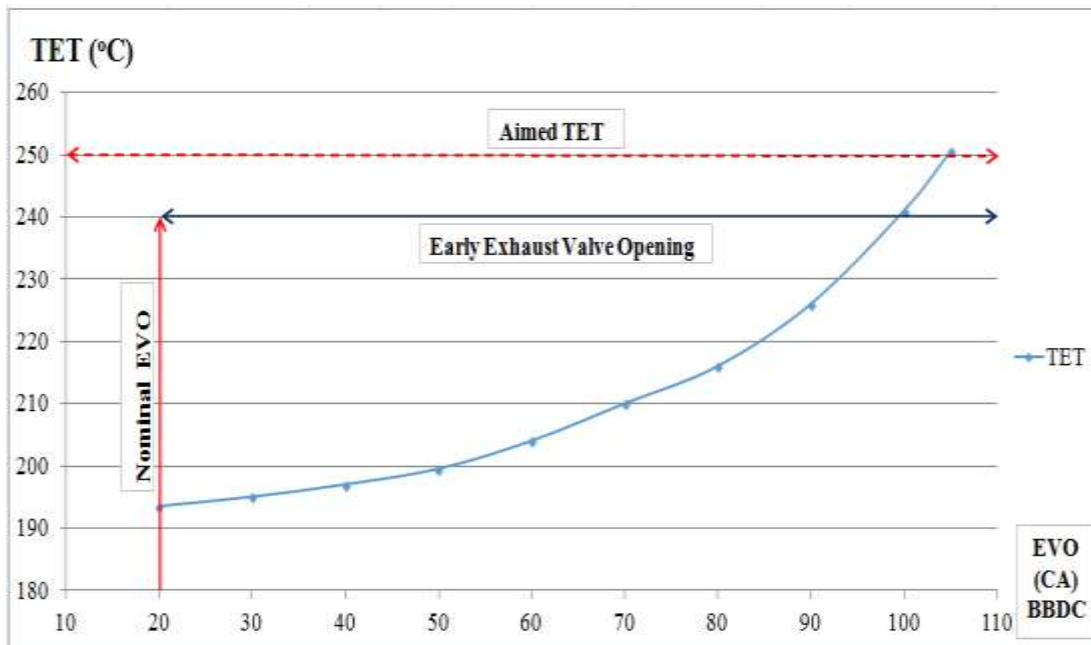


**Figure 4.27 :** TET change for advanced EVO.

It is definite that EEVO is indeed beneficial to obtain 55°C TET rise for a low loading case (2.50 bar bmep) at 1200 rpm engine speed and 250°C TET target line can be reached when sufficient advancement is applied. Also, when exhaust flow along EEVO is analyzed in the sytem on Figure 4.28 below, it can be derived that it is steadily increasing along EEVO.

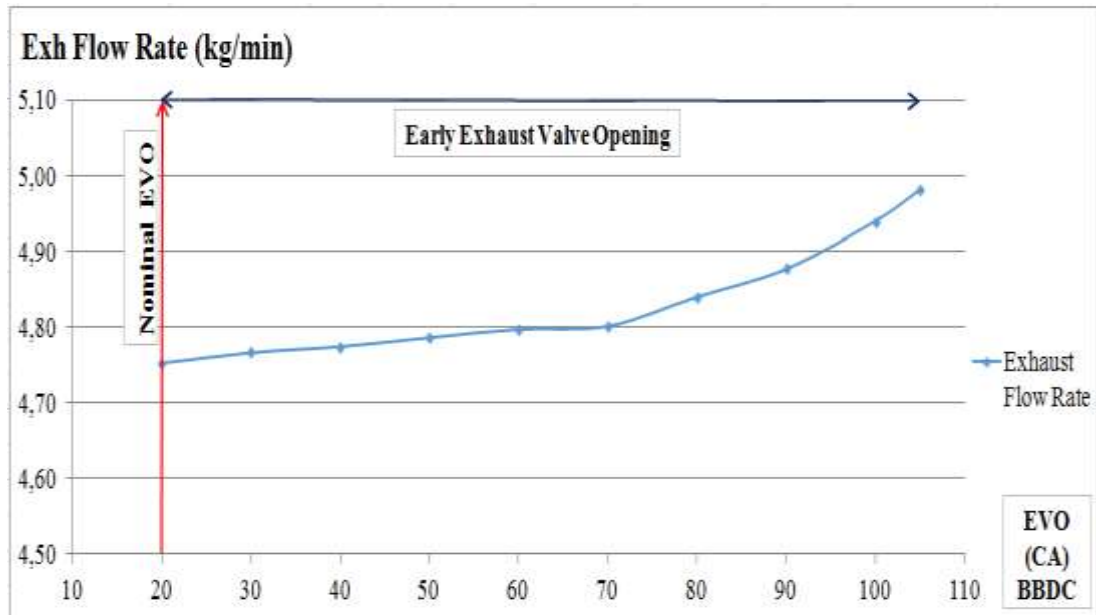


**Figure 4.28 :** Exhaust flow rate variation with advanced EVO.

Exhaust flow is constantly rising in the system because fuel injection rate is increasing rapidly in the system as shown on Figure 4.29. This excessive fuel need is added to the system for advanced EVO timings and results in higher exhaust flow.

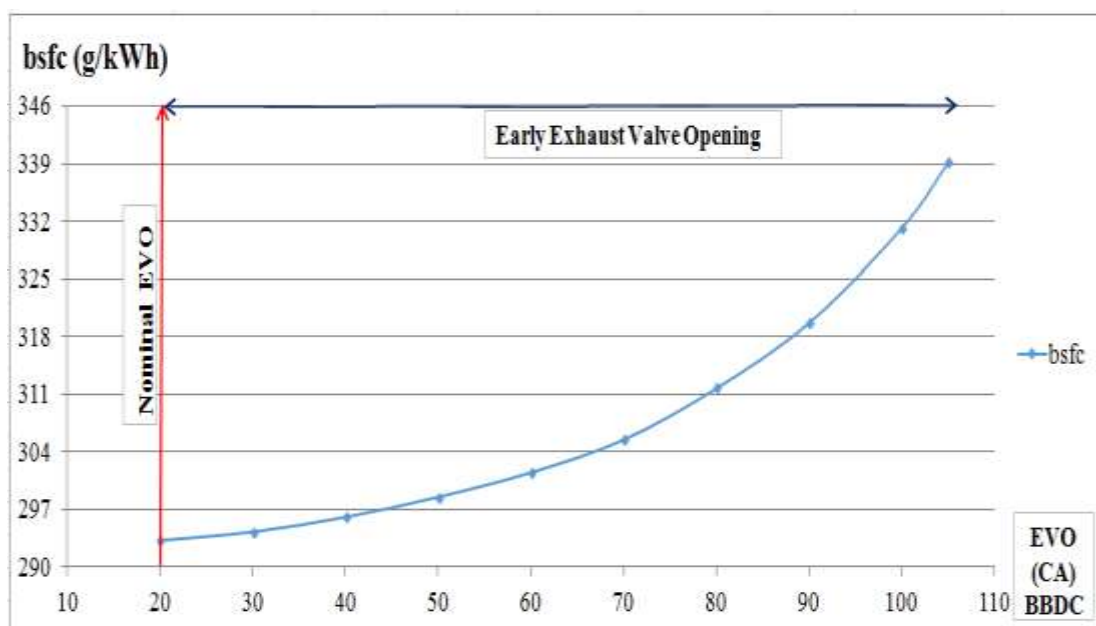


**Figure 4.29 :** Fuel consumption change with EEVO.

The EEVO seems to be only VVT strategy to increase both TET and exhaust flow rate which are the two significant parameters for rising heat transfer from exhaust gases to the catalyst substrates on aftertreatment systems. However, it has a considerable negative effect. It causes high fuel consumption penalty. In fact, when Figure 4.30 below is examined explicitly, it can be understood why this VVT method requires higher fuel consumption in comparison to nominal EVO timing.

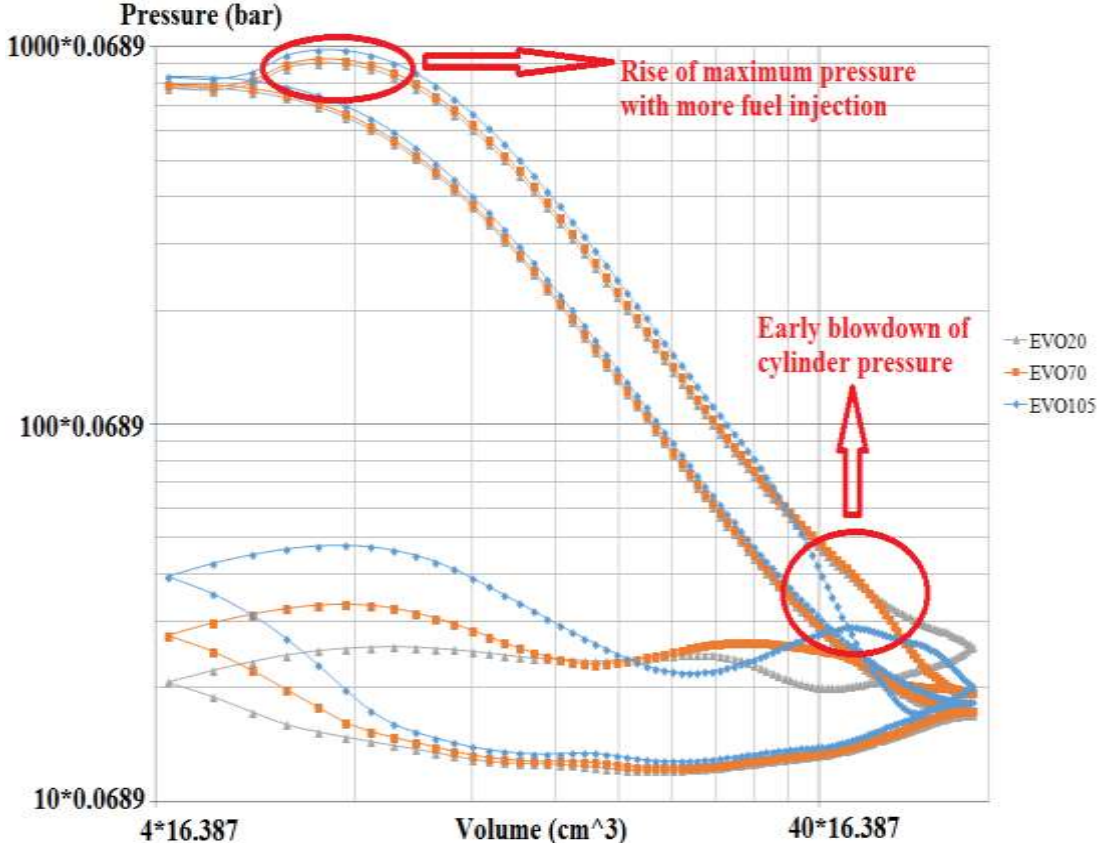


**Figure 4.30 :** Pressure - volume diagrams for EEVO.

Nominal (EVO20, 20 degrees CA before BDC), EVO70 (50 degrees CA advanced from nominal) and EVO105 (85 degrees CA advanced from nominal) timings are compared on Figure 4.30 above. It is seen that as the opening is taken earlier than nominal timing, expansion phase is cut off in the cycle and there is an earlier blowdown in pressure for EVO70 and EVO105 compared to nominal. Therefore, more fuel should be injected into the cylinders in order to compensate the reduced expansion work. It is seen that EVO105 and EVO70 have higher maximum pressures than nominal EVO20. This is in fact due to consuming more fuel to hold engine loading constant. However, combining EEVO with EIVC can be useful, because EIVC is fuel-saving and it can decrease the fuel penalty caused by EEVO.

#### 4.5 Application of Combined EIVC and EEVO on the System

On the previous sections, it is seen that EEVO is the best option to obtain both high TETs and also high exhaust gas flow rates. But, it has a major drawback, it increases the required fuel for the same engine loading in the system. Since EIVC is fuel-saving, these two VVT methods can be applied together as shown on Figure 4.31 below.

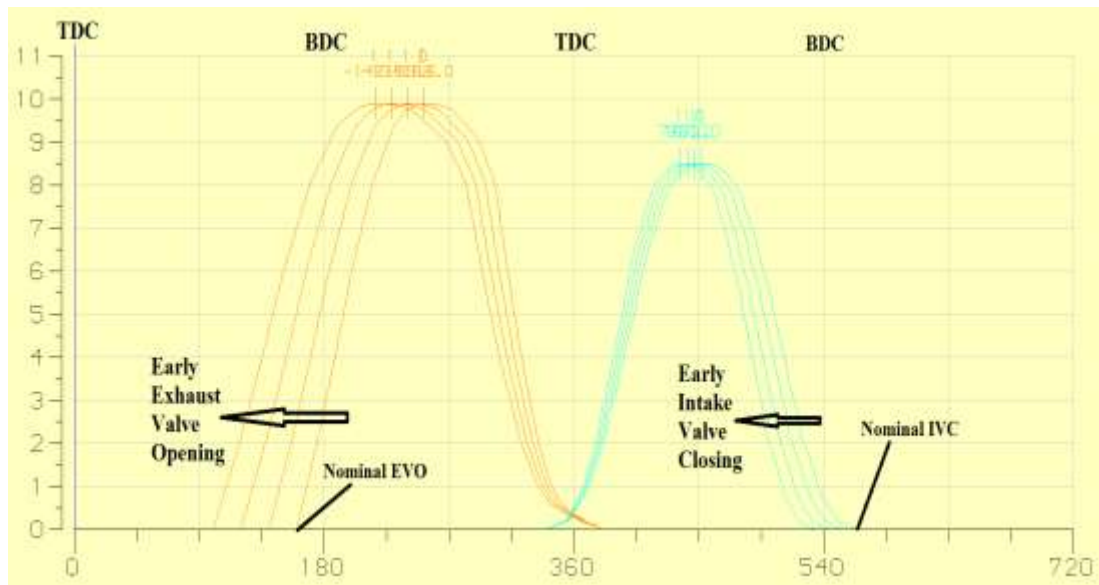


**Figure 4.31 :** Combined EEVO and EIVC valve lift profiles.

TET change is demonstrated below on Figure 4.32 for this EIVC&EEVO combined VVT strategy. TET rises for both advanced EVO and advanced IVC.

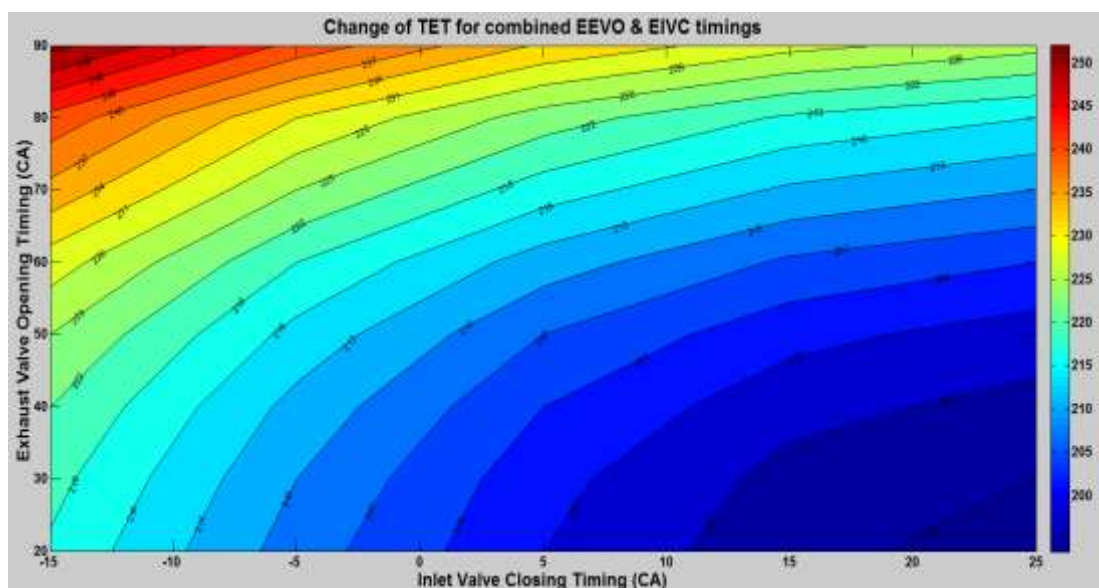


**Figure 4.32 :** Rise of TET ( $^{\circ}$ C) via combined EIVC & EEVO.

It can be derived that utilizing combined EIVC&EEVO method is definitely effective for reaching greater than 250°C exhaust gas temperatures. IVC does not have to be advanced until 40 degrees CA BBDC as studied previously on the validation section. Instead, advancing it 15 degrees CA BBDC is sufficient when EVO is also advanced 70 degrees CA from the nominal timing. Moreover, when exhaust flow rate variation on Figure 4.33 below is examined, it is decreasing for valve point EVO90 and IVC-15 as expected due to the earlier IVC. However, it is not as dramatic as the one achieved on the validation part where IVC is advanced 65 CA from the stock valve timing. It is seen that when only IVC is used to exceed 250°C TET target temperature, exhaust gas flow rate reduces almost 36 %. Yet, EIVC&EEVO application results in a drop of 17 % in comparison to nominal valve timing while achieving the same high TET in the system.

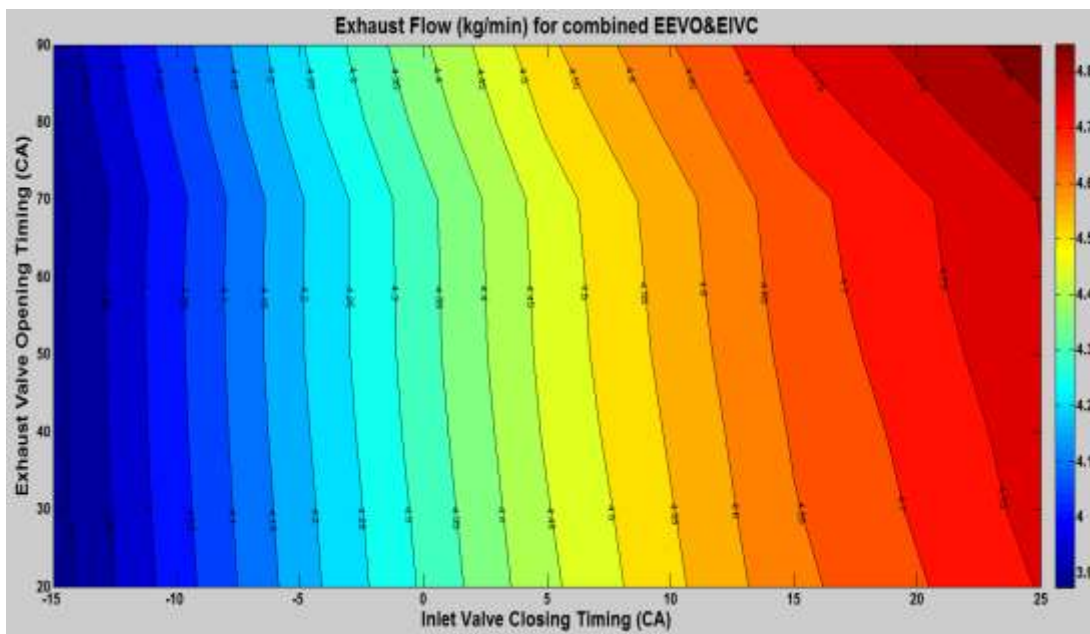


**Figure 4.33 :** Exhaust flow rate change along EEVO & EIVC.

There is no doubt that the method is beneficial for both enabling diesel engine performance with exhaust gas temperatures above 250°C and also providing relatively higher exhaust gas flow rates in comparison to the case where only IVC is swept to earlier timings to attain greater than 55°C TET rises in the system. However, as emphasized previously, the intention is to gain high exhaust gas temperature increase for different engine loading cases without rising the required fuel consumption to hold the engine loading constant. Therefore, fuel consumption variation for EEVO&EIVC on Figure 4.34 should be examined.

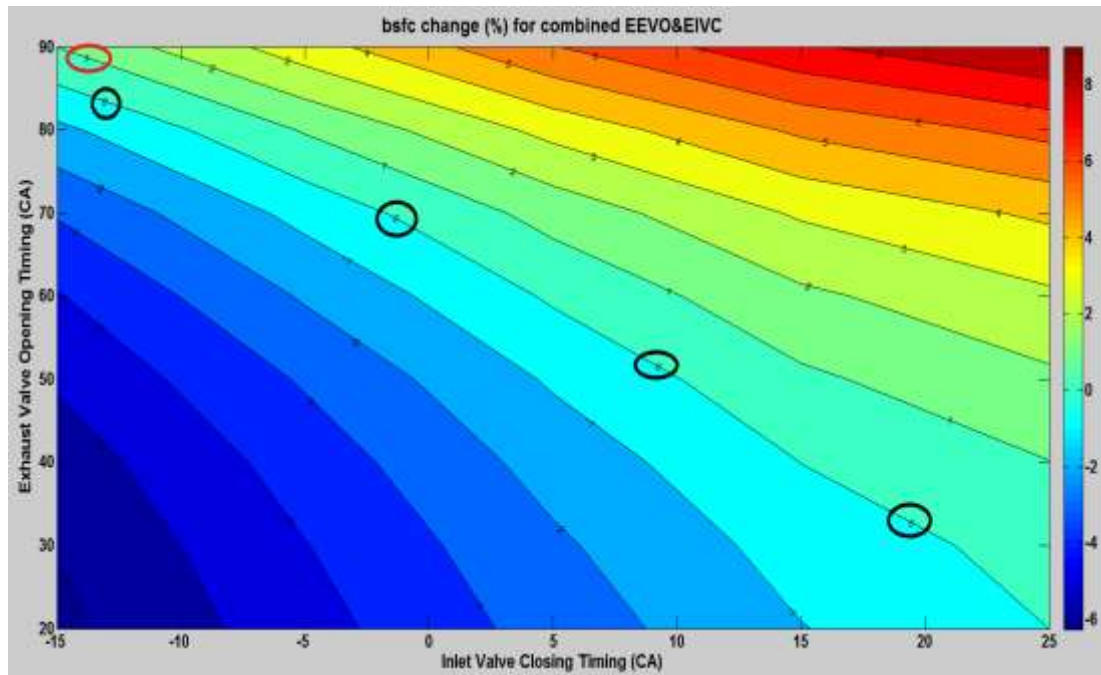


**Figure 4.34 :** bsfc change (%) variation compared to nominal valve timings along combined EEVO & EIVC.

The rise and decrease on fuel consumption need for constant load can be explicitly seen on the figure above. As expected, lower fuel is required to keep loading constant for EIVC due to lower PMEPs and more fuel must be injected into the system for EEVO parts because of the sharp blowdown of the pressure and shortened expansion phase. However, for the combined application, there is a zero fuel consumption penalty line and this line also crosses the part where high TETs are achieved. There is only 1 % fuel consumption penalty in comparison to nominal timing for 90 degrees CA BBDC EVO and 15 degrees CA BBDC IVC timings. EIVC's fuel-efficiency effect compensates the fuel rise need due to EEVO, however, fuel penalty is unavoidable when EVO is earlier than 80 degrees CA BBDC. Therefore, change of inlet and exhaust maximum valve lifts will be examined to decrease this fuel penalty while TET exceeds 250°C.

#### **4.6 Application of Variable Inlet and Exhaust Maximum Valve Lifts**

Nominal inlet and exhaust maximum valve lifts are 8.50 mm and 9.90 mm respectively as specified previously on Table 4.2. While change of opening and closing timings of valves are investigated before, these max. lifts can also be changed in the system in order to observe the effects on TET, exhaust flow and bsfc. Max. lift alteration is shown on Figure 4.35 below.

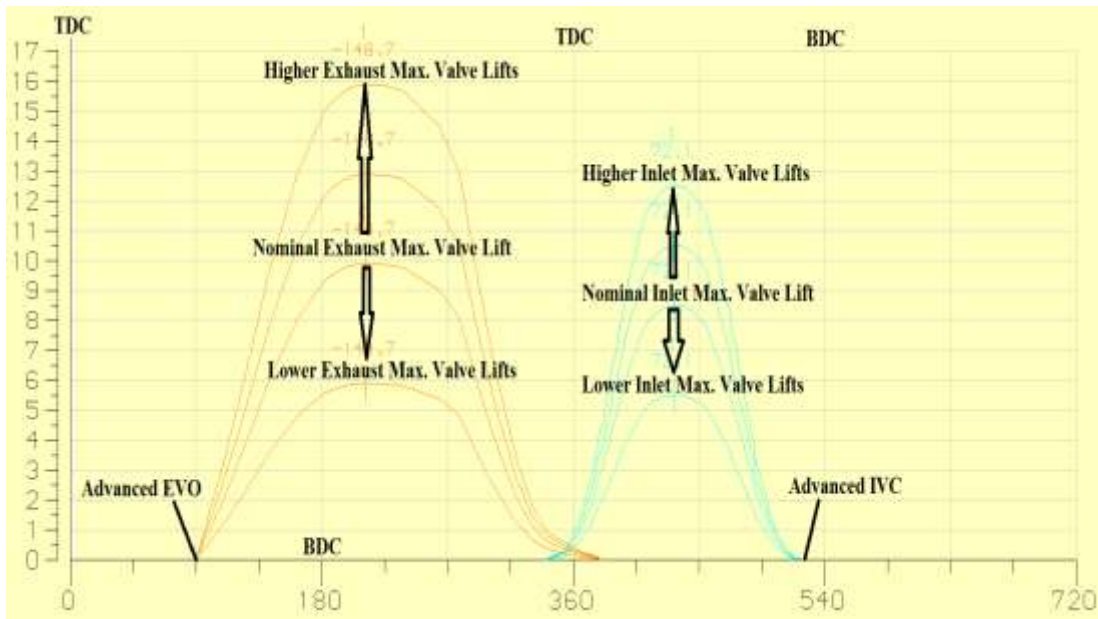


**Figure 4.35 :** Higher and lower valve lift profiles of inlet & exhaust.

The changings on max. lifts are applied for the 70 degrees advanced EVO and 40 degrees CA advanced IVC timings. Firstly, change of inlet max. lift is examined. Then, impact of exhaust max. lift will be analyzed. Finally, effect of changing those both max. valve lifts will be investigated.

#### 4.6.1 Change of inlet maximum valve lift

TET and bsfc change for different inlet max. valve lifts are demonstrated on Figure 4.36 below. Inlet max. lift is increased and decreased while exhaust max. lift is fixed.

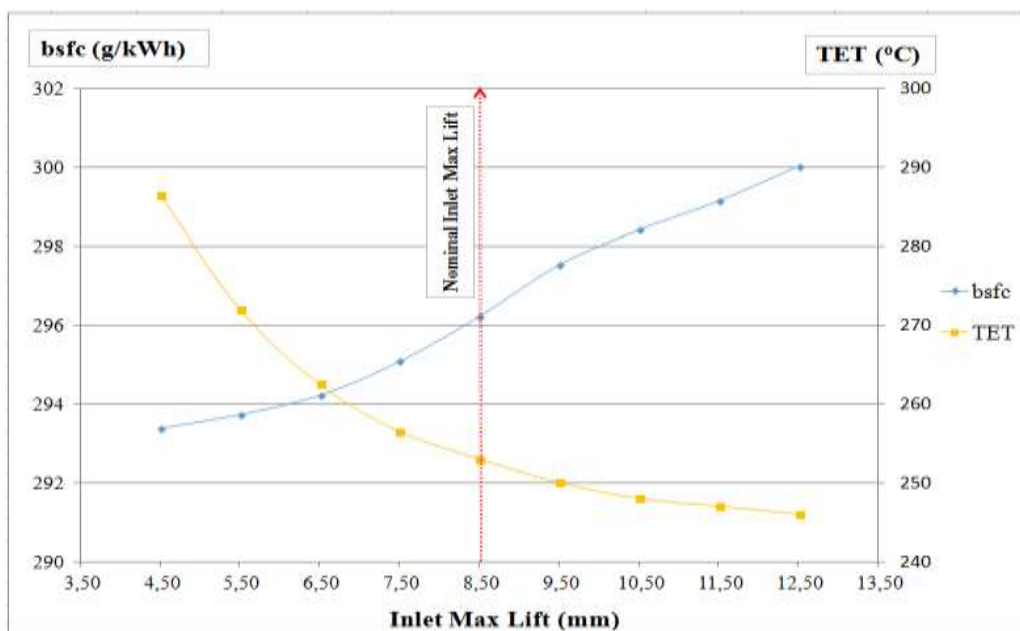


**Figure 4.36 :** TET and bsfc along higher and lower inlet maximum valve lifts.

When the figure above is examined, TET is decreasing for higher max. lifts. It also increasing for lower inlet max. lifts. In other words, it is inversely proportional with the inlet max. lifts. This is because at higher max. lifts, volumetric efficiency is rising and excessive air causes TET to drop. Higher air induction also increases the PMEP in the system and results in higher bsfc in comparison to nominal max. lift. In order to reduce the 1 % fuel consumption penalty, using smaller inlet max. lifts seems to be practical. But exhaust flow change below on Figure 4.37 should also be considered.

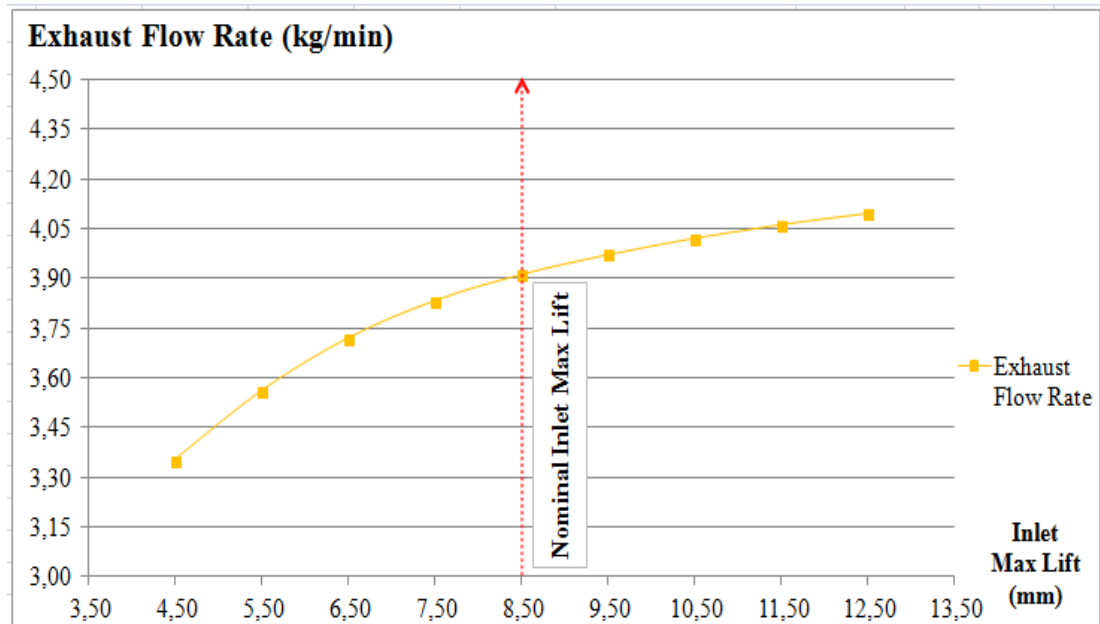


**Figure 4.37 :** Exhaust flow rate change for higher and lower inlet max. valve lifts.

On the validation section, it is seen that EIVC decreases both volumetric efficiency and exhaust flow rate. The same is valid for lower inlet max. lifts too. It is shown on Figure 4.37 above that very low inlet max. lifts leads to the sharp reduction of exhaust flow rate. While it is beneficial to diminish the fuel requirement, change of exhaust max. lifts should also be examined in order not to cause an abrupt decrease on exhaust flow in the system.

#### 4.6.2 Change of exhaust maximum valve lift

It seems from the former section that utilizing lower inlet max. valve lifts is promising to lessen the 1 % fuel consumption penalty. However, changing only inlet max. lifts while exhaust max. lift is constant is affecting exhaust flow rate negatively in the system. Therefore, exhaust max. lifts are taken lower and higher than the nominal lift. Change of bsfc and TET for different exhaust max. lifts are shown on Figure 4.38 below.

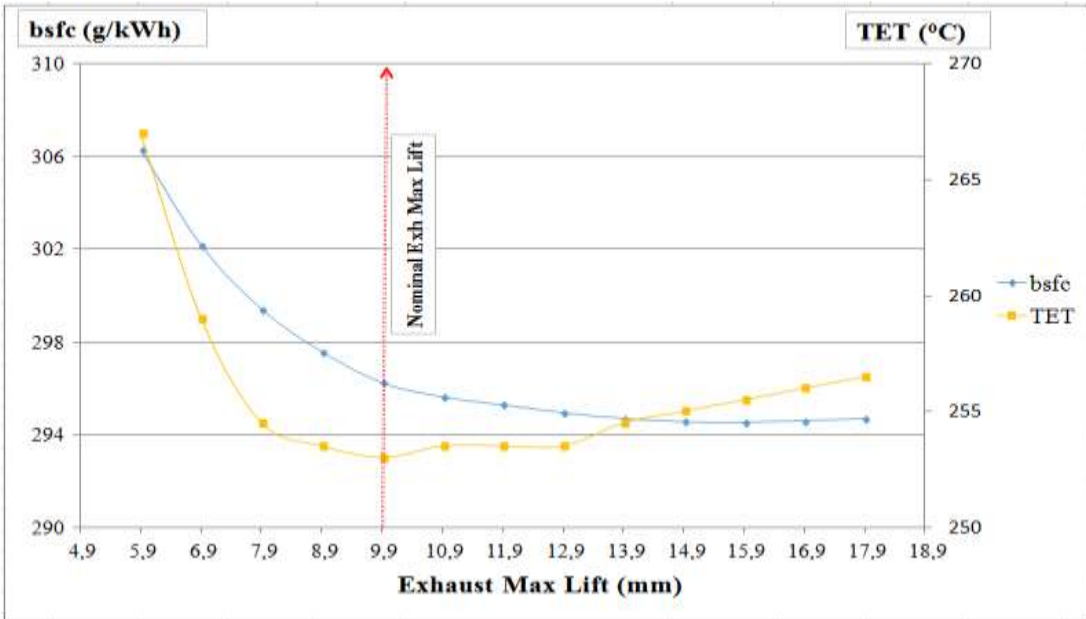


**Figure 4.38 :** TET and bsfc along higher and lower exhaust maximum valve lifts.

As it is shown on the Figure 4.38 above, although increasing exhaust max. lifts does not have a significant effect on TET, it is useful for decreasing the bsfc. This may come from the reason that more exhaust gases can be released at higher lifts and more fresh air inducts into the system for the next cycle. The benefit goes to negligible values for very high lift values. Lower max. lifts result in greater fuel penalty and higher TETs. The rise in TET stems from the increased residual exhaust gases in the cylinder. Incomplete discharge of exhaust gases and more backflow of exhaust gases into the intake port cause reduction of exhaust flow rate as seen on Figure 4.39 below too.

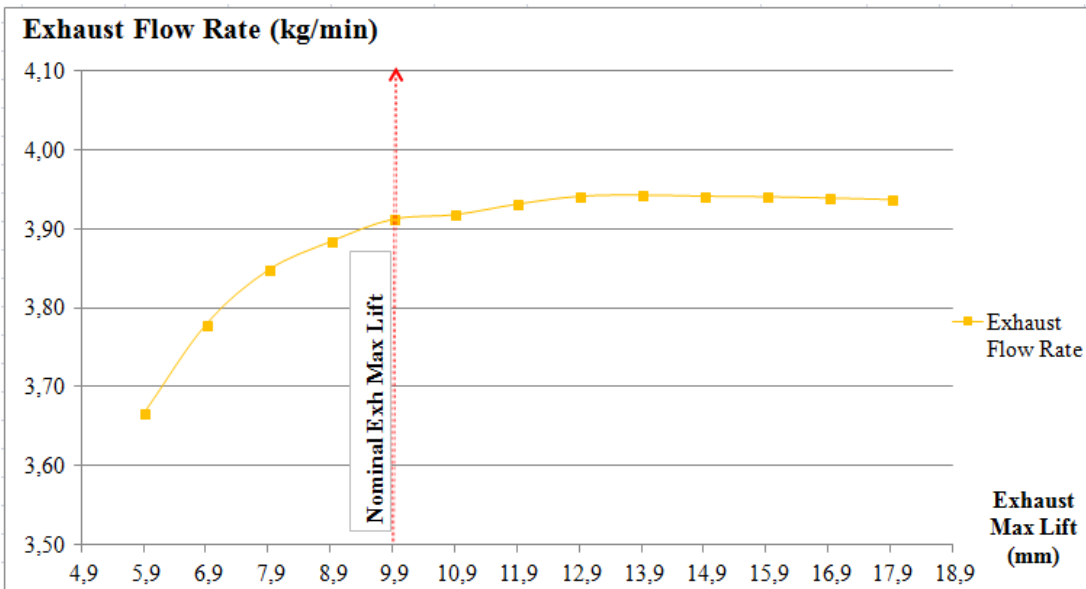


**Figure 4.39 :** Exhaust flow rate change for higher & lower exhaust max. valve lifts.

It can be derived from the change of both inlet&exhaust max. valve lifts that using lower inlet and higher exhaust max. lifts seem to be the best option in the system so as to have a diesel engine performance without fuel penalty in comparison to nominal valve timings and maximum lifts. On the next part, the impacts of utilizing this method at 1200 rpm engine speed and 2.50 bar bmep constant engine loading will be examined.

#### 4.6.3 Using lower inlet and higher exhaust maximum valve lifts

On former sections, it is seen that decreasing inlet and increasing exhaust max. valve lift is expected to be beneficial for attaining higher than 250°C TET without fuel consumption penalty. Therefore, effect of this variable max. lift method is examined in this part. The first parameter examined is change of TET. Variation of TET at lower inlet and higher exhaust max. valve lifts are shown in Figure 4.40 below.

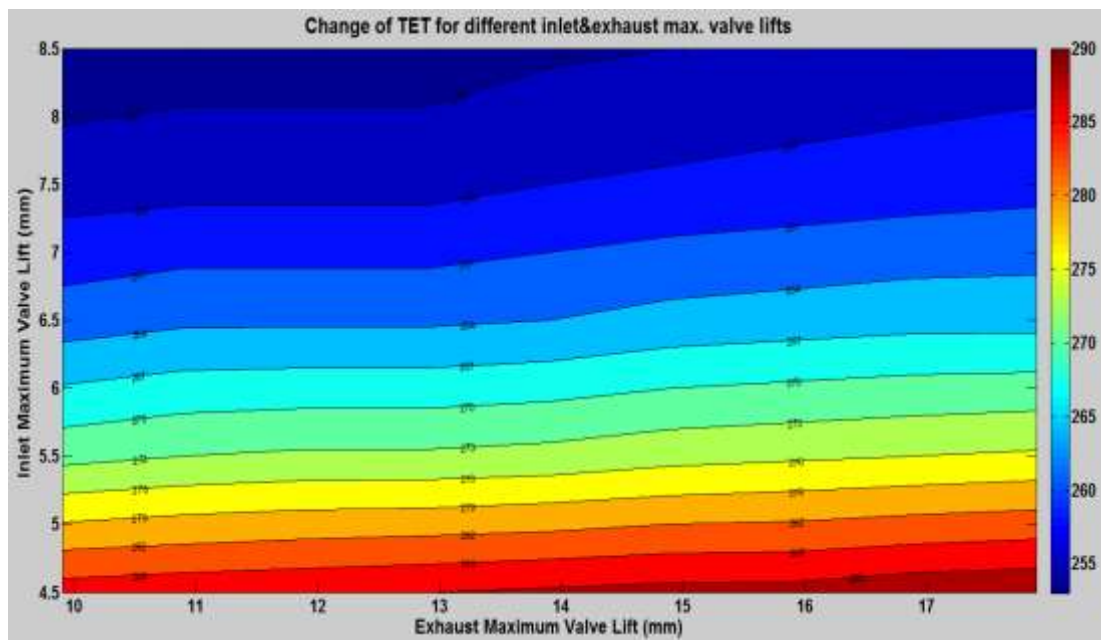


**Figure 4.40 :** TET (°C) for lower inlet and higher exhaust maximum valve lifts.

As it is demonstrated on Figure 4.40 above, TET is rising sharply when inlet max. lift is decreased lower values than the nominal lift. Increasing exhaust max. valve lift does not have a significant effect on TET as expected. As seen previously on Figure 4.36 TET becomes almost the same along exhaust lifts. At least, it can be asserted that there is not a negative effect on TET. For the smallest inlet and higher exhaust max. lift, TET reaches close to 290°C. It is much higher than 250°C. Indeed, the higher the TET is, the faster the thermal management process is. It can speed up the

heat transfer from the exhaust gases to the catalyst substrate and rise the conversion efficiency in a faster manner. However, increasing only TET is not sufficient. Heat transfer depends also on exhaust gas flow. Therefore, exhaust flow rate going directly to the aftertreatment system should also be considered. Change of exhaust flow rate is shown on Figure 4.41 below.

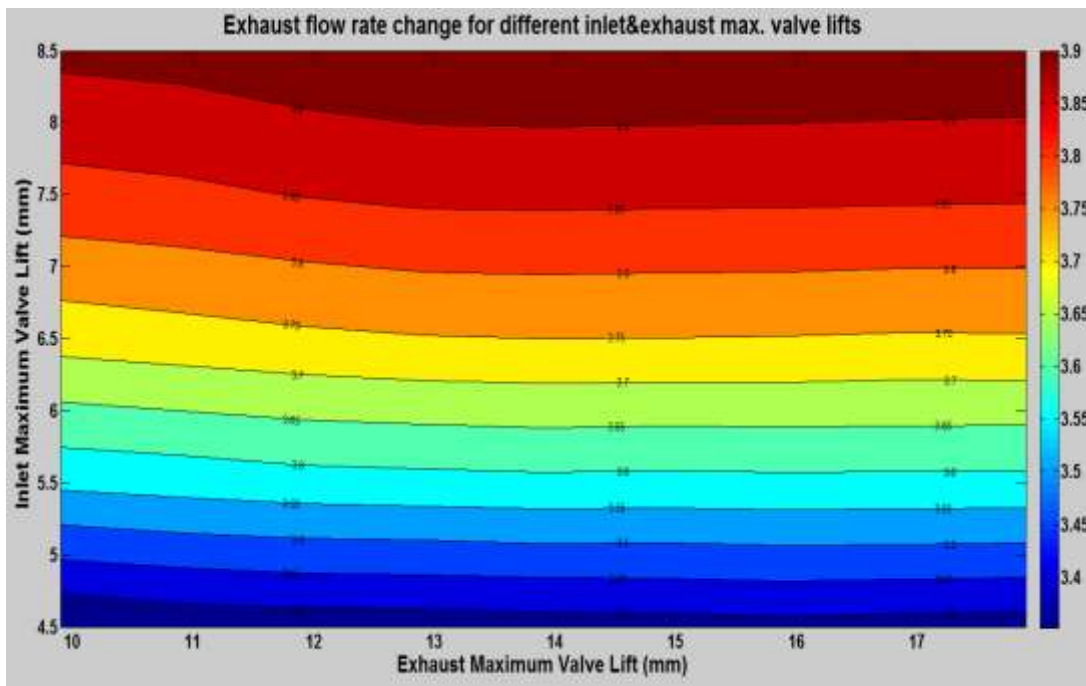


**Figure 4.41 :** Exhaust flow rate (kg/min) change for lower inlet and higher exhaust maximum valve lifts.

When the variation of exhaust flow rate on Figure 4.41 above is analyzed, it can be derived that exhaust max. lifts do not have an important impact on the flow rate. This is similar to the results calculated on Figure 4.39. However, flow rate is reducing dramatically for the lower inlet max. lifts. This is also an expected result. Because air induction reduces at smaller inlet max. lifts and that leads to decreased exhaust flow rate.

The exhaust flow rate decreased to almost 3 kg/min when IVC is advanced 65 degrees CA from the nominal timing on the validation. That is equal to virtually 36 % reduction in comparison to nominal timing. It is observed on Figure 4.41 that although the decrease on exhaust flow rate seems to be above 3 kg/min, there is no doubt that the fall is significant. But, inlet max. lift does not have to be decreased to close to 4.5 mm value on Figure 4.41. Since, TET is still higher than 250°C at higher than 4.5 mm lift cases. However, in order to determine which area on the figure can be most appropriate to utilize on the system, change of bsfc should also be

considered. The fuel consumption requirement variation is seen on Figure 4.42 below.

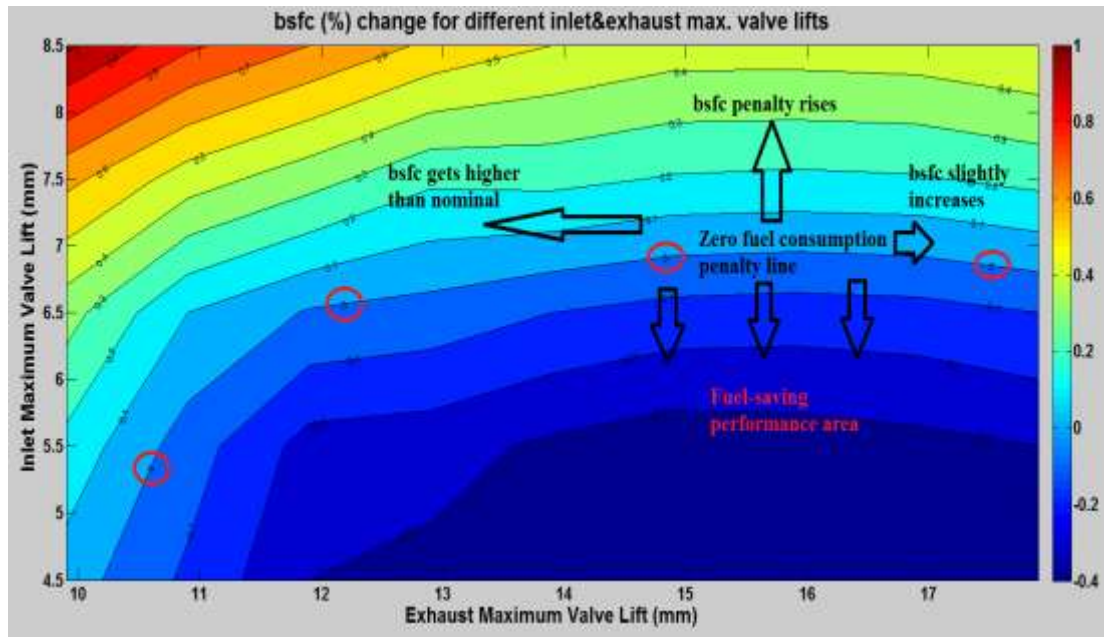


**Figure 4.42 :** bsfc change (%) variation in comparison to nominal max. valve lifts.

It is definite that decreased inlet and increased exhaust max. lifts are reducing the 1 % fuel consumption penalty to zero and even to below zero (fuel efficient) engine performance. However, fuel efficient zones have very low exhaust flow rates. That may affect the thermal power ( $m_{\text{exhaust flow}} * C_p * TET$ ) negatively. Therefore, change of thermal power on Figure 4.43 below is also examined to decide most proper zone.

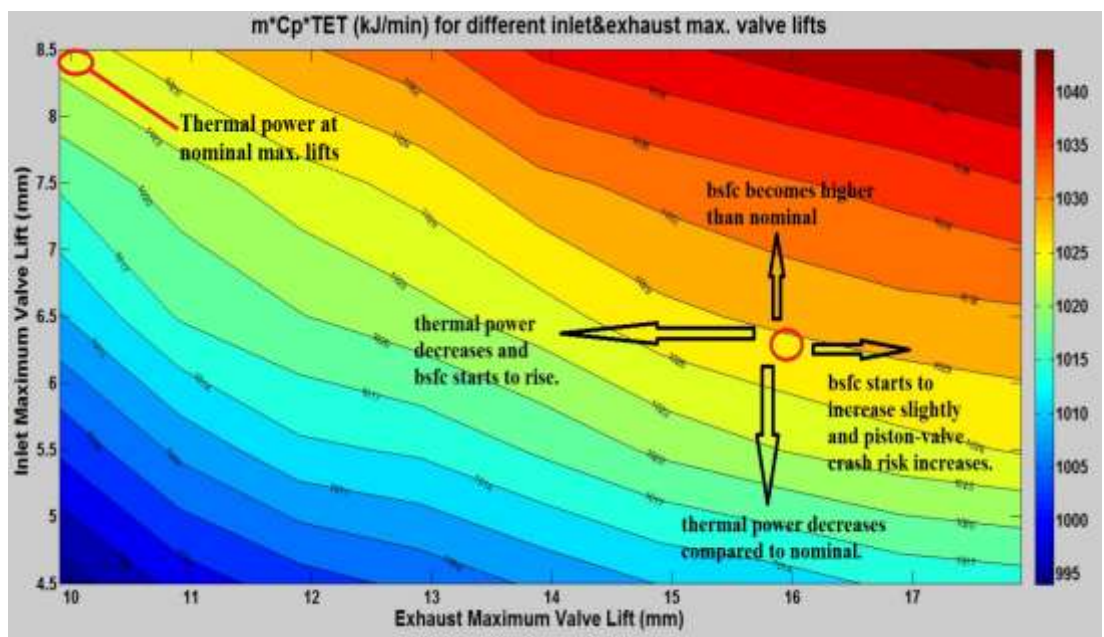


**Figure 4.43 :**  $m_{\text{exhaust flow}} * C_p * TET$  variation for different maximum valve lifts.

When thermal power variation for different inlet and exhaust max. valve lifts are analyzed on Figure 4.43 above, it is seen that thermal power at nominal valve lifts can be obtained at lower inlet and higher exhaust max. lifts. That means the rise on TET observed on Figure 4.40 can compensate the reduction on exhaust flow rate seen earlier on Figure 4.41 at least on some parts of the graph. Other than this constant thermal power line, points have both advantages and disadvantages and the circled area is chosen considering these pros and cons.

The circled area on the figure is 6.5 mm inlet and 15.9 exhaust max. lift point. At that point, thermal power is slightly higher than the nominal. However, there is no fuel consumption penalty as shown on Figure 4.42. When we go upward from that point, thermal power increases, but bsfc penalty rises too. For the lower points, the area is fuel saving, however, exhaust flow rate falls and so does thermal power. On the right side of that point, bsfc begins to increase slightly, there is not a significant change on the thermal power and also it increases the risk of piston-valve crash. There is no need to take extra risks while no extra benefit comes from increasing exhaust max. lift further than that point. On the left side of that circle point, once again the system starts to perform with higher fuel injection rate and also thermal power begins to lessen. The circled point satisfies the zero fuel consumption penalty and enables 265° C TET which is higher than 250°C target temperature. Moreover, exhaust flow rate decreases to only 3.75 kg/min which is 21 % less than the nominal. When compared with the 36 % reduction achieved on the validation part, the circled point definitely improves the exhaust flow rate in the system too.

The application is explained on the former sections for a particular point, 1200 rpm engine speed and 2.50 bar bmep engine loading. And it is seen that the application can be successful when EEVO and EIVC is combined with proper inlet and exhaust max. lifts (lower inlet and higher exhaust max. lifts). After noticing the benefits of the method on this special point, the study can be extended to other performance points of the diesel engine. The nominal TET and exhaust flow rate variation were calculated previously on Figure 4.17 and Figure 4.18 on section 4.3. Now, the method can be applied to different engine speeds (from 1000 rpm to 2000 rpm engine speed) and engine loadings (from 1 bar to 5 bar) in order to observe where it is most effective and also at which points it is least effective or has no effect at all on TET and exhaust flow rate.

#### 4.7 Application of EIVC & EEVO with Low Inlet and High Exhaust Max. Lifts

On the previous section, the VVT strategy with low inlet and high exhaust max. lifts was found to be useful for rising TET and thermal power of the exhaust gases without requiring any excessive fuel consumption compared to nominal valve timings. The application area can now be widened to observe the effect on the whole engine performance zone.

TET change for different engine speeds and various engine loadings with the VVT method can be seen on Figure 4.44 below. IVC timings are advanced 40 degrees CA from nominal timing and inlet and exhaust max. lifts are kept at 6.50 mm and 15.90 mm as applied on the former section. For the same IVC and EVO timings and max. lifts on other points, fuel consumption penalty becomes higher or lower than the one achieved on nominal timings. Therefore, only EVO is advanced more or less than 90 degrees CA BBDC in order to attain zero bsfc penalty on those performance points too.

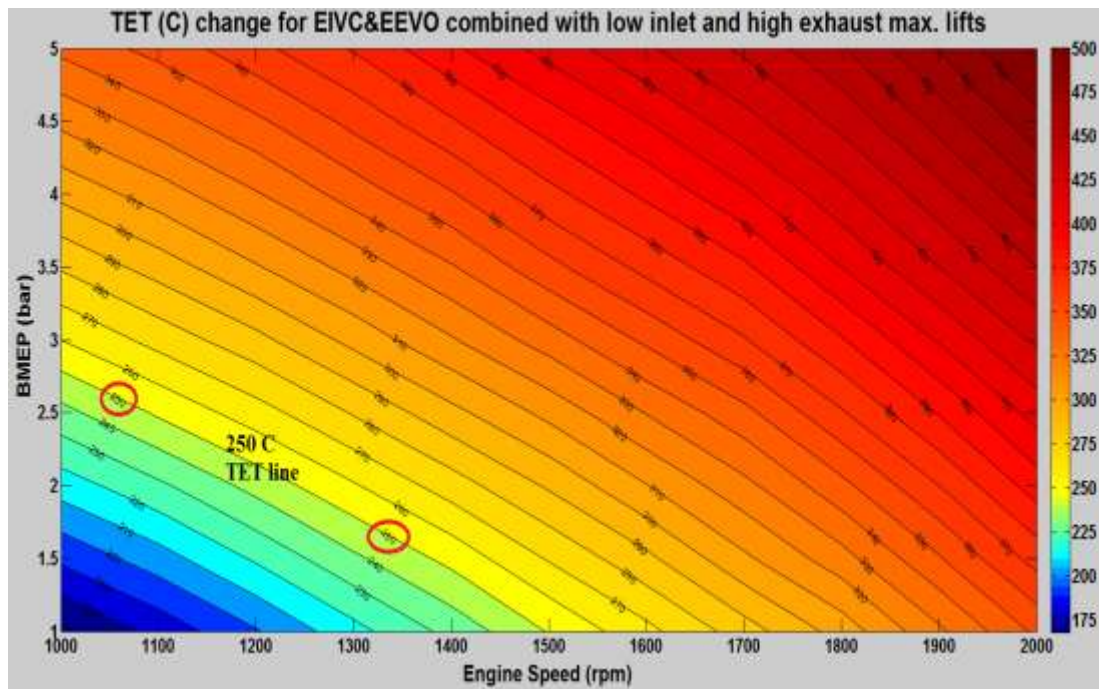


**Figure 4.44** : TET ( $^{\circ}$ C) variation on diesel engine performance zone.

As it is shown on Figure 4.44 above, TETs increase in all parts of the performance zone in comparison to the nominal TETs achieved on Figure 4.17. 250 $^{\circ}$ C target TET line is decreased to lower engine loadings. For instance, it reduced from 4.50 bar to almost 2.75 bar for 1000 rpm engine speed and from 3.50 bar to 1.0 bar for 1500 rpm

engine speed. Moreover, engine speeds higher than 1500 rpm have TETs greater than 250°C and low speed and low loading points are much closer to 250°C compared to nominal TETs. However, when the figure is examined explicitly, it can be derived that the method is especially beneficial for higher engine speeds and higher engine loadings. Also, there is still a performance area below 2.50 bar bmep for low engine speeds where TET is below 250°C. This can also be seen by examining the TET rise change on Figure 4.45 below.

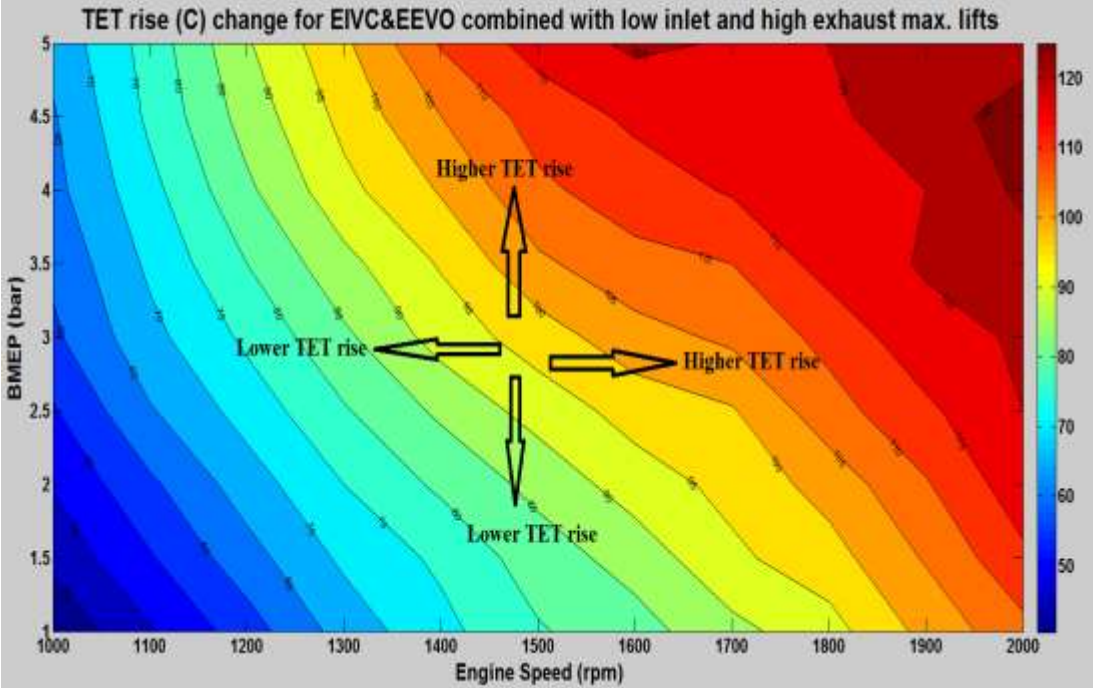


**Figure 4.45 :** TET rise (°C) variation with VVT on diesel engine performance zone.

As it is demonstrated above on Figure 4.45, TET rise is getting higher when engine speed or engine loading is increased. This is because more fuel is needed for these performance areas. In contrast, lower fuel injection rate is sufficient to achieve lower engine speeds and lower engine loadings. In fact, this is why those points have TETs much lower than 250°C at nominal valve timings and results in lower conversion efficiency on aftertreatment systems. However, the method is capable of increasing the TET up to 75°C for these low speed & low loading area and that results in more efficient exhaust thermal management system for most of the diesel engine performance zone. Also, since the TET rise requirement decreased on those points, some other methods (for instance electrically heating or different injection strategies) can be applied on the system in order to reduce the 250°C TET line further down to lower engine loadings.

Exhaust flow change should also be analyzed because heat transfer to the catalyst substrate depends also on exhaust gases flow rate. Similar to Figure 4.18 calculated on section 4.3 for nominal valve timings, the VVT method leads to the exhaust flow variation on the performance area shown on Figure 4.46 below.

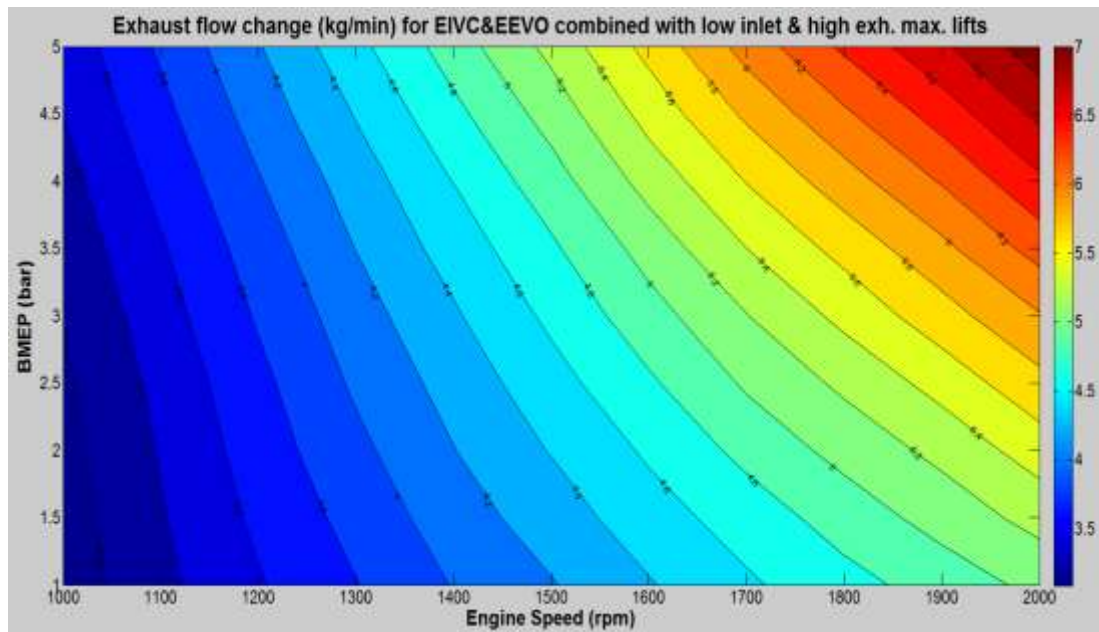


**Figure 4.46 :** Exhaust flow variation with VVT on diesel engine performance zone.

As expected, exhaust flow rate decreases with the application in comparison to nominal timings. This is even better seen on Figure 4.47 below which shows the exhaust flow rate reduction percentage compared to nominal timings.

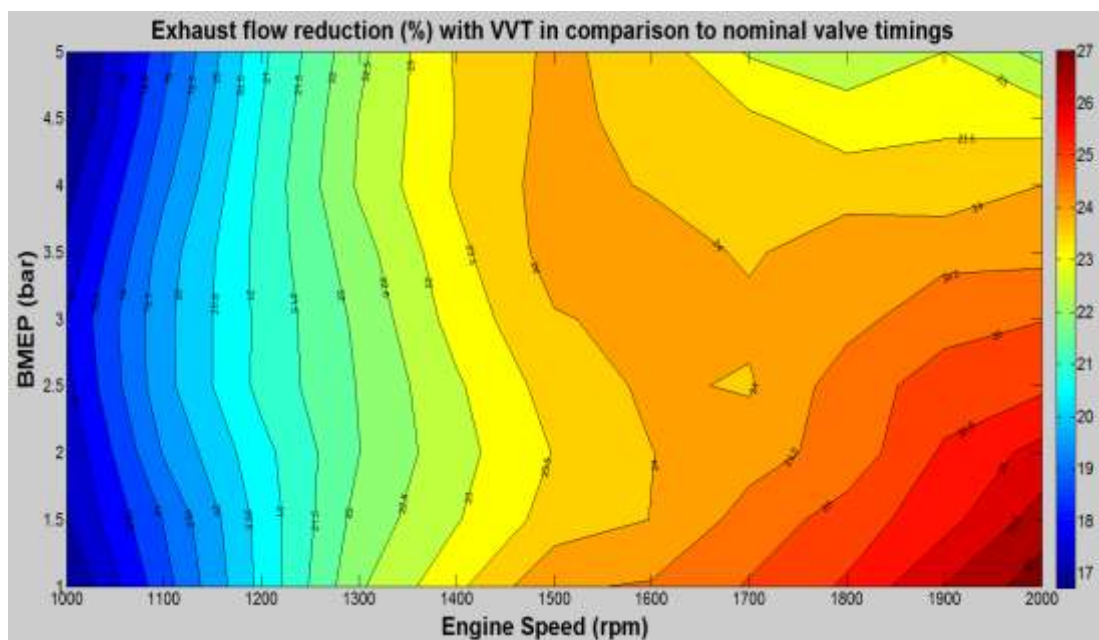


**Figure 4.47 :** Exhaust flow rate reduction compared to nominal valve timings.

It can be derived from Figure 4.47 above that the method causes greater reductions on high engine speed cases. At high engine speeds, more air should be inducted into the cylinder for the same time period. The flow rate is faster than low engine speeds and using EIVC on those areas may decrease the air inducted (in percentage) more than lower engine speeds. However, on these points, exhaust flow is already much higher than lower speeds for both nominal valve timings and also for the VVT case. Therefore, exhaust flow rate reduction on low speeds is more important than higher speeds. High reductions on those points can affect the heat transfer to the catalyst substrate negatively. But as seen on Figure 4.47 above, the reductions are relatively low for low engine speeds. It can be deduced that the intention to keep exhaust flow reductions at smaller percentage is achieved for the performance zone. If it is remembered, the flow rate had to be decreased 36 % on the validation for reaching higher than 250°C TET. On low loading & low engine speed zone, the reduction is lower than that and TETs are much higher than nominal.

Exhaust flow rates decrease, however, TETs are rising for the same points on the performance map. It is not known whether increased TET compensates the reduced exhaust flow rate. Therefore, method's impact on the thermal power ( $m_{\text{exhaust flow}} \cdot C_p \cdot \text{TET}$ ) of the performance area must also be analyzed. Using Figure 4.17 and 4.18 on section 4.3, thermal power change for nominal valve timings can be obtained with the Figure 4.48 seen below.

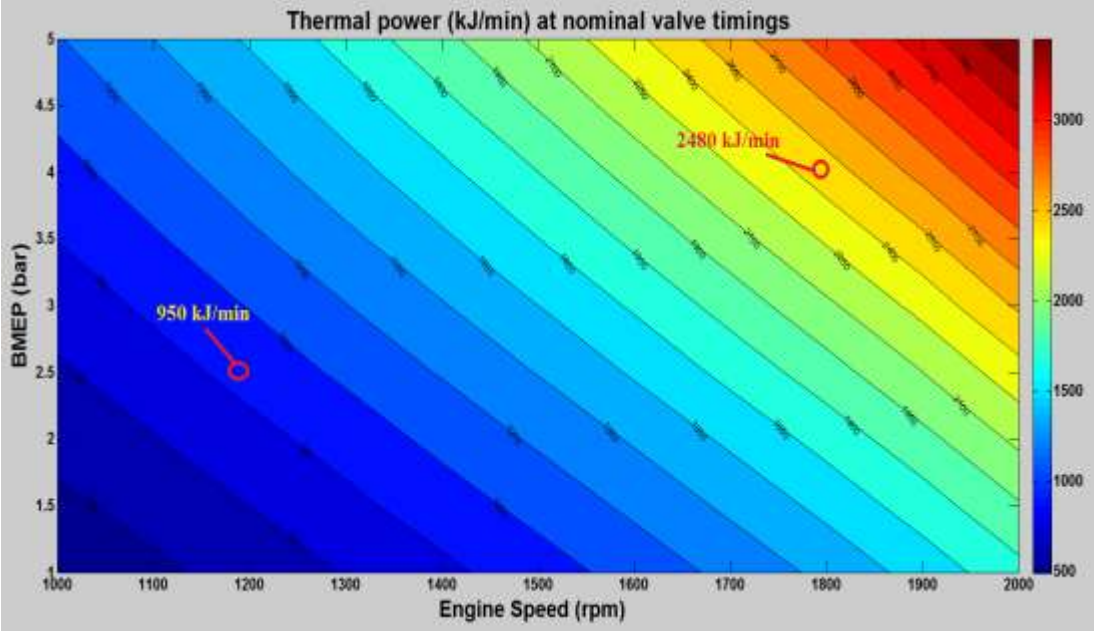


**Figure 4.48 :** Variation of thermal power at nominal valve timings.

As it is demonstrated above on Figure 4.48, thermal power of the diesel engine is increasing for higher engine speeds and higher engine loadings. Two points are chosen to show the change on thermal power with numbers. One of them is at a low speed and low engine loading case and the other is a high speed and high engine loading point. As expected, there is a high thermal power difference between those points. However, when Figure 4.49 below is examined; with the VVT method, these two separate points have both higher thermal power compared to nominal timings. This can be better observed on the thermal power rise variation on Figure 4.50 below.

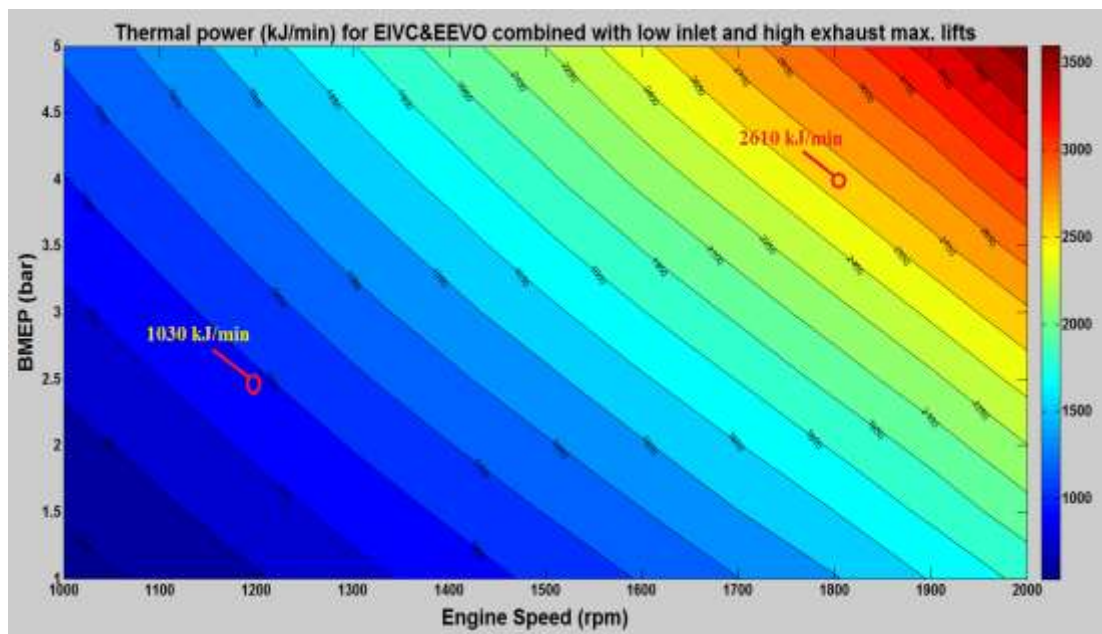


**Figure 4.49 :** Thermal power change with VVT and low inlet & high exh. max. lifts.

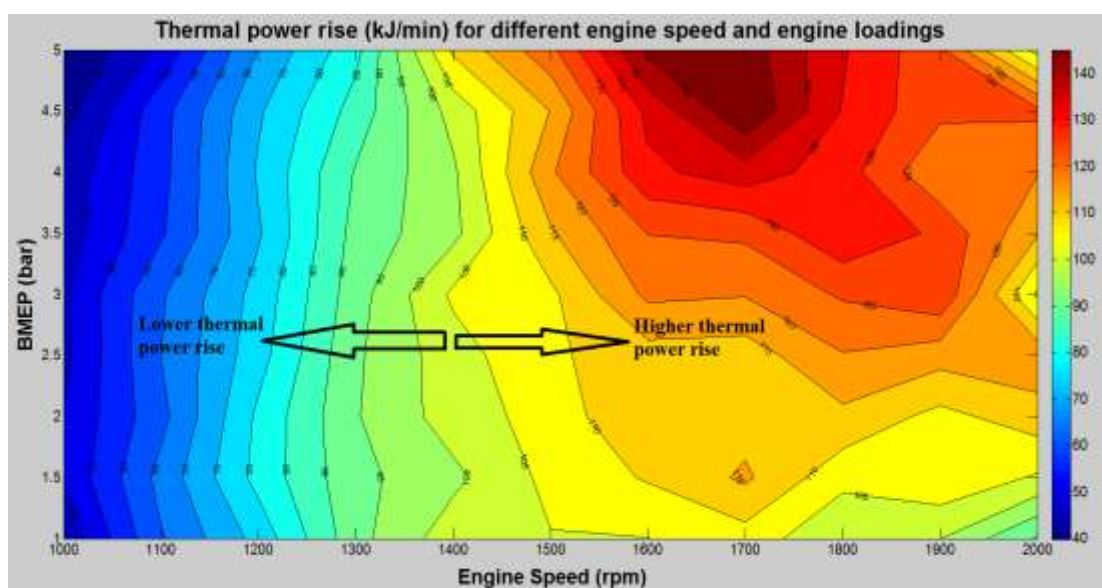


**Figure 4.50 :** Thermal power rise with VVT and low inlet & high exh. max. lifts.

As it is shown above on Figure 4.50, greater thermal power rise can be attained on higher engine speeds and higher engine loading cases. Although exhaust flow rates decrease more at these points, it is known from Figure 4.45 that TET rise on high engine speeds is much higher than lower engine speeds. Therefore, TET rise percentage becomes much higher than the exhaust flow reduction percentage on these points and thermal power increases in comparison to nominal valve timings. On the other hand, thermal power increases for low engine speeds too. The rise may be lower than high engine speeds, however, it is important to note that exhaust flow rate decreases for these points too and TET rise obtained is still capable of raising the thermal power without requiring any fuel consumption penalty.

To summarize the VVT method applied on this section; after validating the results of the simulation with experimental results by using EIVC and LIVC, the effects of IVC timings on other engine performance parameters are examined and it is seen that it affects the exhaust flow rate negatively.

## **5. CONCLUSIONS**

In this section of the study, conclusions obtained from the simulations are given and general evaluation of the study is made. Then, some recommendations for the future studies concerning utilization of VVT on increasing the efficiency of exhaust thermal management systems are explained.

### **5.1 Conclusions**

The emission criteria for these widely used machines has become stricter and stricter since 1994 and it seems it will be more stringent in the future too. Particularly, environmental protection agencies are really sensitive about the negative effects of high rates of emissions. Therefore, diesel engines with low rates of emissions has become the first goal of engine manufacturers.

Modern aftertreatment systems are definitely effective at reducing the NO<sub>x</sub>, unburned HCs, CO and PM emissions from diesel engines. Engine producers are generally preferred to use these exhaust thermal management systems to meet the emission limits. However, these systems have a major drawback. They are temperature-reliant. In other words, catalyst substrates in these systems need at least 250°C in order to acquire an efficient emission conversion efficiency. This can only be achieved when exhaust gas temperatures releasing from diesel engines can be kept above 250°C temperature. But, particularly at low engine speed and at low engine loading conditions, exhaust gas temperatures become much lower than 250°C. Therefore, emission standards cannot be attained for these cases due to the inefficient aftertreatment systems.

As the problem is stated in an explicit manner, a method should be applied to diesel engine for these low speed, low loading performance zone in order to overcome the less efficient exhaust thermal management. Therefore, the primary objective of this study is stated as the utilization of VVT on a Cummins ISB type, six-cylinder, turbocharged and intercooled diesel engine so as to rise TET values higher than

250°C and provide more efficient aftertreatment system for more areas on the engine performance map.

The diesel engine simulated with LES has experimental results at 1200 rpm and 2.50 bar bmep engine loading. These results are obtained by sweeping the IVC timings backward and forward from nominal timing [68]. The simulation results show good correlation with those experimental results. The first goal of the study is to have a validated simulation model in order to predict TET for different engine speed and engine loading cases. Therefore, the similarity between simulation and experimental results for TET and volumetric efficiency proves the reliability of the simulation model.

EIVC and LIVC are definitely effective for increasing TET for low loading engine cases. It is proved in the simulation that up to 55°C TET rise can be accomplished when IVC is closed earlier and later than nominal timing. The loading is managed constant at 2.50 bar bmep at 1200 rpm by changing the fuel injection rate. It is seen that while up to 100 degrees CA retardation is needed to satisfy greater than 250°C exhaust gas temperatures, only 65 degrees CA advancing is sufficient to achieve same target TET point. Not only do these early and late sweepings raise TETs close to 250°C, but also they lead to fuel-saving by decreasing the pumping losses in the system. The lower pumping losses come from the decreased volumetric efficiency values at these timings which reduce the air induction into the system.

Although early or late IVC is a good solution to increase TETs beyond 250°C, these valve timings have a negative effect on the system too. They result in a major reduction of exhaust flow rate in comparison to nominal timing. The decrease is up to 36 % with EIVC since the volumetric efficiency goes lower than 65 % in the earliest timing. For LIVC, the reduction is up to 30 % because the volumetric efficiency is close to 70 % for the latest closing timing. However, this is still a substantial decline compared to nominal exhaust flow rate value.

Exhaust flow rate is important in the system because heat transfer from the exhaust gases to the catalyst substrates depend on both TET and exhaust flow rate. So, increasing TET above 250°C with a high reduction on exhaust flow rate cannot be as effective as expected on aftertreatment systems, particularly for low loading cases where higher TET rises are demanded to reach 250°C temperature. Therefore, other

valve timings are examined in the system in order to combine with EIVC and provide same high TETs with higher exhaust flow rates. While changing other valve timings, the limit is stated as there will not be any fuel consumption penalty in comparison to nominal valve timings and nominal maximum lifts.

LIVO is not really effective at rising TET. It also decreases the exhaust flow rate. EEVC is indeed found to be an attractive solution to increase TETs. Advancing 35 degrees CA from nominal closing timing is adequate to reach higher than 250°C. However, it results in approximately 25 % exhaust flow rate reduction compared to nominal closing timing. When EEVO is examined it is seen that this method increases TETs rapidly and also it does not have a negative effect on exhaust flow rate, even has positive effect for higher advanced EVO timings. But this method has a cost on the system too. It also raises the fuel consumption in the system. Since EIVC is found to be fuel-efficient, EIVC and EEVO combination is preferred to be utilized in the system.

EIVC&EEVO combination results in TET very close to 250°C. IVC is only advanced 40 degrees CA from nominal and EVO is advanced 70 degrees CA from nominal opening timing. Less advanced IVC timing is sufficient to achieve 250°C TET compared to the validation case where IVC has to be advanced 65 degrees CA from nominal closing timing. Therefore, exhaust flow rate reduction becomes only 18 % in comparison to nominal case. However, this method causes a little bit more than 1 % fuel consumption penalty in the system.

Change of inlet and exhaust maximum valve lifts is investigated so as to minimize the 1 % fuel injection rate rise in the system. It is shown that lower inlet maximum lifts result in TET rise and bsfc reduction in the system. Increased TET comes from the lower air induction and decrease in fuel penalty stems from the lower pumping losses in the system. It is also demonstrated that higher exhaust maximum lift does not have a significant effect on TET and exhaust flow rate. Yet, it is useful to lessen the bsfc. As the exhaust gases are better released with higher exhaust maximum lifts and there is lower residual gases for the next cycle, the system may need lower fuel to achieve the same engine loading with this method. Therefore, combined EIVC and EEVO can be improved more by lower inlet maximum lifts and higher exhaust maximum lifts for obtaining higher TETs without fuel consumption penalty. Thermal power of exhaust gases can be kept constant without any need of extra fuel.

Finally, as the method is successful to meet high TETs with lower reduced exhaust flow rates compared to validated case, it is considered that it can be applied to different engine speeds and engine loadings. When it is implemented for engine speeds from 1000 rpm to 2000 rpm and engine loadings changing from 1.0 bar bmep to 5.0 bar bmep, it is seen that 250°C target TET line can be declined to lower engine loadings with this method. For instance, the system needs to be at least 4.25 bar bmep engine loading at 1200 rpm speed to attain 250°C temperature. However, the method reduced that engine loading to almost 2.25 bar bmep. Up to 120°C TET rise can be obtained in the system. It is generally seen that high engine speed and high engine loading cases have higher TET rises and lower speed and lower loading conditions. Therefore, lower than 2.50 bar engine loading and lower than 1500 rpm engine speed conditions are still below 250°C temperature. However, the temperatures are higher than nominal valve timings and the system does not require fuel consumption penalty.

Exhaust flow reduction is inevitable for the whole engine performance map due to the advanced IVC timings. However, when thermal power at nominal valve timings is compared with the one achieved via VVT, it can be derived that thermal power of exhaust gases rises on the whole engine performance zone. In other words, high TET rise compensates the reduction on exhaust flow rate and even increases the thermal power on the system. More importantly, this is accomplished without requiring any additional fuel injection. Thermal power rise is up to 140 kJ/min. But the rise reduces down to 50 kJ/min for low loading and low engine speed cases. Similar to TET rise graph, higher thermal power raise is calculated at high speed and high loading conditions.

## **5.2 Recommendations for Future Work**

Thermal management of exhaust gases is indeed a complicated task. Different valve timing methods has different positive and negative effects on the efficiency of aftertreatment systems. While EIVC and LIVC increases the TET, they also reduce the exhaust flow rate significantly. When EEVO is considered as a solution, although it rises rapidly the TET, it has a major negative effect on bsfc. It is obvious that there is always a tradeoff in the system when VVT is applied into the system for higher than 250°C TET values.

The simulation has similar results with the experiments at 1200 rpm and 2.50 bar bmep engine loading. However, there is not experimental results for combined EIVC and EEVO cases and also lower inlet and higher exhaust maximum valve lifts. Modeling results should be validated with experimental results in the future for this VVT method at least for some low loading and low engine speed cases where there needs more TET rise to attain 250°C. Simulation can only be improved to achieve realistic results by comparing the model results with experimental results.

Also, VVT search can be specified for a particular engine load and engine speed case. In this study, the method is applied for the whole engine performance zone. Although it seems to be successful for most of the area, IVO and EVC timings can also be changed for some points to acquire more TET rise. Moreover, change of inlet and exhaust maximum valve lifts can be altered differently for different speed and loading cases. The important point here is that a deeper analysis is required to find out which VVT strategy is the most appropriate to satisfy adequate thermal management of exhaust gases for different engine loading points without causing fuel consumption penalty or at least with the lowest fuel rise.

VVT proved to be a useful method in earlier studies for thermal management of exhaust gases. The same is valid in this study too. However, for low engine speed and low engine loading cases, it is seen that utilizing only VVT is not sufficient to reach greater than 250°C temperatures. Therefore, other methods can be combined with VVT particularly at these points. Multiple fuel injection, high injection pressure, late fuel injection and exhaust gas recirculation can be some of the methods to combine with VVT. However, these methods may require some tradeoffs in the system too similar to different VVT methods. Therefore, the combination should be optimized for particular engine performance points.

Inlet and exhaust valve lift profiles can be changed. In this study, only maximum lift values are altered and it is seen that change of lifts can affect the system slightly. However, different lift profiles for different engine loadings may be beneficial for TET rise or decreasing fuel consumption penalty. The distance between piston and valve at TDC should be considered while valve lift profiles are changed in order not to cause a piston-valve crash in the system. Actually, simulation programs like LES can give the user the chance to alter valve profiles easily for many different cases. Therefore, several points can be examined in a shorter time using these programs.

Another VVT option is to apply EVO during intake valve timing or vice versa. Opening EVO during intake valve timing may result in backflow of exhaust gases into the cylinder before combustion and increase TET. However, if more exhaust gases flows back into the cylinder, that may affect combustion negatively and results in bsfc rise in the system. There is another tradeoff here too. The duration of the opening timing of exhaust should be optimized for different engine speed and loading situations.

Besides, effect of VVT on transient states of the diesel engine can be examined in the future. In this study, the loadings are kept constant by increasing or decreasing the fuel injection rate in the system. However, diesel engines do not perform in a steady state manner all the time. The loadings can be required to increase rapidly in some situations from lower bmep to higher bmep or vice versa. For instance, EIVC and LIVC may not be as appropriate as the steady state case to obtain greater than 250°C TETs. Because these timings result in a major volumetric efficiency reduction and that may affect the engine negatively while trying to go from a lower loading to higher loading. There will be different tradeoffs for transient cases when VVT is implemented and it is worthwhile to investigate in future studies.

## REFERENCES

- [1] **Url-1** <<http://www.cumminsemissionsolutions.bitnamiapp.com>>, On-Highway Emissions Regulations, date retrieved 30.08.2016.
- [2] **Url-2** <[http://www3.epa.gov/region1/eco/diesel/basic\\_info.html](http://www3.epa.gov/region1/eco/diesel/basic_info.html)>, Environmental Protection Agency Standards for New Trucks and Buses, date retrieved 30.08.2016.
- [3] **Charlton, S., Dollmeyer, T., and Grana, T.** (2010). Meeting the us heavy-duty epa 2010 standards and providing increased value for the customer. *SAE International Journal of Commercial Vehicles*, 3(1):101-110, 2010.
- [4] **Akiyoshi, T., Torisaka, H., Yokota, H., Shimizu, T., Ninomiya, H., and Narita, H.** (2011). Development of efficient urea-scr systems for epa 2010-compliant medium duty diesel vehicles. *SAE Paper 2011-01-1309*, 2012, pp. 6-18.
- [5] **Johnson, T. V.** (2012). Vehicular emissions in review. *SAE International Journal of Engines*, 5(2):216-234, 2012.
- [6] **Girard, J., Cavataio, G., Snow, R., and Lambert, C.** (2008). Combined Fe-Cu SCR systems with optimized ammonia to NOx ratio for diesel NOx control. *SAE International Journal of Fuels and Lubricants*. 1(1): 580-589, 2008.
- [7] **Lambert, C., Hammerle, R., McGill, R., Khair, M., and Sharp, C.** (2004). Technical advantages of urea SCR for light-duty and heavy-duty diesel vehicle applications. *SAE Trans 2004; 113(4):580-589*, 2004.
- [8] **Koebel, M., Elsener, M., and Kleemann, M.** (2000). Urea-SCR: a promising technique to reduce NOx emissions from automotive diesel engines. *Catal Today 2000; 59(3): 335-345*.
- [9] **Mojghan, N., Raymond, C., Howard, H., and Aydin, C.** (2015). Development of emission control systems to enable high NOx conversion on heavy duty diesel engines. *SAE International Journal of Engines*, 8(3):1144-1151, 2015.
- [10] **Stanton, D., Charlton, S., and Vajapeyazula, P.** (2013). Diesel engine technologies enabling powertrain optimization to meet US greenhouse gas emissions. *SAE International Journal of Engines*, 6(3):1757-1770, 2013.
- [11] **Walker, A.** (2004). Controlling particulate emissions from diesel vehicles. *Top Catal 2004; 28(1-4): 165-170*.
- [12] **Allanson, R., Blakeman, P., Cooper B., Hess, H., Silcock, P., and Walker, A.** (2002). Optimising the low temperature performance and regeneration efficiency of the continuously regenerating diesel particulate filter (CR-DPF) system. *SAE Paper 2002-01-0428*, 2002, pp.5-10.

- [13] **Stadlbauer, S., Waschl, H., Schilling, A., and del Re, L.** (2013). DOC temperature control for low temperature operating ranges with post and main injection actuation. *SAE technical paper 2013-01-1580, 2013.*
- [14] **Song, X., Surenahalli, H., Naber, J., Parker, G., and Johnson, J. H.** (2013). Experimental and modeling study of a diesel oxidation catalyst (DOC) under transient and CPF active regeneration conditions. *SAE Paper 2013-01-1046, 2013, pp.10-11. 1*
- [15] **Ye, S., Yap, Y. H., Kolaczowski, S. T., Robinson, K., and Lukyanov, D.** (2012). Catalyst 'light-off' experiments on a diesel oxidation catalyst connected to a diesel engine - Methodology and techniques. *Chemical Engineering Research and Design. Vol. 90, pp.834-845, 2012.* DOI: 10.1016/j.cherd.2011.10.003.
- [16] **Asmus, T. W.** (1982). Valve events and engine operation. *SAE Paper no. 820749.*
- [17] **Gray, C.** (1988). A review of variable engine valve timing. *SAE Paper no. 880386.*
- [18] **Dresner, T. and Barkan, P.** (1989). A review and classification of variable valve timing systems. *SAE Paper no. 890674.*
- [19] **Ahmad, T. and Theobald, M. A.** (1989). A survey of variable valve actuation technology. *SAE Paper no. 891674.*
- [20] **Stone, R. and Kwan, E.** (1989). Variable valve actuation mechanisms and the potential for their application. *SAE Paper no. 890673.*
- [21] **Ham, Y. Y. and Park, P.** (1991). The effects of intake valve events on engine breathing capability. *SAE Paper no. 912470.*
- [22] **Demmelbauer-Ebner, W., Dachs, A. and Lenz, H. P.** (1991). Variable valve actuation systems for the optimization of engine torque. *SAE Paper no. 910447.*
- [23] **Kreuter, P., Heuser, P. and Schebitz, M.** (1992). Strategies to improve SI-engine performance by means of variable intake lift, timing and duration. *SAE Paper no. 910447.*
- [24] **Lancefield, T. M., Gayler, R. J. and Chattopadhyay, A.** (1993). The practical application and effects of a variable event valve timing system. *SAE Paper no. 930825.*
- [25] **Shiga, S., Yagi, S., Morita, M., Matumoto, T., Karasawa, T., and Nakamura, H.** (1996). Effects of early-closing of intake valve on the engine performance in a spark-ignition engine. *The Japan Society of Mechanical Engineers. No. 95-1118, pp. 1659-1665.*
- [26] **Moro, D., Ponti, F., and Serra, G.** (2001). Thermodynamic analysis of variable valve timing influence on SI engine efficiency. *SAE Technical Paper Series 2001-01-0667.*
- [27] **Sher, E., and Bar-Kohany, T.** (2002). Optimization of variable valve timing for maximizing performance of an unthrottled SI engine - a theoretical study. *Energy. 27 (2002). pp 757-775.*

- [28] **Hong, H., Parvate-Patil, G. B., and Gordon, B.** (2004). Review and analysis of variable valve timing strategies - eight ways to approach. *Proceedings of the Institution of Mechanical Engineers, Part D: Journal of Automobile Engineering*. 2004 Vol. 218, pp. 1179-1200.
- [29] **Cao, L., Zhao, H., Jiang, X., and Kalian, N.** (2005). Understanding the influence of valve timings on controlled autoignition combustion in a four-stroke port fuel injection engine. *Proceedings of the Institution of Mechanical Engineers, Part D: Journal of Automobile Engineering*. 2005 Vol. 219, pp. 807-823.
- [30] **Çınar, C., and Akgün, F.,** (2007). Effect of intake valve closing time on engine performance and exhaust emissions in a spark ignition engine. *Journal of Polytechnic*. Vol: 10, No: 4, pp. 371-375.
- [31] **Fontana, G., and Galloni, E.** (2009). Variable valve timing for fuel economy improvement in a small spark-ignition engine. *Applied Energy*. Vol:86, pp. 96-105.
- [32] **Boretti, A.** (2010). Use of variable valve actuation to control the load in a direct injection, turbocharged, spark-ignition engine. *SAE International No. 2010-01-2225*.
- [33] **Khan, S. A., and Ayyappath, P.** (2014). Design and development of variable valve timing and lift mechanism for improving the performance of a single cylinder two wheeler gasoline engine. *SAE Paper No. 2014-01-1699*.
- [34] **Endo, S., Otani, T., and Kakinai, A.** (1988). An improvement of pumping loss of high boosted diesel engines. *SAE Paper No. 885102*.
- [35] **Leonard, H. J., Stone, C. R., and Charlton, S. J.** (1991). Parametric investigation of variable valve timing applied to a turbocharged diesel engine. *SAE Paper No. 910453*.
- [36] **Özsoysal, O. A., Söğüt, O. S., Şahin, C., and Sağ, O. K.** (1995). An analytical investigation of variable valve timing on a high speed turbocharged multi-valve marine diesel engine. *ECOS'95, Efficiency, Costs, Optimization, Simulation and Environmental Impact of Energy Systems. July 11-15, ISTANBUL*.
- [37] **Özsoysal, O. A., Söğüt, O. S., Şahin, C., and Sağ, O. K.** (1995). An analytical investigation of variable valve timing on a high speed turbocharged multi-valve marine diesel engine. *ECOS'95, Efficiency, Costs, Optimization, Simulation and Environmental Impact of Energy Systems. July 11-15, ISTANBUL*.
- [38] **Stone, C. R., Leonard, H. J., Elliott, C., Newman, M. J., Charlton, S. J., and Johnston, D. N.** (1995). Parametric investigation of variable valve timing applied to a turbocharged diesel engine. *Proceedings of the Institution of Mechanical Engineers, Part A: Journal of Power and Energy*. Vol:209, pp. 297-311.
- [39] **Benajes, J., Reyes, E., and Lujan, J. M.** (1996). Intake valve pre-lift effect on the performance of a turbocharged diesel engine. *SAE Technical Paper Series, No. 960950*.

- [40] **Lancefield, T., Methley, I., Rase, U., and Kuhn, T.** (2000). The application of variable event valve timing to a modern diesel engine. *SAE Technical Paper Series, 2000-01-1229*.
- [41] **Tai, C., Tsao, T. C., Schörn, N. A., and Levin, M. B.** (2002). Increasing torque output from a turbodiesel with camless valvetrain. *SAE Technical Paper Series, 2002-01-1108*.
- [42] **Lancefield, T.** (2003). The influence of variable valve actuation on the part load fuel economy of a modern light-duty diesel engine. *SAE Technical Paper Series, 2003-01-0028*.
- [43] **Parvate-Patil, G. B., Hong, H., and Gordon, B.** (2004). Analysis of variable valve timing events and their effects on single cylinder diesel engine. *SAE Technical Paper Series, 2004-01-2965*.
- [44] **Murata, Y., Kusaka, J., Odaka, M., Daisho, Y., Kawano, D., Suzuki, H., Ishii, H., and Yuichi, G.** (2006). Achievement of medium engine speed and load premixed diesel combustion with variable valve timing. *SAE Technical Paper Series, 2006-01-0203*.
- [45] **Nevin, R. M., Sun, Y., Gonzalez, M. A., and Reitz, R. D.** (2007). PCCI investigation using variable intake valve closing in a heavy duty diesel engine. *SAE Technical Paper Series, 2007-01-0903*.
- [46] **Sugiyama, T., Hiyoshi, R., Takemura, S., and Aoyama, S.** (2007). Technology for improving engine performance using variable mechanism. *SAE Technical Paper Series, 2007-01-1290*.
- [47] **He, X., Durrett, R. P., and Sun, Z.** (2008). Late intake valve closing as an emissions control strategy at Tier 2 Bin 5 engine-out NO<sub>x</sub> level. *SAE Technical Paper Series, 2008-01-0637*.
- [48] **Yang, B., and Keller, P.** (2008). Analysis of diesel engine emissions reduction by late intake valve close and VTG turbocharger using 1-D simulation. *SAE Technical Paper Series, 2008-01-2444*.
- [49] **Deng, J., and Stobart, R.** (2009). BSFC investigation using variable valve timing in a heavy duty diesel engine. *SAE Technical Paper Series, 2009-01-1525*.
- [50] **Dembinski, H.** (2009). Miller-cycle on a heavy duty diesel engine. *Master of Science Thesis. KTH Industrial Engineering and Management Machine Design, SE-100 44, Stockholm*.
- [51] **Tomoda, T., Ogawa, T., Ohki, H., Kogo, T., Nakatani, K., and Hashimoto, E.** (2010). Improvement of diesel engine performance by variable valve train system. *International Journal of Engine Research. Vol:11, pp. 331-344*.
- [52] **Modiyani, R., Kocher, I., Van Alstine, D. G., Koeberlein, E., Stricker, K., Meckl, P., and Shaver, G.** (2011). Effect of intake valve closure modulation on effective compression ratio and gas exchange in turbocharged multi-cylinder engines utilizing EGR. *International Journal of Engine Research. Vol:12, pp. 617-631*.

- [53] **Kitabatake, R., Minato, A., Inukai, N., and Shimazaki, N.** (2011). Simultaneous improvement of fuel consumption and exhaust emissions on a multi-cylinder camless engine. *SAE International No. 2011-01-0937*.
- [54] **Lemaire, J., Mustel, W., and Zelenka, P.** (1994). Fuel additive supported particulate trap regeneration possibilities by engine management system measures. *SAE Technical Paper Series No. 942069*.
- [55] **Bouchez, M., and Dementhon, J. P.** (1994). Strategies for the control of particulate trap regeneration. *SAE Technical Paper Series No. 2000-01-0472*.
- [56] **Mayer, A., Lutz, Th., Lammle, Chr., Wyser, M., and Legerer, F.** (2003). Engine intake throttling for active regeneration of diesel particle filters. *SAE Technical Paper Series No. 2003-01-0381*.
- [57] **Joshi, A., Chatterjee, S., Sawant, A., Akerlund, C., Andersson, S., Blomquist, M., Brooks, J., and Kattan, S.** (2006). Development of an actively regenerating DPF system for retrofit applications. *SAE Technical Paper Series No. 2006-01-3553*.
- [58] **Singh, P., Thalagavara, A. M., Naber, J. D., Johnson, J. H., and Bagley, S. T.** (2006). An experimental study of active regeneration of an advanced catalyzed particulate filter by diesel fuel injection upstream of an oxidation catalyst. *SAE Technical Paper Series No. 2006-01-0879*.
- [59] **Parks, J., Huff, S., Kass, M., and Storey, J.** (2007). Characterization of in-cylinder techniques for thermal management diesel aftertreatment. *SAE Technical Paper Series No. 2007-01-3997*.
- [60] **Chen, P., and Wang, J.** (2014). Control-oriented model for integrated diesel engine and aftertreatment systems thermal management. *Control Engineering Practice. Vol.22, pp. 81-93*.
- [61] **Schwoerer, J., Kumar, K., Ruggiero, B., and Swanbon, B.** (2010). Lost-motion VVA systems for enabling next generation diesel engine efficiency and aftertreatment optimization. *SAE International No. 2010-01-1189*.
- [62] **Fessler, H. and Genova, M.** (2004). An electro-hydraulic "lost motion" VVA system for a 3.0 liter diesel engine. *SAE International No. 2004-01-3018*.
- [63] **Bohac, S. V. and Assanis, D. N.** (2004). Effect of exhaust valve timing on gasoline engine performance and hydrocarbon emissions. *SAE International No. 2004-01-3058*.
- [64] **De Ojeda, W.** (2010). Effect of variable valve timing on diesel combustion characteristics. Miller-cycle on a heavy duty diesel engine. *SAE International No. 2010-01-1124*.
- [65] **Honardar, S., Busch, H., Schnorbus, T., Severin, C., Kolbeck, A. F., and Korfer, T.** (2011). Exhaust temperature management for diesel engines assessment of engine concepts and calibration strategies with regard to fuel penalty. *SAE Technical Paper Series, 2011-24-0176*.

- [66] **Wickström, A.** (2012). Variable valve actuation strategies for exhaust thermal management on a hd diesel engine. *Master of Science Thesis. KTH Industrial Engineering and Management. Stockholm, Sweden.*
- [67] **Ehleskog, M., Gjürya, S., and Denbratt, I.** (2012). Effects of variable inlet valve timing and swirl ratio on combustion and emissions in a heavy duty diesel engine. *SAE Technical Paper Series, 2012-01-1719.*
- [68] **Garg, A.** (2013). Exhaust thermal management using intake valve closing timing modulation. *Master of Science Thesis. Purdue University. West Lafayette, Indiana. December 2013.*
- [69] **Garg, A., Magee, M., Ding, C., Roberts, L., Shaver, G., Koeberlein, E., Shute, R., Koeberlein, D., McCarthy, J., and Nielsen, D.** (2016). Fuel-efficient exhaust thermal management using cylinder throttling via intake valve closing timing modulation. *Proceedings of the Institution of Mechanical Engineers, Part D: Journal of Automobile Engineering. March 2016, vol. 230 no. 4, pp. 470-478. DOI: 10.1177/0954407015586896.*
- [70] **Gehrke, S., Kovacs, D., and Eilts, P.** (2013). Investigation of VVA-based exhaust management strategies by means of a HD single cylinder research engine and rapid prototyping systems. *SAE International 2013-01-0587.*
- [71] **Roberts, L., Magee, M., Shaver, G., Garg, A., McCarthy, J., Koeberlein, E., Holloway, E., Shute, R., Koeberlein, D., and Nielsen, D.** (2014). Modeling the impact of early exhaust valve opening on exhaust thermal management and efficiency for compression ignition engines. *International Journal of Engine Research. Epub ahead of print 6 October 2014. DOI: 10.1177/1468087414551616.*
- [72] **Roberts, L. E.** (2014). Analysis of the impact of early exhaust valve opening and cylinder deactivation on aftertreatment thermal management and efficiency for compression ignition engines. *Master of Science Thesis. Purdue University. West Lafayette, Indiana. December 2014.*
- [73] **Zammit, J. P., McGhee, M. J., Shayler, P. J., Law, T., and Pegg, I.** (2014). The effects of early inlet valve closing and cylinder disablement on fuel economy and emissions of a direct injection diesel engine. *Energy 79 (2015), pp. 100-110.*
- [74] **Magee, M.** (2014). Exhaust thermal management using cylinder deactivation. *Master Thesis. Purdue University. West Lafayette, Indiana. May 2014.*
- [75] **Zhang, X., Wang, H., Zheng, Z., Reitz, R. D., and Yao, M.** (2016). Effects of late intake valve closing (LIVC) and rebreathing valve strategies on diesel engine performance and emissions at low loads. *Applied Thermal Engineering, Volume 98, pp. 310-319. April 2016.*
- [76] **Ding, C.** (2014). Thermal efficiency and emission analysis of advanced thermodynamic strategies in a multi-cylinder diesel engine utilizing valve-train flexibility. *PhD Thesis. Purdue University. West Lafayette, Indiana. December 2014.*

- [77] **Ding, C., Roberts, L., Fain, D. J., Ramesh, A. K., Shaver, G. M., McCarthy, J., Ruth, M., Koeberlein, E., Holloway, E. A., and Nielsen, D.** (2015). Fuel-efficient exhaust thermal management for compression ignition engines during idle via cylinder deactivation and flexible valve actuation. *International Journal of Engine Research*. DOI: 10.1177/1468087415597413.
- [78] **Bharath, A. N., Kalva, N., Reitz, R. D., and Rutland, C. J.** (2014). Use of early exhaust valve opening to improve combustion efficiency and catalyst effectiveness in a multi-cylinder RCCI engine system - a simulation study. *ASME 2014 Internal Combustion Engine Division Fall Technical Conference, ICEF 2014. October 19-22, 2014, Columbus, IN, USA*.
- [79] **Bharath, A. N., Yang, Y., Reitz, R. D., and Rutland, C.** (2015). Comparison of variable valve actuation, cylinder deactivation and injection strategies for low-load RCCI operation of a light duty engine. *SAE International 2015-01-0843*.
- [80] **Url-3** <<http://www.lotuscars.com/engineering/engineering-software>>, Lotus Engine Simulation v5.07f, date retrieved 01.05.2014.
- [81] **Sezer, İ.** (2011). Alternative gaseous fuels in PFI spark ignition engines. *Journal of the Energy Institute, 2011. Vol.84, No.4*.
- [82] **Heywood, J. B.** (1988). *Internal combustion engine fundamentals*. McGraw-Hill Book Company, New York.
- [83] **Winterbone, D. E., and Pearson, R. J.** (2000). *Theory of engine manifold design – Wave action methods for IC Engines*. Professional Engineering Publications, London.
- [84] **Winterbone, D. E., and Pearson, R. J.** (1999). *Design techniques for engine manifolds : wave action methods for IC engines*. Professional Engineering Publications, London.
- [85] **Pearson, R. J., Bassett, M. D., Fleming, N. P., and Rodemann, T.** (2002). *Lotus Engineering software - an approach to model-based design*. Lotus Engineering. Hethel, Norfolk.
- [86] **Sandoval, D., and Heywood, J. B.** (2003). An improved friction model for spark-ignition engines. *SAE Paper no. 2003-01-0725*.
- [87] **Patton, K. J., Nitschke, R. G., and Heywood, J. B.** (1989). Development and evaluation of a friction model for spark ignition engines. *SAE Paper no. 890836*.
- [88] **Benson, R. S.** (1982). *The thermodynamics and gas dynamics of internal combustion engines (Volume 1)*. Clarendon Press, 1982.
- [89] **Watson, N. and Pilley, A. D.** (1980). A combustion correlation for diesel engine simulation. *SAE Paper 800029*.
- [90] **Sezer, İ.** (2011). *Gaseous fuels in PFI spark ignition engines. 6<sup>th</sup> International Advanced Technologies Symposium (IATS'11), 16-18 May 2011, Elazığ, Turkey*.

- [91] **Ghazal, O. H.** (2013). Effect of inlet valve variable timing in the spark ignition engine on achieving greener transport. *World Academy of Science, Engineering and Technology, Vol:5, 2013-10-05.*
- [92] **Annand, W. J. D.** (1963). Heat transfer in the cylinders of reciprocating internal combustion engines. *Proceeding of the Institution of Mechanical Engineers, Vol. 177, pp. 983-990.*
- [93] **Benson, R. S. and Whitehouse, N. D.** (1979). *Internal combustion engines: a detailed introduction to the thermodynamics of spark and compression ignition engines, their design and development (Volume 1).* Oxford : Pergamon Press, 1979.
- [94] **Watson, N. and Janota, M. S.** (1982). *Turbocharging the internal combustion engine.* John Wiley&Sons, 1982.

## **APPENDICES**

**APPENDIX A:** Steady State Test Data Figures.

**APPENDIX A : Steady State Test Data Figures.**

Label	default cylinder
Bore (mm)	107,0000
Stroke (mm)	124,0000
Cyl Swept Volume (l)	1,11501
Total Swept Volume (l)	6,69007
Con-rod Length (mm)	192,00
Pin Off-Set (mm)	0,00
Compression Ratio	17,30
Clearance Volume (l)	0,068406
Phase (ATDC)	0,00
Combustion Model	
Open Cycle HT	
Closed Cycle HT	
Surface Areas	
Surface Temperatures	
Scavenge-Cylinder	

**Figure A.1 :** Insertion of main technical specs of the cylinder.

Test Point	Speed (rpm)	Friction Option	Cylinder Data	Cylinder No.	FMEP (bar)	Efficiency (l-1)	Main Bearing Type	No. of Mains	Main Dia. (mm)	Main Bg. Length (mm)	Crankpin Type	Pin Dia. (mm)
1	1000	Sandoval and Heywood	Common	All			In-line Default	4	64,2000	23,7540	In-line Default	60,9900
2	1100	Sandoval and Heywood	Common	All			In-line Default	4	64,2000	23,7540	In-line Default	60,9900
3	1200	Sandoval and Heywood	Common	All			In-line Default	4	64,2000	23,7540	In-line Default	60,9900
4	1300	Sandoval and Heywood	Common	All			In-line Default	4	64,2000	23,7540	In-line Default	60,9900
5	1400	Sandoval and Heywood	Common	All			In-line Default	4	64,2000	23,7540	In-line Default	60,9900
6	1500	Sandoval and Heywood	Common	All			In-line Default	4	64,2000	23,7540	In-line Default	60,9900
7	1600	Sandoval and Heywood	Common	All			In-line Default	4	64,2000	23,7540	In-line Default	60,9900
8	1700	Sandoval and Heywood	Common	All			In-line Default	4	64,2000	23,7540	In-line Default	60,9900
9	1800	Sandoval and Heywood	Common	All			In-line Default	4	64,2000	23,7540	In-line Default	60,9900
10	1900	Sandoval and Heywood	Common	All			In-line Default	4	64,2000	23,7540	In-line Default	60,9900
11	2000	Sandoval and Heywood	Common	All			In-line Default	4	64,2000	23,7540	In-line Default	60,9900

**Figure A.2 :** Friction assumption of the simulation model.



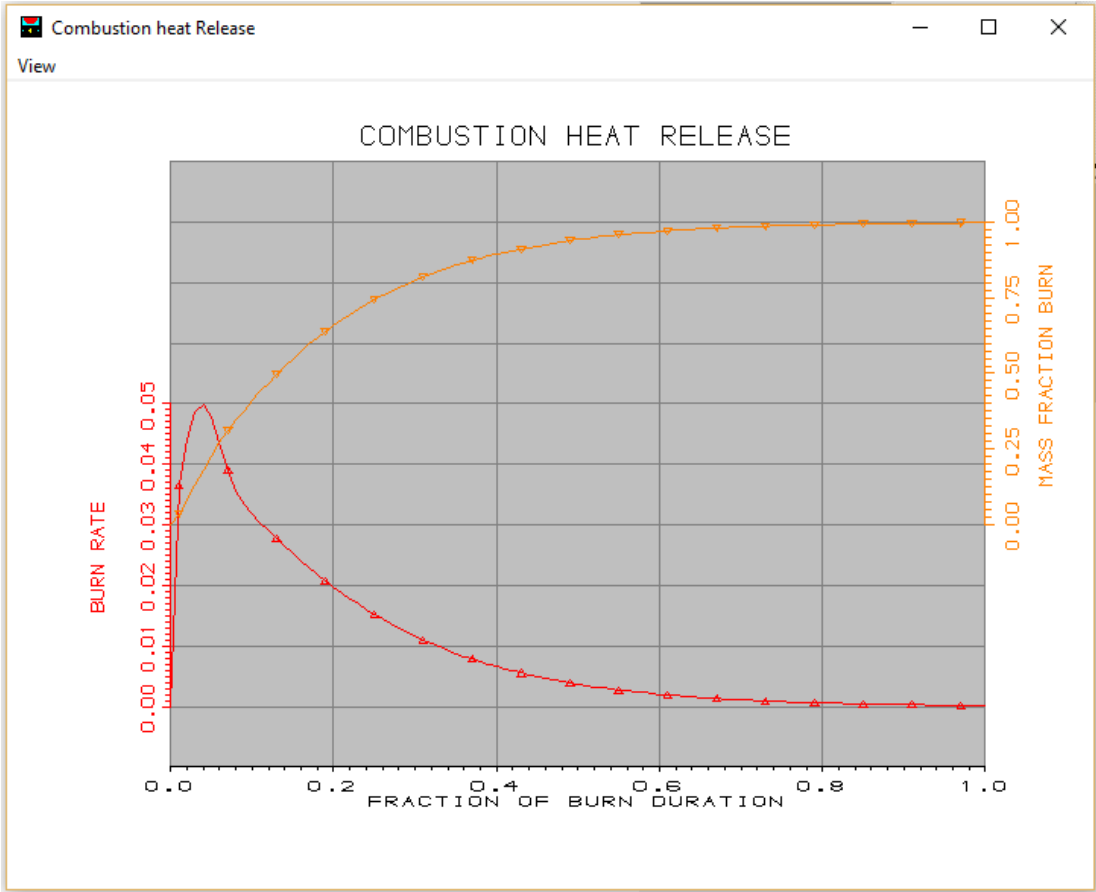


**Figure A.4 :** Combustion heat release graph.

The interface shows the following configuration for the Annand heat transfer model:

- Heat Transfer Model Type: **Annand**
- Annand Heat Transfer Model:
  - Default**: A: 1,100, B: 0,700
  - User**: A: [ ], B: [ ]

**Figure A.5 :** Annand open cycle heat transfer model.

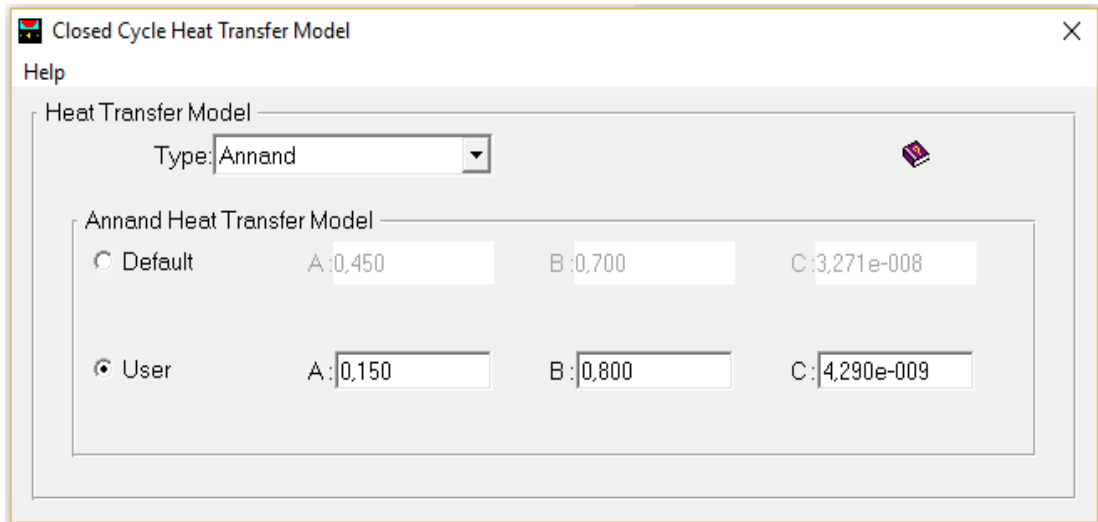


**Figure A.6 :** Annand closed cycle heat transfer model.

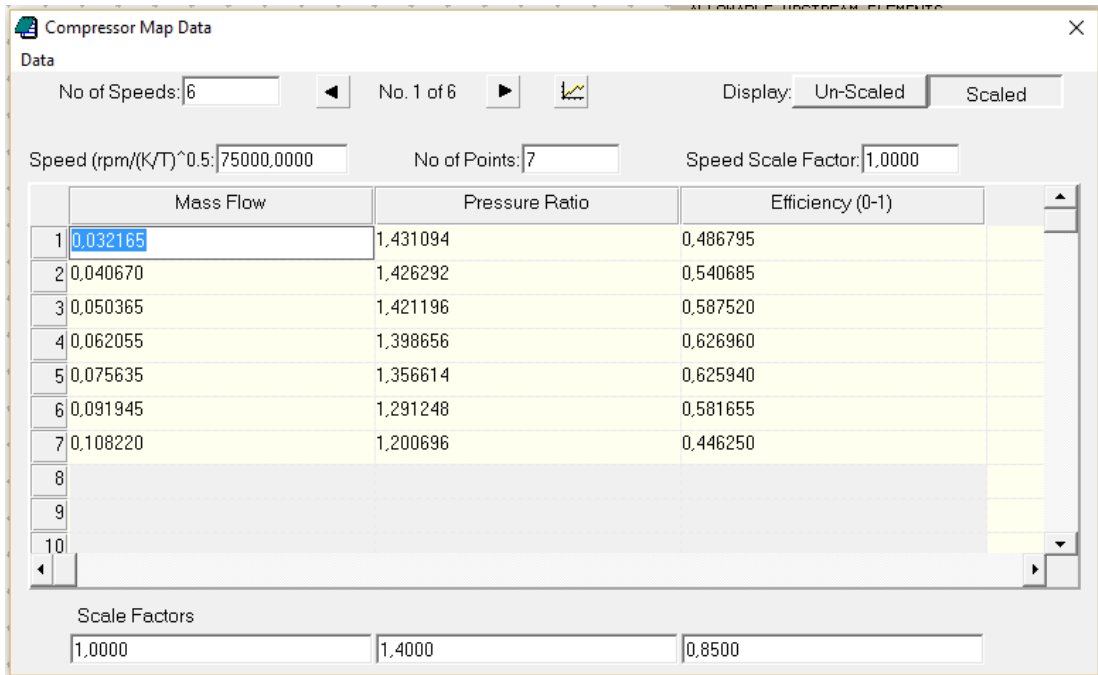


**Figure A.7 :** Compressor map data.



## CURRICULUM VITAE



**Name Surname:** Hasan Üstün BAŞARAN

**Place and Date of Birth:** ÜSKÜDAR / 29.07.1985

**E-Mail:** basaranha@itu.edu.tr

### EDUCATION:

**B.Sc.:** Istanbul Technical University, Naval Architecture and Marine Engineering, 2003-2008.

**M.Sc.:** Istanbul Technical University, Naval Architecture and Marine Engineering Master of Science Program, 2008-2010.

### PROFESSIONAL EXPERIENCE AND REWARDS:

Research Assistant - Istanbul Technical University, Naval Architecture and Ocean Engineering Department, Naval Architecture and Marine Engineering since June 2009.

### PUBLICATIONS, PRESENTATIONS AND PATENTS ON THE THESIS:

- **Başaran, H.Ü.**, 2013: Developing an Analytical Model for a Marine Diesel Engine Test Stand. *15<sup>th</sup> International Congress of the International Maritime Association of the Mediterranean, IMAM 2013 - Developments in Maritime Transportation and Exploitation of Sea Resources*, October 14-17, 2013 A Coruna, Spain.
- **Başaran, H.Ü.**, 2015: Modelling the Effect of Exhaust Valve Timing on Exhaust Thermal Management of a Turbocharged&Intercooled Diesel Engine. *16<sup>th</sup> International Congress of the International Maritime Association of the Mediterranean, IMAM 2015 - Developments in Maritime Transportation and Exploitation of Sea Resources*, September 21-24, 2015 Pula, Croatia.
- **Başaran, H.Ü.**, Özsoysal, O.A., 2016: Modelling the Effect of Variable Valve Timing on Exhaust Thermal Management of a Turbocharged&Intercooled Diesel Engine. *3<sup>rd</sup> International Conference on Maritime Technology and Engineering*, July 4-6, 2016 Lisbon, Portugal.
- **Başaran, H.Ü.**, Özsoysal, O.A., 2016: Modelling the Effect of Intake Valve Closing Timing on Exhaust Thermal Management of a Turbocharged&Intercooled Diesel Engine. *Gemi ve Deniz Teknolojisi Dergisi*, Sayı: 206.

